The stability of continuous cover forests

by

Axel Wellpott

Thesis

Submitted to the University of Edinburgh
for the degree of

Doctor of Philosophy

School of GeoSciences

2008

Acknowledgement

First of all I would like to thank the Forestry Commission for funding my PhD project, which gave me the opportunity to work on the fascinating topic of wind and tree interactions in a team, which is probably the best in the world.

This PhD project continues some of the work started by my principle supervisor Barry Gardiner in the 1990's. Walking in his footsteps was a real challenge. In all the time he gave me a very long lead and let me follow my own ideas, but gave me direction and advice when I needed them. His enthusiasm for the topic, his friendly nature, and his light-hearted approach to life made it a pleasure to work with him.

Maurizio Mencuccini from the University of Edinburgh was my other supervisor. His optimistic and cheerful nature was always epidemic and more than once I left his office in a much better mood than the one I was in when I had entered it.

Beside my two supervisors the Stability team of the Forest Management Division (FMD) was another group which showed great interest in my work. Many of the lively discussions of my data with Bill Mason, Bruce Nicoll, Sophie Hale, and Alexis Achim gave me new ideas for further analysis and helped me to improve the outcome of my thesis. Sophie also had the unpleasant job to read the first drafts of my chapters.

The logging equipment for the field campaign was supposed to be delivered, so that I would only have to plug everything in to collect the data in the field. The equipment was never delivered and therefore I had to set foot into the Northern Research Station workshop for the first time after six months into my PhD. What would I have missed out! The realisation of the field measurements would have been impossible without the support from Dave Brooks, John Strachan, and

Jim Nicholl in the workshop. Worth more than just building water proof boxes and ordering equipment for me was the fact that I received detailed answers to my questions and demonstrations on how everything works. Without this my enthusiasm for data loggers and measuring systems would probably have never evolved. The hours I spent in the workshop were among those that I enjoyed the most throughout my PhD.

For the first field experiment an industrial-PC was needed for final data storage. Unfortunately the budget had already been overspent, when I needed to order one. Thankfully, Roland Vogt from the University of Bale, Switzerland, lent me one from his equipment pool, which was vital for the startoff of the first field campaign.

For the setup of the two experiments I got help from many people. The guys from the Technical Support Unit in Talybont, Wales, did a fabulous job and it was a pleasure to work with them. Thanks go to Justin Chapbell, Brian Jones alias "Dickie", Brian Jones, and Dai Evans. It was a real pleasure to work with them.

Special thanks need to be addressed to Shaun Mochan and Carl Foster. Shaun was on site every time when the mast was erected or lowered. Carl was the head of the Technical Support Unit at the time of the Clocaenog Experiment and was a great help in organising the field work. Carl also deserves special thanks for asking me to go to the pub at the end of a long day in the field, which was probably the worst in my PhD, instead of letting me spend the time on my own in the the hotel room.

Beside the core field team, many students helped in the field. Thanks are addressed to Armand Tene, David Vinué, Nicolas Foulan, and Sophie Bertin.

The experimental stand in Clocaenog Forest is part of the Tyfiant Coed project from the experimental silviculture research group at the University of Wales, Bangor. Arne Pommerening granted permission to carry out our experiments in this stand and Jens Haufe kindly made the detailed stand measurements available, which were used for stability modelling.

Structured forest stands are rare as hens' teeth in Britain. All the more I like to thank Peter Hale (Hale Association) and Ian Robinson (Scottish Woodland) for letting us conduct the second field experiment in one of the stands in the beautiful Kyloe Wood forest, Northumberland.

In August 2007 I attended the "Wind and Trees"-Conference in Vancouver,

Canada, this gave me the possibility to present the results of my PhD to an international audience. My travel expenses were covered by the "Irvine Sinclair fund" and were made available by John Grace from the University of Edinburgh, which is much appreciated.

Finally, I would like to acknowledge my parents and my family, who supported me for all my life. At the same time I apologise for not visiting them as often as they deserved during my time in Scotland.

Abstract

World-wide, wind damage causes major economical losses to commercial forestry, in particular in windy climates such as in the British Isles. Wind risk models are valuable tools for forest management planing to predict and minimise the risk of wind damage. British foresters use the ForestGALES model which predicts the critical wind speed and risk for forest stands in Britain. Due to a number of factors the number of British forests that are managed under low impact silviculture systems is increasing. The associated stand structure is more irregular than those under standard management and the ForestGALES model is at the moment not able to predict the critical wind speed for these structured stands. The aim of this PhD project was to collect field data to help in the development of the ForestGALES model for application in irregularly structured forest stands.

Two field campaigns were carried out in which wind and tree interactions were investigated. Wind profiles, turbulence, and turning moment at the tree base were measured with high temporal resolution for a group of nine trees in both field studies.

The first experiment took place in a mature even-aged Sitka spruce forest stand, which appeared to be more stable than model calculations anticipated. Differences in wind loading between the individual trees were calculated and related to tree properties. Absolute turning moments were positively correlated with tree properties such as diameter at breast height, tree height, and stem weight. The estimated turning moment for tree failure for the strongest tree in the sample was more than five times higher than the value for the weakest one. However, due to their dominance and their exposed position in the stand, the bigger trees also experienced higher wind drag. The results suggest that the balance between individual tree resistive moment and applied moments is such

that the critical wind speeds for damage are similar. This implies that trees are adapted to some extent to their local wind climate.

Post-damage surveys from continental Europe suggest that irregular forests are more stable than regular ones. This hypothesis was tested in the second field campaign in which the wind and tree interactions were compared in two contrasting but adjacent stands. One group of trees was located where an understorey was present, while two other trees were at a location with no understorey. The analysis suggests that the trees with an understorey benefit from the understorey in terms of wind loading and wind damage risk. The results are backed up by the comparison of the turbulence characteristics for different wind directions and the comparison of the wind profiles at the two locations. These confirm that there is reduced momentum transfer to the overstorey in the presence of an understorey.

Contents

Appendices

List of Figures

List of Tables

List of Symbols

Symbol	Name	Unit
A	crown area	m^2
C_D	drag coefficient	–
cr	crown radius	m
c_{reg}	regression constant for estimating M_{over}	$\mathrm{N\,m\,kg^{-1}}$
d	zero plane displacement	m
dbh	diameter at breast height (1.3 m)	m
$dist$	distance	m
D	average spacing of stand	m
E	Young's modulus	Pa
F	force	N
F_D	drag	N
f_{CW}	additional turning moment due to overhanging crown mass	Nm
f_{edge}	edge factor	–
f_{knot}	knot factor	–
g	standard gravity (9.81)	$\mathrm{m\,s^{-2}}$
GF	gust factor	–
h	tree height	m
h_{100}	stand top height	m
h_C	canopy height	m
k	Von-Karman constant (0.40)	–
Kt_a	Kurtosis of Variable a	–
L	Obukhov length ($L = -u_*^3/k\beta\overline{w'\Theta'}$)	m
L_u	horizontal Eulerian length scale	m
L_w	vertical Eulerian length scale	m
m	mass	kg
M	turning moment	Nm
M_{break}	breaking moment	Nm
M_{crit}	critical moment	Nm
M_{over}	overturning moment	Nm
MOR	modulus of rupture	Pa

Symbol	Name	Unit
r	Pearson's correlation coefficient	–
R^2	coefficient of determination	–
Sk_a	Skewness of variable a	–
TMC	**T**urning **M**oment **C**oefficient	kg
u	horizontal wind speed component	$\mathrm{m\,s^{-1}}$
u_*	friction velocity	$\mathrm{m\,s^{-1}}$
u_{break}	wind speed which breaks tree or stand	$\mathrm{m\,s^{-1}}$
u_{over}	wind speed which overturns tree or stand	$\mathrm{m\,s^{-1}}$
u_{crit}	critical wind speed for tree or stand failure	$\mathrm{m\,s^{-1}}$
u_h	horizontal wind speed at canopy top	$\mathrm{m\,s^{-1}}$
w	vertical wind speed component	$\mathrm{m\,s^{-1}}$
z	height	m
z_0	roughness length	m
α	scale parameter of the Weibull distribution	–
γ	shape parameter of the Weibull distribution	–
ρ	air density (1.226)	$\mathrm{kg\,m^{-3}}$
τ	shear stress	$\mathrm{N\,m^{-2}}$
τ	Kendall's rank correlation coefficient	–
ε	strain	–

List of Abbrevations

Abbrevation	Name
cdf	cumulative distribution function
cr-rad	crown radius
cr-base	crown base
cr-class	crown class
pdf	probability density function
rp	return period
wd	wind direction
BA	basal area
CCF	continuous cover forestry
CI	competition index
DAMS	**D**etailed **A**spect **M**ethod of **S**coring
DWD	German Weather Service
LES	large eddy simulation
RMA	relative momentum absorption
RMSE	root mean square error
STS	strain transducer signal
SW	stem weight
VITA	**V**ariable **I**nterval **T**ime **A**veraging
WHC	**W**ind **H**azard **C**lassification

Chapter 1

Introduction

1.1 Wind damage

Wind damage is along with wildfires the main natural process which acts as starting point for natural regeneration and increasing diversity in forest stands (Quine, 2001; Ruel and Pineau, 2002). Therefore wind damage is seen as a valuable disturbance from an ecological point of view. However, from a forest managers perspective, who has to fullfill economical targets, it is difficult to see the benefits of wind damage. Non salvaged wind thrown timber can be a source of insect pests (Bouget and Duelli, 2004) and logging wind damaged stands is dangerous, time consuming, and costly. Major storm events come along with logistic problems. The national Swedish fleet of harvesters on its own was not capable to tidy up the wind thrown timber quickly enough after the storm event *Gudrun* in winter 2005, to salvage the thrown trees and prevent insect outbreaks. Thus efforts were undertaken, although the costs for harvesting and storing exceeded in many cases the value of the timber (Björheden, 2007). After the storm event *Lothar* in 1999, the salvaged timber flooded the market, leading to a drastic decrease in timber prices (prices for roundwood dropped by at least 30 %) (ECE/FAO, 2000).

Compared to continental Europe Britain's wind climate is much more severe (Troen and Petersen, 1989). Wind damage makes up about 20 % of the annual timber production excluding major storm events (Rollinson, 1987). In addition to financial loss windthrow is also blamed for many accidents in the aftermath, when the wind thrown timber is salvaged.

So there are reasons to spend efforts on minimising wind throw in plantation

forests. The conflict between ecology and economy is solved by using forest management systems, which to some extent mimic natural disturbance events. Several management types have been implemented, which promote the growth of natural regeneration, while an overstorey is still present. Such techniques are the opposite of the traditional clear felling/restocking system, which has been common practise in Britain for at least a century (Schütz, 2001; Mason and Kerr, 2004).

In times in which climate change and its consequences are discussed everywhere the question rises whether forest stands will suffer an increased risk of wind damage in the future. Since normal crop rotation periods cover time spans of decades, forestry is very much affected. A profound understanding of all factors influencing stand stability is therefore necessary for reliable predictions.

1.2 Wind risk models

Wind risk models calculate the critical wind speed required for wind damage as a function of site and stand characteristics and are designed to give support in forest management decision processes. Model calculations allow the estimation of the impact of forest management on the windthrow risk of a stand and are able to predict future wind risk as the stand matures using yield tables or growth models.

The earliest efforts in Britain to support forest managers in estimating the windthrow risk of a particular site, resulted in the **W**ind **H**azard **C**lassification (WHC), which provides a score in the range of one to six (Miller, 1985). The score is based on physical measurements and should therefore be relatively objective. However, only site specific information are used in its calculations and no stand or silviculture information. Nevertheless is the scoring system still in use today and provides a valuable site classification system for British foresters.

Purely empirical wind risk models have been described in the literature (Mitchell et al., 2001). These models are based on the statistical analysis of windthrow observations. The windthrow risk is estimated using regression analysis, where stand characteristics are used only as estimators. The portability of any statistical model to different conditions and its extrapolation for conditions the model has not been validated for is always an issue (Lanquaye-Opoku and Mitchell, 2005).

In contrast to statistical models a mechanistical approach aims to mimic the physical processes of tree uprooting or failure. The two most widely used wind risk models in this category are ForestGALES and the HWIND model (Peltola, 1996a; Dunham et al., 2000; Gardiner et al., 2000, 2008).

The structure of the two models is very similar. Both models calculate the resistance to overturning and breaking for the average tree in the stand as a function of soil type, stand cultivation, tree species, and stand characteristics. The critical wind speed required for damage is reached when the wind induced turning moment exceeds the tree's critical turning moment. The method of distributing the wind energy onto the tree is different in the two models. ForestGALES predicts the average shear stress on each tree (*roughness method*), while HWIND calculates the wind profile in the stand to predict the mean wind loading. Since it is not the mean turning moment that damages the tree but the maximum turning moment, both models use an empirically derived *gustfactor*. This factor represents the ratio of maximum to mean turning moment and is calculated from stand characteristics (tree height, spacing, distance from edge).

To estimate the likelihood that the critical wind speed is exceeded, the two models have wind climate modules incorporated. ForestGALES uses a windiness scoring system called DAMS (available for Britain), while HWIND uses the WAsP model to estimate wind speed distributions at the location of the stand. The wind speed distributions are then used to calculate the return periods for the predicted critical wind speed.

Due to their mechanistical approach the two models have been configured for many other countries. So far the ForestGALES model has been adapted for Canada, New Zealand, France, and Japan (Ruel et al., 2000; Moore and Quine, 2000; Cucchi et al., 2005; Kamimura and Shiraishi, 2007).

At the moment the ForestGALES model calculates the wind risk for the mean tree in the forest and therefore the model is not able to account for the variability of wind risk that occurs in irregular stands. These shortcomes prevent the application of the wind risk model for stands that are managed under a continuous cover system. However, recent model developments perform calculations at the individual tree level rather than at the stand level (e.g. Ancelin et al., 2004). Schelhaas et al. (2007) modification of the HWIND model even takes inter-tree interaction (crown contact) into consideration.

1.3 Turbulence above forests

The airflow above a canopy is different from the one above a plane surface. It was Raupach et al. (1996) who worked out that the turbulent structure above a canopy is better described by the mixing of two layers that flow with different speeds instead of a boundary layer approach (see Fig. 1.1).

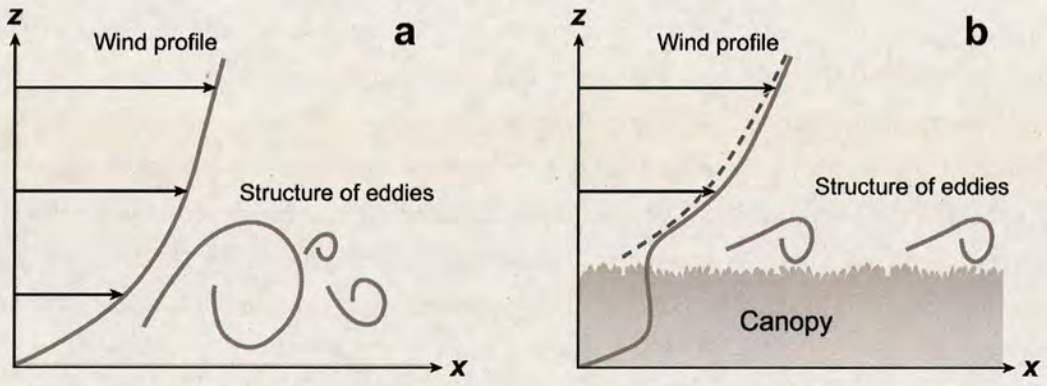

Figure 1.1: Sketch of a boundary layer (a) and a mixing layer (b) (taken from de Langre (2008)).

The two main characteristics of a mixing layer are (1) the inflection point of the wind profile and (2) the occurrence of coherent structures which scale with canopy height and dominate the transport of any scalar (momentum, heat, water vapour, etc.). Such structures are visible as *Honamis* in crop fields (Inoue, 1955; Finnigan, 1979; Py et al., 2005; de Langre, 2008), as cat's paws on a water surface (Dorman and Mollo-Christensen, 1973), and are audible as travelling gusts on a windy day in a forest. Gardiner (1995) showed that the occurrence of coherent structure correlates with maxima in time series of turning moments that trees experience and concluded that these gusts are responsible for wind damage. Allen (1996) pushes the interpretation to the limit and relates the direction of overturned trees to the hairpin shape of coherent gusts.

The theoretical development of such coherent structures is shown in Figure 1.2. The formation of Kelvin-Helmholtz waves is the starting point for the creation of the coherent structures, which travel about 1.8 times faster than the mean wind speed at canopy top. However, in reality the several stages of development shown in Figure 1.2 are not as separated as the drawing suggests. All the processes take place at the same time and the coherent structures are superimposed onto the general atmospheric turbulence. Most of the knowledge of these structures has been gathered from the single point time series analysis from turbulence

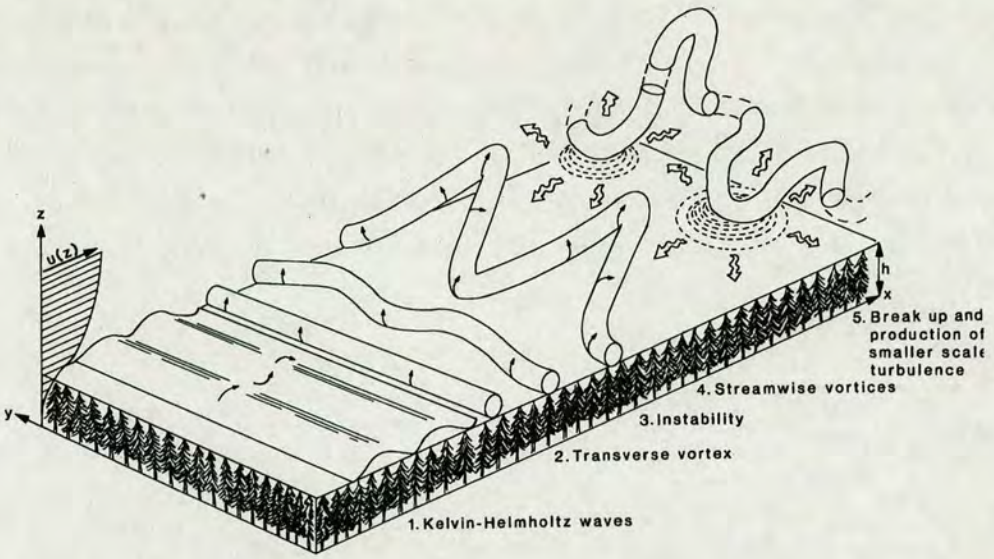

Figure 1.2: Formation of coherent structures above a forest canopy (after: Finnigan and Brunet (1995), taken from Quine et al. (1995)).

measurements applying Taylor's frozen turbulence axiom. The occurrence of gusts can be identified by ramp structures in time series of momentum flux or air temperature (Gao et al., 1989; Shaw et al., 1989; Bergström and Högström, 1989; Collineau and Brunet, 1993; Shaw et al., 1995).

More recently Py et al. (2006) assigned an active part to the canopy in forming those coherent structures by a lock-in mechanism. Their results from experiments in two different crops revealed that the length scale of the coherent structures is interlocked with the eigenfrequency of the underlying canopy over a wide wind speed range. Marshall (1998) observed the same phenomenon in data from wind tunnel experiments with modelled forests. Those results raise the question of whether the same principles hold true for natural forest canopies and whether the stand can be manipulated in a way that benefits its stability. Moore and Maguire (2004) showed that the eigenfrequency of several tree species is linearly related to the ratio of height to the squared diameter at breast height. Therefore an irregular forest stand with a wide range of tree's eigenfrequencies might result in less severe turbulence, which in conclusion would lower the risk of wind damage (Gardiner, 1995).

The air flow at forest edges differs from the one deeper inside a forest stand. It takes several tree heights (about 10 h) before the turbulence has fully adapted to the new surface and the turbulence has reached steady state conditions (Marshall

et al., 2002; Yang et al., 2006). Trees that are closer than three tree heights from the edge have to withstand less drag compared to those further away. This is one of the reasons why wind damage does usually not originate at forest edges of established stands (Mitscherlich, 1974). Processes at stand edges are not the subject of discussion in this work, but work on this topic is widely available in the literature (e.g. Peltola and Kellomäki, 1993; Irvine et al., 1997; Morse et al., 2002).

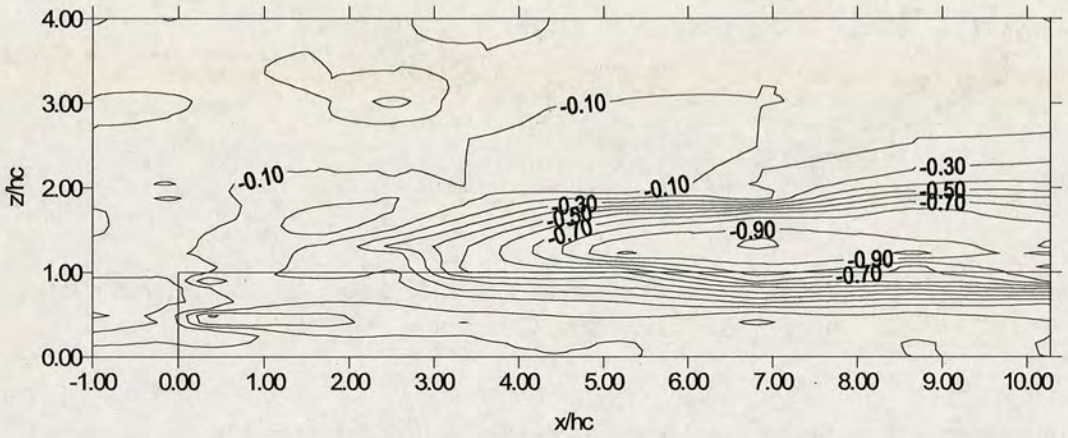

Figure 1.3: Contour plot of atmospheric shear stress along a forest transect. Axes are normalised by canopy height (h_C) (Morse et al., 2002).

The assumption of steady state conditions further away from the forest edge leads to the conclusion that the production of turbulence equals its dissipation, which means that the atmospheric shear stress (τ) is fully transferred to the trees of the forest stand (Gardiner, 1995). Together with the assumption that the zero plane displacement (d) can be regarded as the acting height (Thom, 1971) and the fact that the area a single tree occupies is governed by stand density, the turning moment for individual trees can be calculated. Gardiner (1994) measured turning moments of three trees and the atmospheric shear stress and found good agreement between measurements and calculations.

1.4 Mechanics of wind damage

1.4.1 Resistance to wind damage

Tree failure can be distinguished into two major types:

- mechanical failure of the tree which causes stem breakage, and

- failure of root anchorage which causes overturning.

Some authors subclassify into more categories than these two by specifying which part of the tree failed (Bazzigher and Schmid, 1969). Different tree failure types can occur in the same forest stand. However, wind damage in Britain occurs most of the time due to overturning, since many soils are waterlogged which restricts root development (Ray and Nicoll, 1998).

Stem breakage occurs when the curvature of the stem exceeds its flexibility. The stiffness of a cylinder, which is a good representation for a tree trunk, is proportional to its cubed diameter. Hence a small increase in diameter results in a big increase in rigidity. It is believed that trees are able to optimise their shape in a way that the mechanical stress is constant for the entire tree profile (Metzger, 1893). As a consequence this means that the likelihood of structural failure is the same along the tree trunk.

The resistance to overturning is governed by the root-soil resistance, which itself is determined by the distribution of the roots, soil type, and water content (Nicoll et al., 2006b). Bigger root-plate dimensions result in higher overturning resistance. There is evidence that the root-plate resistance changes during a storm event by cyclic loading and gradual loosening of the soil-root connection (O'Sullivan and Ritchie, 1993). In dense stands, the roots of neighbouring trees can be interweaved, so that a separation into two root plates is not feasible.

For obvious reasons reliable root information is almost impossible to access without destructive sampling methods, which makes that information unsuitable as input parameter for wind risk models. However, good relationships have been found between overturning moment and above ground tree properties. The analysis of more than 2,000 tree pulling tests in Britain revealed that the overturning moment can be parametrised using information on tree species, stem weight, soil type, and rooting depth (Nicoll et al., 2006a). Tree pulling experiments from other countries and species, which are not native to Britain, found similar relationships, which makes this an universal approach (Achim et al., 2005; Byrne and Mitchell, 2007). The assumptions are backed up by Cheng and Niklas (2007), who found a good correlation between the above and below ground biomass in 1,534 forested communities.

1.4.2 Wind loading on trees

The drag force (F_D) on a tree can be calculated from the density of the fluid (ρ) and the profiles of horizontal wind speed (u), crown area (A), and drag coefficient (C_D).

$$F_D = \rho \cdot \int_0^z A(z) \cdot C_D(z) \cdot u(z)^2 \ \mathrm{d}z \tag{1.1}$$

As trees are not rigid obstacles, like for example buildings, the application of this equation is more complicated. Branches and twigs are flexible and bend. The tree crown streamlines and therefore projected area and drag coefficient are also functions of wind speed. Mayhead (1973) measured the drag coefficient of several species of British forest trees in a wind tunnel. Rudnicki et al. (2004) did the same for several species from British Columbia. Due to size limitations only small individuals or tree tops were measured. Because juvenile wood is more flexible than mature wood, it is questionable whether the values from the wind tunnel are realistic. Another problem is that the air flow in a wind tunnel is less turbulent compared to the free atmosphere, which also leads to systematic underestimation of the drag coefficient.

1.4.3 Dynamics of wind-tree interaction

Trees have to be considered as dynamic structures. An instantaneously applied force causes the tree to sway around its rest position before it returns to it after several sway circles. The dynamic character of the wind and tree interaction has been suggested to be an important reason why the calculated forces required to damage are overestimated (Oliver and Mayhead, 1974).

In the simplest dynamic model, a tree can be represented by a rigid rod with a rotary spring and damper at the bottom (Flesch and Wilson, 1999). Kerzenmacher and Gardiner (1998) developed a more sophisticated model with more degrees of freedom. Their model adjusted the rigidity, mass, and damping coefficient for each 1 m section of the tree.

From concurrent time series of turbulence and tree response the mechanical transfer function can be calculated as (Mayer, 1987; Peltola, 1996b):

$$S_{yy} = H_m^2 \cdot S_{uu} \tag{1.2}$$

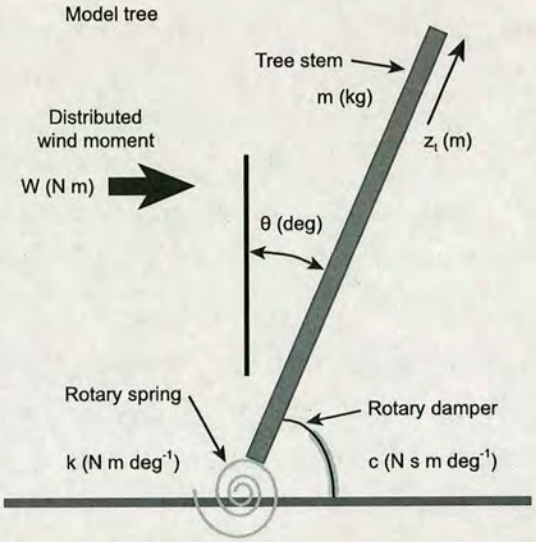

Figure 1.4: Simple tree model with rotary spring and rotary damper (taken from Flesch and Wilson (1999)).

where S_{yy} and S_{uu} are the spectra of turning moment and horizontal wind speed, respectively. The form of the mechanical transfer function agrees with the one of a damped harmonic oscillator (Gardiner, 1992), with a pronounced peak at the eigenfrequency of the tree. A second much less pronounced peak can be found close to the frequency of the tree's second mode. The tree response will be less severe the bigger the difference is between the eigenfrequency and the peak in the spectrum of the horizontal wind speed. This made Peltola (1996b) conclude that "we have to grow small fat trees" to increase the stability of forest stands. Theoretically a resonant effect would be possible, where the amplitude of turning moment over successive sways builds up. However, no one has observed this phenomenon so far in the field.

Taking only the eigenfrequency of the whole system "tree" into consideration is a simplification. More sophisticated approaches would take the coupling of branches, subbranches, etc. into account, where each hinge has its own spring and damper characteristics (Sellier and Fourcaud, 2005). Scannell (1984) found "simple relationships between the natural frequency modes of the tree element", which is an effective way to maximise the tree damping. An idea of the efficiency of the coupling of branches and trunk is given by the field experiments from Moore (2002), who found out that 80 % of the branch mass of Douglas-fir trees needs to be removed before a significant impact on the eigenfrequency of the whole system is recognisable.

Last but not least, the tree dynamic response is also strongly affected by stand structure. Crown clashing dissipates a lot of swaying energy. Milne (1991) estimated the proportion of (1) interference of branches with those of neighbours, (2) aerodynamic drag on foliage, and (3) damping in the stem to be 5/4/1. Although the values cannot easily be transferred to other forest stands the numbers highlight the importance of the interaction between neighbouring trees.

The very complex structure of trees and the complex response to dynamic wind loading makes it difficult to reproduce the natural situation in a wind tunnel model. Field measurements are therefore always necessary to support any result derived from wind tunnel studies (or computer modelling).

1.5 Adaptive growth

Although trees are not able to escape the environment they are living in, they are able to adapt to their environment within certain physiological limits. The response to mechanical stimulation was already observed in the 19th century (Knight, 1803; Metzger, 1893) and has been termed *thigmomorphogenesis* by Jaffe (1973). Experiments with seedlings showed that plants had higher stem diameters when they were regularly shaken compared to a control, which was not shaken (e.g. Rees and Grace, 1980; Stokes et al., 1997). It is believed that this is triggered by the release of ethylene in cells (Telewski, 1995). However, wind is just one factor affecting growth among many others. But its influence can be seen clearly where sheltered and non sheltered environments are located close to each other.

Thigmomorphogenesis does not stop at the soil surface. The root system is also subject to adaptation, which includes the circumference of the root plate, direction of the first order roots, and the general root shape (Nicoll and Ray, 1996; Ruel et al., 2003; Nicoll et al., 2005, 2006b). The work from Urban et al. (1994) suggests that the adaptation of the root system is triggered more quickly than the response in the trunk.

As a practical implication this means that trees, if they have sufficient time, are well adapted to the wind climate they are exposed to. A change in exposure caused by thinning can elevate the risk of wind damage. The regularly observed higher amount of wind damage in recently thinned stands is a consequence of the lack of time for the trees to adapt (Somerville, 1980; Cremer et al., 1982;

Gardiner and Quine, 1994).

The fact that trees are still potentially vulnerable to wind throw can be explained by the fact that wind is not the only constraint to the vitality of a tree. In a forest, individuals compete for light and nutrition and tree growth is a trade off between going for height to experience an improved light regime, and going for thickness, which results in improved structural strength (James et al., 1994).

1.6 Forest management and wind damage

Gale events which cause wind throw in forests are often divided into catastrophic and endemic ones. Miller (1985) defined the threshold to be an hourly mean wind speed of $40\,\mathrm{m\,s^{-1}}$. There is a consensus in the literature that the influence of silviculture practise is neglegible in a catastrophic event. Although the catastrophic events get more attention in the media the amount of wind damage in Britain concerned with those events is less than that related with endemic damage. Rollinson (1987) accredits an average loss of 6 % of the total production to catastrophic events and 20 % to endemic events for a time period of 30 years.

It is in the nature of the wind speed distribution that a small change in stability has a big influence on the likelihood, that the critical wind speed is exceeded. Therefore, even small increases in mechanical stability can have a significant impact on the probability of wind damage (Mason, 2002).

The traditional management system in Britain is a clearfelling-restocking system. All trees of a forest stand are harvested at a time and restocking takes place after lying the site idle for some years. British forest policy set the target to move forward from this simple silvicultural system to a more sophisticated one, where forest stands are managed in a way that a canopy is maintained throughout the lifetime of the site, avoiding clearfelling. For Wales for example the target is to transfer 50 % of the forest area into continuous cover forests (CCF) by the year 2020 (Mason, 2002). In general the selected stands are attributed with a higher quality in terms of biodiversity and visual impact. Most other European countries have a long tradition of continuous cover forestry and clear felling is prohibited today, although clearfelling and restocking has been also common both in Central Europe and Scandinavia.

The high number of mature stands in Britain makes it difficult to introduce CCF on a broader scale. Such stands are vulnerable to any kind of thinning, which is essential to improve the light conditions at the forest floor. A sufficient light regime is a precondition for the establishment of natural regeneration, which is a first step towards an irregular stand structure (Hale et al., 2004). The transformation of these forest stands is one of the major challenges for British silviculture at the beginning of the 21st century. However, it won't either be sensible nor possible to transform all British forest stands into CCF. Some of the stands are too exposed and any thinning would result in an unreasonable high wind risk.

The three major components that have an effect on wind damage are (1) soil, (2) wind climate, and (3) silviculture (Mitchell, 1995). Although man has started to alter the climate on a worldwide scale the first two components are more or less out of our control, which leaves only silviculture for manipulating stand stability. The management has both an influence on the local wind climate and the future tree growth. A general recommendation is to start the thinning of stands at early stages of the stand development and to thin more often while removing less timber (Cremer et al., 1977; Mason and Quine, 1995).

1.7 Research Aims

For the parametrisation of wind risk models, that are able to simulate irregular stand structures, information of wind and tree interaction on the individual tree level are required. The data from two field experiments are the basis for the analysis in this work. The analysis focuses on the relationship between wind speed and turning moments that individual trees experience. The research aims are:

1. to validate several modules of the ForestGALES model independently with the detailed data from a field experiment in a mature even-aged Sitka spruce forest. The results should identify, which modules need further improvement.

2. to model the relationship between wind speed and turning moment for individual trees with the aim of estimating the individual risk of wind damage.

3. to predict the turning moment of individual trees with the help of individual

tree parameters as estimators, which will be applicable to irregular stand structures.

4. to quantify the differences in wind loading on individual trees for two different stand structures (regular and irregular) and to compare the results with those from wind tunnel studies.

1.8 Overview of thesis

The thesis consists of four main chapters (2-5), which are intended for publication. These chapters should be self contained and understandable on their own. Therefore repetition of some aspects is unavoidable.

Chapter 2: In the second chapter several modules of the ForestGALES model are validated using data from a field survey undertaken in a mature pure even-aged stand in Clocaenog Forest, Wales. The model predicts a return period for wind damage of one year for this stand. However, no wind damage was recorded for at least ten years.

A major assumption of the model in the calculations of the turning moment at the tree base is the way in which atmospheric shear stress is distributed onto the individuals of the forest stand. The analysis of turning moment data from a group of nine adjacent trees shows that the assumption, that every tree is exposed to the same wind loading, is not valid and that the drag the individual trees experience covers a wide range. The aerodynamic characteristics of the trees are too different and they cannot be assumed to be identical, and hence the current ForestGALES model approach is found to be oversimplistic for use in mature complex stands.

Chapter 3: The wind and turning moment relationships for the nine Sitka spruce trees in Clocaenog Forest are analysed more in detail in Chapter 3. Quadratic model fitting of the wind speed and the turning moment measurement for the nine trees gives R^2 values greater than 0.75 in eight out of nine cases. Due to the differences in tree properties the estimated moments for breaking and overturning are very different for the nine trees. The critical turning moment for the strongest tree is more than 5 times bigger than it is for the weakest tree in the sample. Naturally greater stability (higher stem mass) is correlated with an exposed position in the

stand and hence higher wind loading. Diameter at breast height is the best estimator of turning moments. Predicted critical wind speeds suggest that taller and bigger trees in the stand are at higher risk of failure than the smaller trees.

Chapter 4: The validation of some of the ForestGALES modules in Chapter 2 revealed the necessity to develop a new approach to calculate the wind loading at a single tree level. In this chapter the performance of several distance-dependent competition indices is tested for predicting wind loading at a single tree level. It is shown that even simple indices are able to explain most of the observed variance. However, the analysis also shows that wind direction has an impact on the wind and turning moment relationship. The occurrence of a gap increases the wind loading on the tree for the same wind speed, which indicates that the wind penetrates deeper into the canopy in such cases.

In a next step, the indices are used to simulate the influence of different thinning scenarios on the stability of the stand. The three scenarios differ in the way the trees are chosen for harvesting. The predicted mean critical wind speeds for the three scenarios after the thinning are very similar. However, the analysis for the distribution of critical wind speed classes shows that the scenario in which the tallest trees are removed from the stand creates the most vulnerable stand.

Chapter 5: Work from continental Europe suggests that irregular stand structures are more stable than regular ones. However, most evidence comes from post damage surveys, which brings some difficulties in interpretation.

The wind and tree interactions of nine trees were measured in two nearby locations. The stand at the two locations had the same overstorey crop but showed differences in the understorey. Due to silvicultural trials one location features an understorey, while the other does not. The direct comparison of the measured turning moment and the estimated critical wind speeds suggest that the overstorey trees benefit from the presence of an understorey in terms of wind loading and stability. This is supported by the analysis of wind profiles and turbulence characteristics which also suggests that more momentum is absorbed by the overstorey if no understorey is present.

Chapter 6: The final chapter summarises the results from the previous ones and

finishes with some recommendations for further work.

Appendix: The appendix consists of three parts. The first part describes the use and the calibration procedure for the strain transducers that were used to measure the turning moment. The two following parts describe the setup of the measuring system for the two field experiments.

References

Achim A, Ruel JC, and Gardiner BA, 2005: Evaluating the effect of precommercial thinning on the resistance of balsam fir to windthrow through experimentation, modelling, and development of simple indices. *Canadian Journal of Forest Research*, 35, 1844–1853.

Allen JRL, 1996: Windblown trees as a palaeoclimate indicator: The character and role of gusts. *Palaeogeography Palaeoclimatology Palaeoecology*, 121, 1–12.

Ancelin P, Courbaud B, and Fourcaud T, 2004: Development of an individual tree-based mechanical model to predict wind damage within forest stands. *Forest Ecology and Management*, 203, 101–121.

Bazzigher G and Schmid P, 1969: Sturmschäden und Fäule. *Schweizerische Zeitschrift für Forstwesen*, 10, 521–535.

Bergström H and Högström U, 1989: Turbulence exchange above a pine forest. *Boundary-Layer Meteorology*, 49, 231–263.

Björheden R, 2007: Possible effects of the hurricane Gudrun on the regional Swedish forest energy supply. *Biomass and Bioenergy*, 31, 617–622.

Bouget C and Duelli P, 2004: The effects of windthrow on forest insect communities: A literature review. *Biological Conservation*, 118, 281–299.

Byrne KE and Mitchell SJ, 2007: Overturning resistance of western redcedar and western hemlock in mixed-species stands in coastal British Columbia. *Canadian Journal of Forest Research*, 37, 931–939.

Cheng DL and Niklas KJ, 2007: Above- and below-ground biomass relationships across 1534 forested communities. *Annals of Botany*, 99, 95–102.

Collineau S and Brunet Y, 1993: Detection of turbulent coherent motions in a forest canopy Part I: Wavelet analysis. *Boundary-Layer Meteorology*, 65, 357–379.

Cremer KW, Borough CF, McKinnell FH, and Carter PR, 1982: Effects of stocking and thinning on wind damage in plantations. *New Zealand Journal of Forestry Science*, 12, 244–268.

Cremer KW, Myers BJ, van der Duys F, and Craig IE, 1977: Silvicultural lessons from the 1974 windthrow in radiata pine plantations near Canberra. *Australian Forestry*, 40, 274–292.

Cucchi V, Meredieu C, Stokes A, de Coligny F, Suárez J, and Gardiner BA, 2005: Modelling the windthrow risk for simulated stands of Maritime pine (*Pinus pinaster* Ait.). *Forest Ecology and Management*, 213, 184–196.

Dorman GE and Mollo-Christensen E, 1973: Observation of the structure on moving gust patterns over a water surface ('cat's paws'). *Journal of Physical Oceanography*, 3, 120–132.

Dunham R, Gardiner B, Quine C, and Suárez J, 2000: *ForestGALES - A PC-based wind risk model for British forests*. Forestry Commission, Edinburgh, UK.

ECE/FAO, 2000: Effects of the december 1999 storms on European timber markets. In *ECE/FAO Forest products annual market review, 1999-2000*. United Nations Publications.

Finnigan J, 1979: Turbulence in waving wheat I. Mean statistics and Honami. *Boundary-Layer Meteorology*, 16, 181–211.

Finnigan J and Brunet Y, 1995: Turbulent airflow in forests on flat and hilly terrain. In Coutts MP and Grace J, eds., *Wind and Trees*, chap. 1, pp. 3–40. Cambridge Univ. Press.

Flesch TK and Wilson JD, 1999: Wind and remnant tree sway in forest cutblocks. II. Relating measured tree sway to wind statistics. *Agricultural and Forest Meteorology*, 93, 243–258.

Gao W, Shaw RH, and Paw U KT, 1989: Observation of organized structure in turbulent flow within and above a forest canopy. *Boundary-Layer Meteorology*, 47, 349–377.

Gardiner B, Byrne K, Hale S, Kamimura K, Mitchell SJ, Peltola H, and Ruel JC, 2008: A review of mechanistic modelling of wind damage risk to forests. *Forestry*, 81, 447–463.

Gardiner B, Peltola H, and Kellomäki S, 2000: Comparison of two models for predicting the critical wind speeds required to damage coniferous trees. *Ecological Modelling*, 129, 1–23.

Gardiner BA, 1992: Mathematical modelling of the static and dynamic characteristics of plantation trees. In Franke J and Roeder A, eds., *Mathematical modelling of forest ecosystems*, pp. 40–61. J.D. Sauerländer's Verlag, Frankfurt a. M.

Gardiner BA, 1994: Wind and wind forces in a plantation spruce forest. *Boundary-Layer Meteorology*, 67, 161–186.

Gardiner BA, 1995: The interactions of wind and tree movement in forest canopies. In Coutts MP and Grace J, eds., *Wind and Trees*, chap. 2, pp. 41–59. Cambridge Univ. Press.

Gardiner BA and Quine CP, 1994: Wind damage to forests. *Biomimetics*, 2, 139–147.

Hale SE, Levy PE, and Gardiner BA, 2004: Trade-offs between seedling growth, thinning and stand stability in Sitka spruce stands: A modelling analysis. *Forest Ecology and Management*, 187, 105–115.

Inoue E, 1955: Studies of the phenomena of waving plants ('Honami') caused by wind. Part I. Mechanism and characteristics of waving plants phenomena. *Journal of Agricultural Meteorology*, 11, 18–22.

Irvine MR, Gardiner BA, and Hill MK, 1997: The evolution of turbulence across a forest edge. *Boundary-Layer Meteorology*, 84, 467–496.

Jaffe M, 1973: Thigmomorphogenesis: The response of plant growth and development to mechanical stimulation. *Planta*, 114, 143–157.

James JC, Grace J, and Hoad SP, 1994: Growth and photosynthesis of *Pinus sylvestris* at its altitudinal limit in Scotland. *The Journal of Ecology*, 82, 297–306.

Kamimura K and Shiraishi N, 2007: A review of strategies for wind damage assessment in Japanese forests. *Journal of Forest Research*, 12, 162–176.

Kerzenmacher T and Gardiner B, 1998: A mathematical model to describe the dynamic response of a spruce tree to the wind. *Trees*, 12, 385–394.

Knight T, 1803: Account of some experiments on the descent of sap in trees. *Philosophical Transactions of the Royal Society of London*, 4, 277–289.

de Langre E, 2008: Effects of wind on plants. *Annual Review of Fluid Mechanics*, 40, 141–168.

Lanquaye-Opoku N and Mitchell SJ, 2005: Portability of stand-level empirical windthrow risk models. *Forest Ecology and Management*, 216, 134–148.

Marshall B, 1998: *Wind flow structures and wind forces in forests*. Ph.D. thesis, Jesus College, University of Oxford.

Marshall BJ, Wood CJ, Gardiner BA, and Belcher RE, 2002: Conditional sampling of forest canopy gusts. *Boundary-Layer Meteorology*, 102, 225–251.

Mason WL, 2002: Are irregular stands more windfirm? *Forestry*, 75, 347–355.

Mason WL and Kerr G, 2004: Transforming even-aged conifer stands to continuous cover management. Information Note 40, Forestry Commission, Edinburgh.

Mason WL and Quine CP, 1995: Silvicultural possibilities for increasing structural diversity in British spruce forests: The case of Kielder forest. *Forest Ecology and Management*, 79, 13–28.

Mayer H, 1987: Wind-induced tree sways. *Trees*, 1, 195–206.

Mayhead GJ, 1973: Some drag coefficients for British forest trees derived from wind-tunnel studies. *Agricultural Meteorology*, 12, 123–130.

Metzger C, 1893: Der Wind als maßgebender Faktor für das Wachstum der Bäume. *Mündener Forstliche Hefte*, 3, 35–86.

Miller KF, 1985: Windthrow hazard classification. Leaflet 85, Forestry Commission.

Milne R, 1991: Dynamics of swaying of *Picea sitchensis*. *Tree Physiology*, 9, 383–399.

Mitchell SJ, 1995: The windthrow triangle: A relative windthrow hazard assessment procedure for forest managers. *The Forestry Chronicle*, 71, 446–450.

Mitchell SJ, Hailemariam T, and Kulis Y, 2001: Empirical modeling of cutblock edge windthrow risk on Vancouver Island, Canada, using stand level information. *Forest Ecology and Management*, 154, 117–130.

Mitscherlich G, 1974: Sturmgefahr und Sturmsicherung. *Schweizerische Zeitschrift für Forstwesen*, 125, 199–216.

Moore J and Quine CP, 2000: A comparison of the relative risk of wind damage to planted forests in Border Forest Park, Great Britain, and the Central North Island, New Zealand. *Forest Ecology and Management*, 135, 345–353.

Moore JR, 2002: *Mechanical behaviour of coniferous trees subjected to wind loading*. Ph.D. thesis, Oregon State University, Corvallis.

Moore JR and Maguire DA, 2004: Natural sway frequencies and damping ratios of trees: Concepts, review and synthesis of previous studies. *Trees*, 18, 195–203.

Morse AP, Gardiner BA, and Marshall BJ, 2002: Mechanisms controlling turbulence development across a forest edge. *Boundary-Layer Meteorology*, 103, 227–251.

Nicoll B and Ray D, 1996: Adaptive growth of tree root systems in response to wind action and site conditions. *Tree Physiology*, 16, 891–898.

Nicoll BC, Achim A, Mochan S, and Gardiner BA, 2005: Does steep terrain influence tree stability? A field investigation. *Canadian Journal of Forest Research*, 35, 2360–2367.

Nicoll BC, Berthier S, Achim A, Gouskou K, Danjon F, and van Beek LPH, 2006a: The architecture of *Picea sitchensis* structural root systems on horizontal and sloping terrain. *Trees*, 20, 701–712.

Nicoll BC, Gardiner BA, Rayner B, and Peace AJ, 2006b: Anchorage of coniferous trees in relation to species, soil type, and rooting depth. *Canadian Journal of Forest Research*, 36, 1871–1883.

Oliver H and Mayhead GJ, 1974: Wind measurements in a pine forest during a destructive gale. *Forestry*, 47, 185–195.

O'Sullivan M and Ritchie R, 1993: Tree stability in relation to cyclic loading. *Forestry*, 66, 69–82.

Peltola H, 1996a: Model computations on wind flow and turning moment by wind for Scots pines along the margins of clear-cut areas. *Forest Ecology and Management*, 83, 203–215.

Peltola H, 1996b: Swaying of trees in response to wind and thinning in a stand of Scots pine. *Boundary-Layer Meteorology*, 77, 285–304.

Peltola H and Kellomäki S, 1993: A mechanistic model for calculating windthrow and stem breakage of Scots pines at stand edge. *Silva Fennica*, 27, 99–111.

Py C, de Langre E, and Moulia B, 2006: A frequency lock-in mechanism in the interaction between wind and crop canopies. *Journal of Fluid Mechanics*, 568, 425–449.

Py C, de Langre E, Moulia B, and Hémon P, 2005: Measurement of wind-induced motion of crop canopies from digital video images. *Agricultural and Forest Meteorology*, 130, 223–236.

Quine C, Coutts M, Gardiner B, and Pyatt G, 1995: *Forests and wind: Management to minimize damage*. Forestry Commission Bulletin. HMSO, London UK.

Quine CP, 2001: A preliminary survey of regeneration of Sitka spruce in wind-formed gaps in British planted forests. *Forest Ecology and Management*, 151, 37–42.

Raupach MR, Finnigan JJ, and Brunet Y, 1996: Coherent eddies and turbulence in vegetation canopies: The mixing-layer analogy. *Boundary-Layer Meteorology*, 78, 351–382.

Ray D and Nicoll BC, 1998: The effect of soil water-table depth on root-plate development and stability of Sitka spruce. *Forestry*, 71, 169–182.

Rees D and Grace J, 1980: The effects of shaking on extension growth of *Pinus contorta* Douglas. *Forestry*, 53, 155–166.

Rollinson TJD, 1987: Thinning control of conifer plantations in Great Britain. *Annals of Forest Science*, 44, 25–34.

Rudnicki M, Mitchell SJ, and Novak MD, 2004: Wind tunnel measurements of crown streamlining and drag relationships for three conifer species. *Canadian Journal of Forest Research*, 34, 666–676.

Ruel JC, Larouche C, and Achim A, 2003: Changes in root morphology after precommercial thinning in balsam fir stands. *Canadian Journal of Forest Research*, 33, 2452–2459.

Ruel JC and Pineau M, 2002: Windthrow as an important process for white spruce regeneration. *The Forestry Chronicle*, 78, 732–738.

Ruel JC, Quine C, Meunier S, and Suárez J, 2000: Estimating windthrow risk in balsam fir stands with the ForestGALES model. *The Forestry Chronicle*, 76, 329–337.

Scannell B, 1984: *Quantification of the interactive motions of the atmospheric surface layer and a conifer canopy*. Ph.D. thesis, Cranfield Institute of Technology, Bedford.

Schelhaas M, Kramer K, Peltola H, van der Werf D, and Wijdeven S, 2007: Introducing tree interactions in wind damage simulation. *Ecological Modelling*, 207, 197–209.

Schütz JP, 2001: Opportunities and strategies of transforming regular forests to irregular forests. *Forest Ecology and Management*, 151, 87–94.

Sellier D and Fourcaud T, 2005: A mechanical analysis of the relationship between free oscillations of *Pinus pinaster* Ait. saplings and their aerial architecture. *Journal of Experimental Botany*, 56, 1563–1573.

Shaw RH, Brunet Y, Finnigan JJ, and Raupach MR, 1995: A wind tunnel study of air flow in waving wheat: Two-point velocity statistics. *Boundary-Layer Meteorology*, 76, 349–376.

Shaw RH, Paw U KT, and Gao W, 1989: Detection of temperature ramps and flow structures at a deciduous forest site. *Agricultural and Forest Meteorology*, 47, 123–138.

Somerville A, 1980: Wind stability: Forest layout and silviculture. *New Zealand Journal of Forest Science*, 10, 476–501.

Stokes A, Nicoll B, Coutts M, and Fitter A, 1997: Responses of young Sitka spruce clones to mechanical perturbation and nutrition: Effects on biomass allocation, root development, and resistance to bending. *Canadian Journal of Forest Research*, 27, 1049–1057.

Telewski F, 1995: Wind-induced physiological and developmental responses in trees. In Coutts MP and Grace J, eds., *Wind and Trees*, chap. 14, pp. 237–263. Cambridge Univ. Press, Cambridge.

Thom AS, 1971: Momentum absorption by vegetation. *Quarterly Journal of the Royal Meteorological Society*, 97, 414–428.

Troen I and Petersen E, 1989: *European Wind Atlas*. Risø National Laboratory, Roskilde.

Urban ST, Lieffers VJ, and MacDonald SE, 1994: Release in radial growth in the trunk and structural roots of white spruce as measured by dendrochronology. *Canadian Journal of Forest Research*, 24, 1550–1556.

Yang B, Morse AP, Shaw RH, and Paw U KT, 2006: Large-eddy simulation of turbulent flow across a forest edge. Part II: Momentum and turbulent kinetic energy budgets. *Boundary-Layer Meteorology*, 121, 433–457.

Chapter 2

Validation of the ForestGALES model for a mature Sitka spruce forest

Abstract

ForestGALES is a decision support tool developed for the purpose of estimating the risk of wind damage in British forest plantations. Since the main species in British plantations is Sitka spruce and the traditional management is based on clearfelling/restocking, the model focuses on regular coniferous stand structures. With the increasing use of irregular silviculture systems in British forestry the model needs to be tested for such systems.

The performance of several modules of ForestGALES was tested using the data from a field experiment in a mature Sitka spruce plantation, for which ForestGALES predicts a return period for wind damage of one year. Since the stand withstood several gale events over the last several years the prediction seems to be too pessimistic.

The comparison of the measured experienced turning moments of nine trees revealed, that the wind energy was not distributed equally among the individuals, which is one of the main assumptions in the model. Dominant individuals were more exposed and experienced higher turning moments at the tree base than smaller trees. At the same time they create a sheltered environment for the smaller trees in their surrounding.

The incorrect estimate of the critical wind speed for the stand seemed to be caused by the assumption that members of the stand share the same properties. Although the experimental stand was regularly structured, it contained enough internal variability to invalidate this assumption from an aerodynamic point of view. The estimate of the wind climate is also too pessimistic, which results in a too pessimistic estimate of the likelihood of wind damage for the stand.

2.1 Introduction

Wind damage in forest plantations causes severe economic loss all over the world (Mitchell, 1995). Since Britain suffers from a more severe wind climate than many other parts of the world (Troen and Petersen, 1989), there have been many efforts in Britain to understand the principles that govern the wind and tree/stand-interaction (Fraser, 1964; Busby, 1965; Mayhead, 1973a,b; Miller, 1985). All the knowledge that has been gathered over more than four decades has been implemented into the PC based ForestGALES model. ForestGALES is a decision support tool to calculate the risk of wind damage for British forest stands (Gardiner et al., 2004, 2008). The model assists foresters to estimate the impact of their management on the stability of a stand. The model has been adapted for Canada, New Zealand, France, and Japan (Ruel et al., 2000; Moore and Quine, 2000; Cucchi et al., 2005; Kamimura and Shiraishi, 2007).

ForestGALES was designed for even-aged regularly structured mono-species plantations. Its equations were derived from tree pulling tests (Nicoll et al., 2006), field experiments (Gardiner, 1994, 1995), and wind tunnel studies (Gardiner et al., 1997, 2005). A comparison with the HWIND model showed good agreement between the two models (Peltola et al., 1997; Gardiner et al., 2000). However, there has been no systematic validation of the several modules with data from a single field experiment so far.

Here the data from a field study, in which experienced turning moments and wind parameters in an even-aged Sitka spruce plantation were simultaneously measured, are used to independently validate some of the modules of Forest-GALES.

2.2 The ForestGALES model

2.2.1 General

ForestGALES is a PC-based wind risk model for British forests (Dunham et al., 2000; Gardiner et al., 2004). It replaced the wind hazard classification (WHC), a scoring system which had been in use since the mid eighties (Miller, 1985). The WHC comprises soil and windiness information to classify stands into six risk classes. The shortcomings of this scoring system are that it lacks objectivity and is not able to predict either the timing or amount of damage

(Quine and Bell, 1998). Furthermore it does not account for species differences, site cultivation, or silviculture. Since the initial development of the WHC, the understanding of wind damage has improved and since the design of the WHC did not allow the implementation of this knowledge, it became necessary to follow a new approach.

Development and improvement of ForestGALES is still in process. For Version 2.0 the wind climate module was revised, since it turned out to be too pessimistic (Gardiner et al., 2004). Since then, only minor modifications were implemented in the 2006 release (Version 2.1). The main modules of the model are the:

- tree characteristics and mechanics module,
- wind module, and
- wind climate module.

ForestGALES is configured for British conditions. Hence the focus is on the risk estimation for regular even-aged plantations, which is the most common stand type in Britain. Thus the model is still awaiting the implementation of mixed-species and irregular stands to make it work with more complex silviculture systems (such as single tree selection, shelterwood, group selection).

2.2.2 Resistive moments

Whether a tree fails during a gale or not depends on the relationship between wind-induced turning moment, the tree's stiffness and its anchorage. As soon as the wind-imposed turning moment exceeds either the critical breaking or the overturning moment the tree snaps or overturns, respectively. The trees breaking moment (M_{break} in Nm) is calculated from the tree properties as:

$$M_{break} = \frac{\pi}{32} \cdot f_{knot} \cdot MOR \cdot dbh^3 \tag{2.1}$$

where MOR (Pa) is the modulus of rupture, f_{knot} $(-)$ is an empirical factor for taking the effect of knots into account, and dbh (m) is the tree diameter at breast height (1.3 m).

The overturning moment (M_{over} in Nm) is calculated using a linear relationship:

$$M_{over} = c_{reg} \cdot SW \tag{2.2}$$

where SW (kg) is the tree's stem fresh weight and c_{reg} ($\mathrm{N\,m\,kg^{-1}}$) is an empirical species, soil and rooting depth specific regression coefficient, estimated from more than 2000 treepulling tests (Nicoll et al., 2006).

2.2.3 Wind loading

Roughness method

Two different approaches have been used in wind risk models to calculate the wind loading on trees. The first approach is known as the *wind profile method* and is for example used in the HWIND model (Peltola and Kellomäki, 1993; Peltola et al., 1999). This approach integrates the drag over the canopy height from the wind profile and crown properties. The second approach is the *roughness method*, which is used in ForestGALES and described in more detail below.

Two layers of air moving with different speed create shear stress (τ in $\mathrm{N\,m^{-2}}$). The shear stress is related to momentum flux ($\overline{u'\,w'}$) and can be calculated from turbulence time series as:

$$\tau = \rho \cdot \overline{u'\,w'} \tag{2.3}$$

where u' and w' are the instantaneous deviations from the mean horizontal ($\overline{u}$) and vertical ($\overline{w}$) wind speed and $\overline{u'\,w'}$ is the covariance.

At the forest edge the turbulence characteristics are very different from those several tree heights inside the forest stand. It takes several tree heights before the turbulence has adapted to the underlying surface and steady state conditions are reached (Yang et al., 2006; Dupont and Brunet, 2008). From wind tunnel experiments Morse et al. (2002) found that by a distance of 14.5 tree heights inside the forest the turbulence has adjusted up to twice the canopy height. In the ForestGALES model edge effects are neglected after a distance of 10 tree heights or more downwind of the edge.

The shear stress is apportioned equally onto the individual trees of the stand, so that when D (m) is the average spacing, each tree has to withstand an average shear of $\tau \cdot D^2$ (Raupach, 1994). After Thom (1971) the force can be treated as

if it was acting at the height of the zero-plane displacement (d). Therefore the mean turning moment (M_{mean} in Nm) a tree has to withstand can be calculated as:

$$M_{mean} = \tau \cdot d \cdot D^2 \tag{2.4}$$

Above the zero-plane displacement (d) a logarithmic wind profile for a neutrally layered atmosphere is assumed:

$$u(z) = \frac{u_*}{k} \cdot ln\left(\frac{z-d}{z_0}\right) \tag{2.5}$$

where u ($\mathrm{m\,s^{-1}}$) is horizontal wind speed, u_* ($\mathrm{m\,s^{-1}}$) is friction velocity above the canopy, k (0.4) is the dimensionless Von Karman constant, d (m) is the zero plane displacement, and z_0 (m) is roughness length. The values for d and z_0 are a function of the area index of the canopy, which is related to the leaf area index (Raupach, 1994). Friction velocity is related to shear stress as:

$$\tau = -\rho \cdot u_*^2 \tag{2.6}$$

where ρ ($1.226\,\mathrm{kg\,m^{-3}}$) is air density.

Gustiness

Turbulence above plant canopies shows the characteristics of a mixing layer rather than those of a boundary layer (Raupach et al., 1996). Among other attributes, the mixing layer is defined by coherent structures, which establish from Helmholtz instabilities and dominate the exchange of scalars and momentum transport between the biosphere and the atmosphere (Green et al., 1995; Kruijt et al., 2000). Gardiner (1994) used the variable interval time averaging (VITA) technique to show that the appearance of those structures coincides with peaks in time series of turning moment.

It is believed that trees are adapted to the mean wind speed but get damaged by maximum wind speeds occurring during gust events. Taking this into account is done by implementing a scaling factor called gust factor (GF). This factor is defined as fraction of maximum to mean turning moment:

$$GF = \frac{M_{max}}{M_{mean}} \tag{2.7}$$

The independent variables to calculate the GF in ForestGALES are spacing, tree height, and distance to edge:

$$GF = f(\text{spacing, tree height, distance from edge}) \tag{2.8}$$

For trees that are far enough from the edge ForestGALES estimates the factor to be in the range of 10 to 12 (Gardiner, 1994). The equations for calculating the gust factor were derived mainly from wind tunnel studies (Gardiner et al., 1997).

Critical wind speed

The wind speeds for breaking ($u(h_C)_{break}$) and overturning ($u(h_C)_{over}$) are calculated by inserting the equations for the resistive moments into the wind profile equation. h_C is the height of the canopy top. The two resulting equations are (Gardiner et al., 2000):

$$u(h_C)_{break} = \frac{1}{k \cdot D} \left(\frac{\pi \cdot MOR \cdot dbh^3}{\rho \cdot 32 \cdot GF \cdot (d - 1.3)} \right)^{\frac{1}{2}} \cdot \left(\frac{f_{knot}}{f_{edge} \cdot f_{CW}} \right)^{\frac{1}{2}} \cdot ln \left(\frac{h - d}{z_0} \right) \tag{2.9}$$

$$u(h_C)_{over} = \frac{1}{k \cdot D} \left(\frac{c_{reg} \cdot dbh^2 \cdot h}{\rho \cdot GF \cdot d} \right)^{\frac{1}{2}} \cdot \left(\frac{1}{f_{edge} \cdot f_{CW}} \right)^{\frac{1}{2}} \cdot ln \left(\frac{h - d}{z_0} \right) \tag{2.10}$$

where f_{edge}, and f_{CW} are parameters that take the position relative to the stand edge and the additional turning moment due to overhanging crown mass into consideration.

The results are scaled to 10 m above the zero plane displacement plus the roughness length ($d + z_0$) in the forest. The wind speed values can then be related to the conditions of the weather stations of the Meteorological Office using DAMS.

2.2.4 Wind climate

Calculating the return period for a certain wind speed requires information on the wind climate (wind speed distribution) of the site. The ForestGALES model uses DAMS (**D**etailed **A**spect **M**ethod of **S**coring) to calculate the two parameters of a Weibull distribution for hourly mean wind speed (Bell et al., 1995). DAMS is calculated from site information such as elevation, topographic exposure, aspect, funnelling effects, and general wind zone based on the analysis of long term tatter flag measurements at more than 1,000 locations (Quine and White, 1994). The score is available for Britain on a 50×50 m grid resolution. The method was validated against wind speed data from six 10 m masts in complex terrain and compared with two airflow models (WAsP and MS–Micro/3). The good agreement of the different methods underlines the aptitude of this approach (Suárez et al., 1999). The shape parameter (γ) is assumed to be constant for the whole of Britain (1.85). The second parameter (α), called the scale parameter, is calculated using an empirical linear regression equation, which was derived from long term wind speed measurements (Quine, 2000).

The probability density function (*pdf*) and the cumulative distribution function (*cdf*) of the Weibull distribution are defined as:

$$pdf(u) = \frac{\gamma}{\alpha} \cdot \left(\frac{u}{\alpha}\right)^{(\gamma-1)} \cdot e^{-(\frac{u}{\alpha})^{\gamma}} \quad u \in [0; +\infty] \tag{2.11}$$

$$cdf(u) = 1 - e^{-(\frac{u}{\alpha})^{\gamma}} \tag{2.12}$$

where γ $(-)$ defines the shape and α $(-)$ the scale of the distribution. The number of hours per year that exceed a specific value can be calculated as:

$$n(u) = (1 - cdf(u)) \cdot 365.25 \cdot 24 \tag{2.13}$$

and the return period ($rp(u)$) is defined as the reciprocal ($rp(u) = n(u)^{-1}$).

2.3 Material and methods

2.3.1 Experimental site

The study site was located in Clocaenog Forest, North Wales (53°04′N, 3°35′W). The site is located on a gentle slope facing south (2 %-5 %) about 400 m above sea level. Mean annual precipitation exceeds 1300 mm. The soil type is an intergrade iron pan and the surface is uneven due to the ploughing. The rooting depth is 50 cm.

The light regime on the forest floor is good enough to allow ample natural regeneration to be recruited, which was at the time of the experiment about 10 years old. Seedling growth beneath a canopy is a precondition for a successful implementation of continuous cover forestry (CCF) (Hale et al., 2004). Therefore the stand can be described as a stand in transformation towards CCF (Pommerening and Murphy, 2004; Mason and Kerr, 2004).

The silviculture history of the site is not known in detail. It is suggested that the site was originally heather moor, ploughed to a depth of 15 to 20 cm, and was planted at 5′ × 5′ spacing as a 2/1 or 2/2 row mixture of Sitka spruce (*Picea sitchensis* (Bong.) Carr.) and Scots pine (*Pinus sylvestris* L.) or lodgepole pine (*Pinus contorta* Dougl. ex Loud.) in the years 1948 and 1951. Today the stand is pure Sitka spruce with a density of 292 trees ha^{-1}. The stand had a line thinning in the 1970s, followed by a selective thinning in 1993 (removing 80 to 100 $m^3\,ha^{-1}$) and another selective thinning in 1999/2000 (removing 100 to 120 $m^3\,ha^{-1}$).

The critical hourly mean wind speed for wind damage, as calculated by the ForestGALES model is 14 $m\,s^{-1}$, which corresponds to a return period of less than one year according to the modelled wind climate. However, there are no signs of wind damage and the fact that the last note on wind damage is dated back to 1997, demonstrates that the stand is more stable than anticipated. Since the stand has already passed its rotation period and since the risk of wind damage is considered very high, the suggested best practise would be clear felling of the stand (Miller, 1985).

The study site is part of a silviculture project of the Forestry Commission Wales and the University of Wales, Bangor, monitoring the transformation of plantations to irregular stands. Within this project mensurational and positional data for all trees in the plot (1 ha size) are available for the year 2002.

Table 2.1: Stand characteristics for the experimental stand in Clocaenog Forest. For further details see text. (*dbh*: diameter at breast height, DAMS: Detailed Aspect Method of Scoring, WHC: wind hazard classification score; tree measurements were taken in 2002)

Species	Sitka spruce
Planting year	1951
Density	292 trees ha^{-1}
mean *dbh*	35.8 cm
mean height	26.7 m
Top height	28.4 m
Basal area	30.8 m^2 ha^{-1}
Volume	400 m^3 ha^{-1}
Yield class	20
DAMS	20
WHC	2

2.3.2 Experimental trees

Nine trees in the plot were chosen as experimental trees (see Fig. 2.1). Those trees were located in the north-east corner of the experimental plot and approximately arranged in a 3×3 array. The individual tree properties cover a wide range. Height for the nine trees is in the range of 22.8 to 31.9 m and the diameter at breast height (*dbh*) is in the range 28.5 to 59.8 cm. The values for the nine experimental trees are summarised in Table 2.2.

Table 2.2: Mensurational data for the nine experimental trees (h: tree height, *dbh*: diameter at breast height; measurements were taken in 2005).

ID	h (m)	*dbh* (cm)
4	29.6	59.8
37	31.1	42.2
38	27.3	38.9
39	26.9	35.4
40	28.0	37.6
41	24.1	31.8
42	22.8	28.5
43	30.5	47.2
80	31.9	54.5

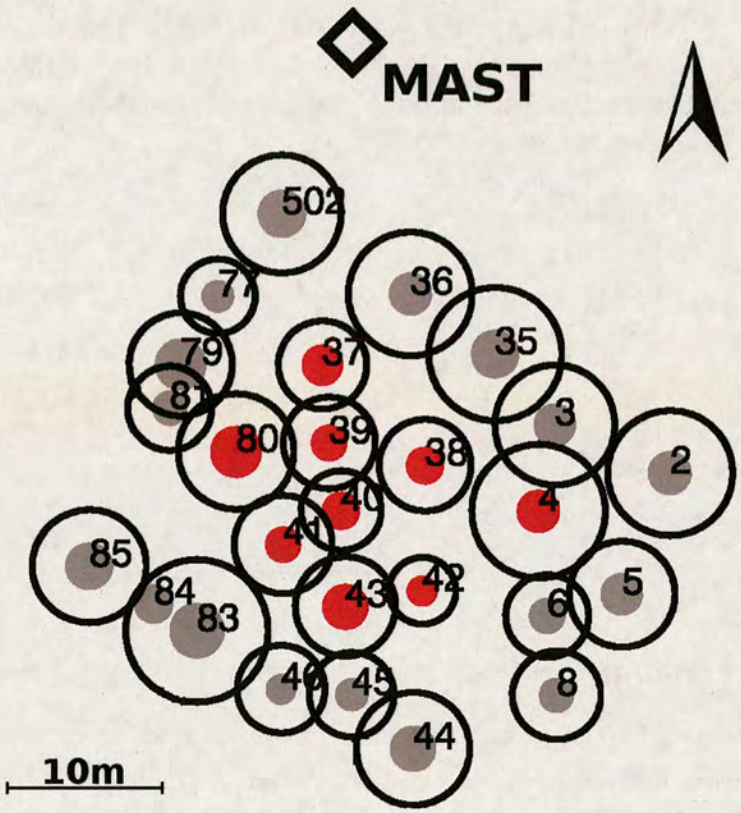

Figure 2.1: Detailed sitemap showing the nine experimental trees (red dots) and their direct neighbours (grey dots). Black circles represent the average crown radii. The meteorological mast was located within the forest stand. Since the experiment was located at the edge of the experimental plot the positions of those trees in proximity of the mast were not measured.

2.3.3 Strain transducers

The turning moments, which the nine experimental trees experience, were measured using strain gauges. These were glued onto strain transducers of the type designed by Guy Blackburn during his PhD project at the Northern Research Station (Blackburn, 1997). A more detailed description of the design and the overall performance of the sensors can be found in Moore et al. (2005). Every experimental tree was equipped with two strain transducers, which were screwed perpendicularly into the tree at about 1.3 m.

Strain gauges change their resistance when the strain transducer is squeezed or pulled as it happens when the tree sways. Because the changes in resistance are very small, the transducers were incorporated into a Wheatstone bridge to obtain a satisfactory resolution.

The signal outputs of the strain transducers were measured with three CR10 data loggers (Campbell Scientific, Logan, US) with a time resolution of 4 Hz. Each CR10 logged six strain transducers. All data loggers were part of a RS485-network. An industrial computer running LOGGERNET software (Version 2.1, Campbell Scientific) was also part of the network and stored all data, which were gathered by the data loggers, as plain text files (ASCII).

Each strain transducer was calibrated individually, by stepwise pulling the trees into two directions with a hand winch (Lugall 4000-20SH-UK, METRELL, UK) while measuring the applied force with a S-type load cell (Model 616, Tedea Huntleigh, US). The relationship between strain transducer signal and applied turning moment was linear.

The whole system was too power demanding to run it permanently. Therefore it was switched on manually when a gale was approaching based on the weather forecast. In total more than 400 hours of data were gathered during the time period May to November 2005.

Strain data analysis

The strain transducers respond to changes in air temperature and tree growth. However, the time scale of the temperature induced signal changes is very long compared to the signal from the tree swaying. Because all of the analysis was carried out at time intervals not longer than 60 minutes, linear detrending of the raw signal is assumed to be appropriate to remove this background trend. For every time interval the offset is also removed. The offset was defined as the most frequently occurring value estimated from a histogram analysis. In the final step the individual calibration coefficients were applied to the raw data.

2.3.4 Wind measurements

A 30 m mast (TallTower, NRG Systems, US) was erected in the forest stand in August 2004. The mast was equipped with eight cup anemometers (NRG♯40, NRG Systems, US; heights (m): 5, 10, 15, 18, 21, 24, 27, 30.8) and two wind vanes (NRG♯200P, NRG Systems, US; heights (m): 15, 27). The four upper cup anemometers and the wind vanes were logged every three seconds (0.33 Hz). The lower four anemometers were logged once every minute.

For the second half of the field experiment (from the 23rd of August 2005) data from an Ultra-Sonic anemometer (USA-1, METEK GmbH, Germany), which

was mounted at 29.8 m height, are available. The data from the sonic were streamed to a serial port of the industrial PC and stored in hourly files using the manufacturer's software (tcopy.exe). The measurement time resolution of the sonic anemometer was set to 10 Hz.

A 10 m mast equipped with a single cup anemometer (A100R, Vector Instruments, Rhyl, UK) and a wind vane (A200P, Vector Instruments, Rhyl, UK) was erected on a clear felled site (53°03′N, 3°28′W) about 3.5 km away from the 30 m mast (see Fig. 2.2). For every hour average wind speed, average wind direction, 3 s maximum wind speed (gust speed) and corresponding wind direction was logged. Data are available for the time period May 2004 until February 2006.

Figure 2.2: Contour map (10 km × 10 km) showing the area around the experimental site and the 10 m mast. Isolines are in 20 m elevation steps.

2.3.5 Wind climate

The wind speed distribution at the site was estimated using the wind data from the 10 m mast and an approximately 15 year long time series from the Meteorological Office station in Rhyl (UK Meteorological Office, 2006). The method used to lengthen the time series from the 10 m mast was the standard *Measure-Correlate-Predict* (MCP) analysis (Derrick, 1992). The concurrent hourly data from the two sites were used for 30 ° sectorwise linear regression analysis. The sector-specific regression coefficients were applied to create an

extended time series for the Clocaenog site. The time series from Rhyl covers the time period 1st of February 1992 until 30th of June 2007. Data availability for this period is 97 %. The overall coefficient of correlation for the overlapping time interval is 0.76. The wind speed distribution of the extended time series is plotted in Figure 2.3.

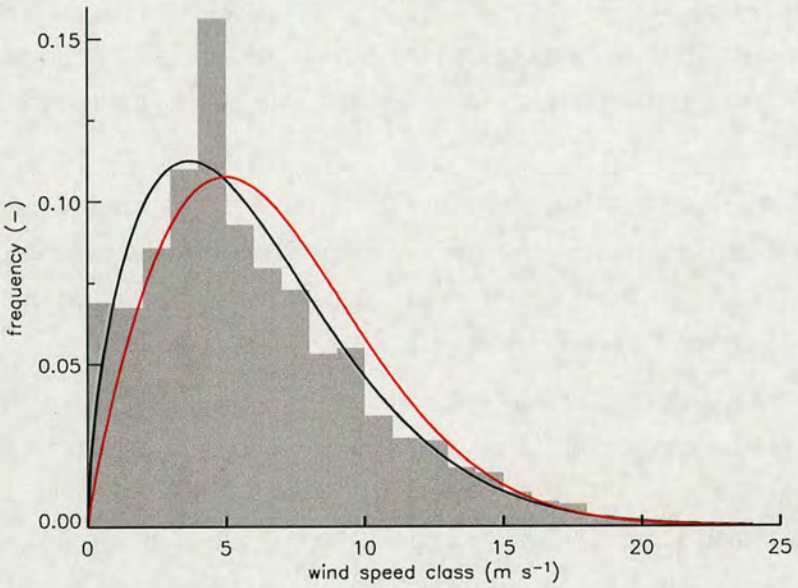

Figure 2.3: Estimated hourly mean wind speed distribution at the 10 m mast in Clocaenog Forest (grey bars; bin size $1\,\mathrm{m\,s^{-1}}$) and fitted Weibull distribution (black line, $\alpha = 1.60$, $\gamma = 6.77$). The red line is the Weibull distribution from the ForestGALES model using DAMS ($\alpha = 1.85$, $\gamma = 7.60$).

2.3.6 Gale events

Since the start of the field experiment in 2005 the stand got hit by two notable gale events. On the 8th of January 2005 the hourly mean wind speed measured at the 10 m mast reached $16.2\,\mathrm{m\,s^{-1}}$. For the same hour the maximum gust speed was $27.0\,\mathrm{m\,s^{-1}}$. This storm event was named *Gudrun* by the Norway weather service and caused severe wind damage in Scandinavian countries. For Sweden the amount of thrown or damaged timber was estimated to be approximately 75 million cubic meter, which equals about the annual harvest of the country (SMHI, 2005).

Another severe storm, which was named *Kyrill* by the German Weather

Service (DWD), took place on the 18th of January 2007. At this time the 10 m mast had already been dismantled. However, at the Meteorological Office weather station in Rhyl higher wind speeds compared to the event in 2005 were recorded. The station recorded 17.8 m s^{-1} and 36.0 m s^{-1} as hourly wind speed and maximum gust speed, respectively. Therefore it is likely that the wind speed in Clocaenog was also higher compared to the 2005 event. In comparison to *Gudrun* the track of the low pressure field passed further south and therefore the main damage during *Kyrill* occurred in central Europe. In most northern federal states of Germany the damage exceeded the one of the *Lothar* storm in 1999 (EFI, 2007).

The two graphs in Figure 2.4 show the time series of wind speed, direction, and air pressure at sea level for the two gale events. In the experimental stand (including the buffer zone) only 1.25 trees ha^{-1} were overturned in the 2007 event (Jens Haufe, personal communication).

From the regression analysis of hourly wind speed data between the 10 m and the 30 m mast, it is possible to estimate the wind speed at the experimental plot for the two gale events. The cup anemometer at 30.8 m is the one closest to the height for which ForestGALES estimates the critical wind speed ($d + z_0$). The analysis showed that the wind direction has a significant impact on the slope of the regression line. Therefore only data points that fall within the wind sector 225 ° to 270 ° are used (see Fig. 2.5), which covers the wind direction of the peak wind speeds for the two gale events. The estimated wind speeds at 30.8 m in the stand for the two events are 11.1 m s^{-1} (*Kyrill*) and 12.2 m s^{-1} (*Gudrun*). Neither of the two values exceeds the one predicted by ForestGALES.

2.3.7 Model validation

The measurements made in this field study enabled the testing of several assumptions of the ForestGALES model regarding the stand characteristics, gust factor, wind loading, and wind climate. The impact of the uncertainties of the different modules on the models output is discussed.

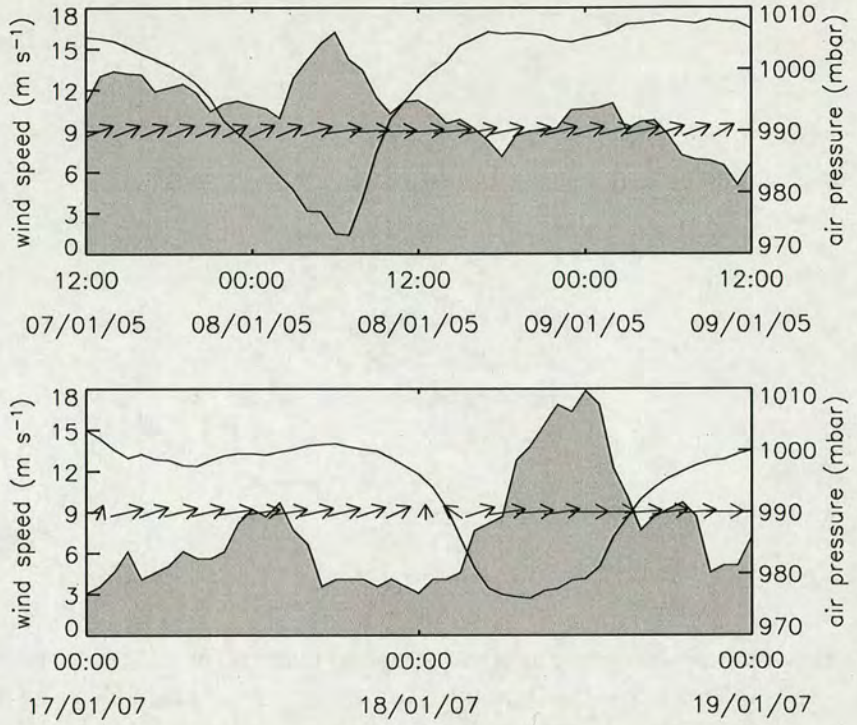

Figure 2.4: Time series of hourly mean wind speed (filled area), wind direction (arrows), and atmospheric air pressure at sea level (line) for the storm events *Gudrun* (8.Jan.2005) and *Kyrill* (17.Jan.2007). The wind data from the first event were measured at the 10 m mast in Clocaenog Forest. For the second event the original wind speed data from the Meteorological Office weather station Rhyl (53°03′N, 3°28′W) were used, because the mast in Clocaenog Forest had already been dismantled. Air pressure data for both events are taken from the Rhyl station.

2.4 Results

2.4.1 Stand and tree characteristics

In the ForestGALES model mean height is calculated from stand top height, because of the wider availability of this parameter in British forestry (Edwards and Christie, 1981). Top height (h_{100}) is defined as the mean height of the 100 largest trees in the stand, where the term largest relates to the *dbh*. For Sitka spruce the regression is:

$$h_{mean} = h_{100} \cdot 1.0467 - 2.1452 \tag{2.14}$$

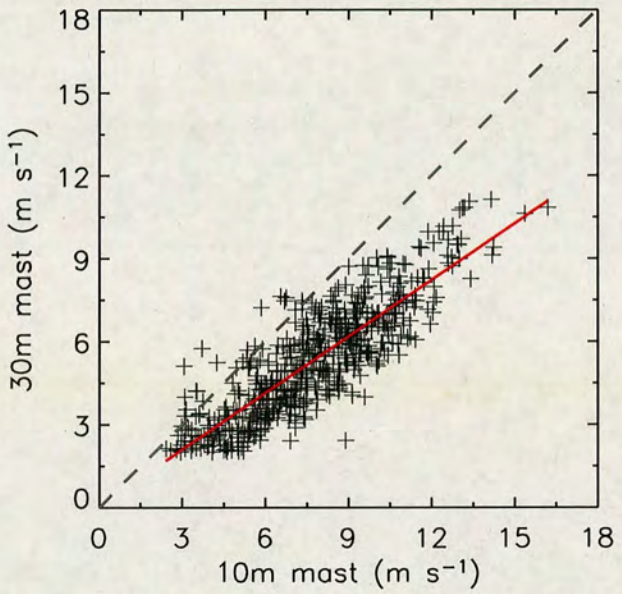

Figure 2.5: Scatter plot of hourly mean wind speed at the 30 m mast (cup anemometer at 30.8 m) plotted versus the 10 m mast. Only data values for the wind sector [225:270] degrees were used ($f(x) = x \cdot 0.68 + 0.05$, $R^2 = 0.85$, $SE = 1.1$, $n = 539$).

Figure 2.6 shows the distributions of tree height and *dbh*. Top and mean height are 28.5 m and 26.8 m, respectively. The calculated value using the above regression results in a value for mean height of 27.7 m, which is 0.9 m taller than the measurements. The overestimation of mean height results in an overestimation of the zero plane displacement and stem weight. The first results in a longer cantilever arm for the acting wind force, which itself increases the turning moment at the tree base. The second factor counteracts this effect. A taller tree has a higher value of stem weight and therefore an increased resistance to overturning.

2.4.2 Gust factor

The comparison of two wind risk models by Gardiner et al. (2000) revealed that the gust factor (GF) is a parameter to which the ForestGALES model is very sensitive to. Therefore an accurate estimation of this parameter is crucial for the performance of the model. The GFs were calculated from 10 min time series as ratios of maximum to mean value of measured turning moment. In Figure 2.7 the measured GFs are plotted versus the 10 min mean wind speed at 30.8 m height.

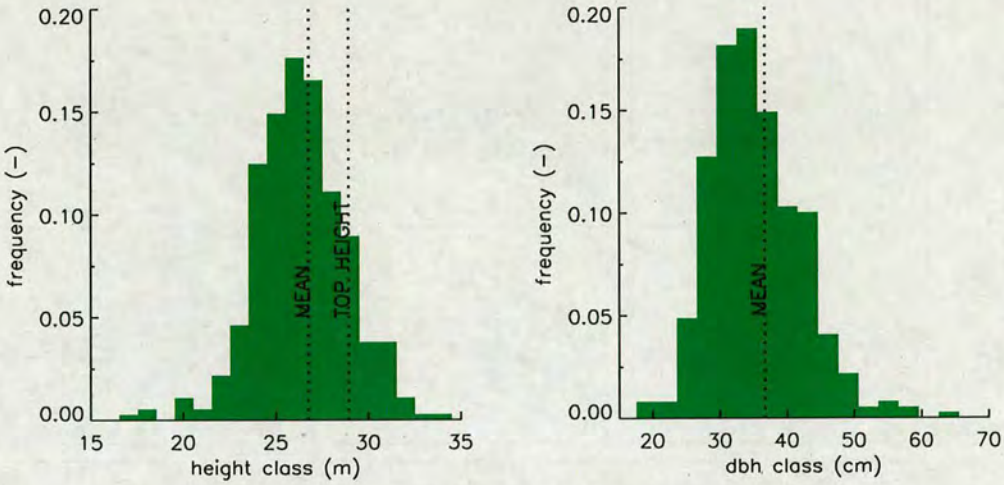

Figure 2.6: Frequency distributions of tree height (1 m bin size) and dbh (3 cm bin size) for the experimental stand in Clocaenog Forest. Total number of trees in the stand was 292.

The value for GF calculated by ForestGALES (using Eq. 2.8) is 10.1, based on average spacing, measured tree height (from Eq. 2.14) and assuming that edge effects are negligible.

All of the nine plots show large scatter. And although some data points exceed the ForestGALES value by more than 50 %, the vast majority of points lie below the ForestGALES value and so do all mean values. In similar field studies Gardiner (1995) "found a consistent ratio of 10–12 between extreme and mean forces on plantation trees", which also exceed the measured ratios of this experiment.

The plots in Figure 2.7 show no trend within the range of measured wind speeds. All mean values are in the interval 6.5 to 8.2. The four smallest mean values correspond to the four tallest trees (80,37,43,4) and the five highest values correspond to the group of smaller trees (40,38,39,41,42). A negative correlation of tree height and GF would explain the differences in GFs from this study and the one from Gardiner (1995), whose trees were only 12 m (median) tall. Gardiner et al. (2005) present results from wind tunnel studies which also suggest that the individual gust factor varies with tree height.

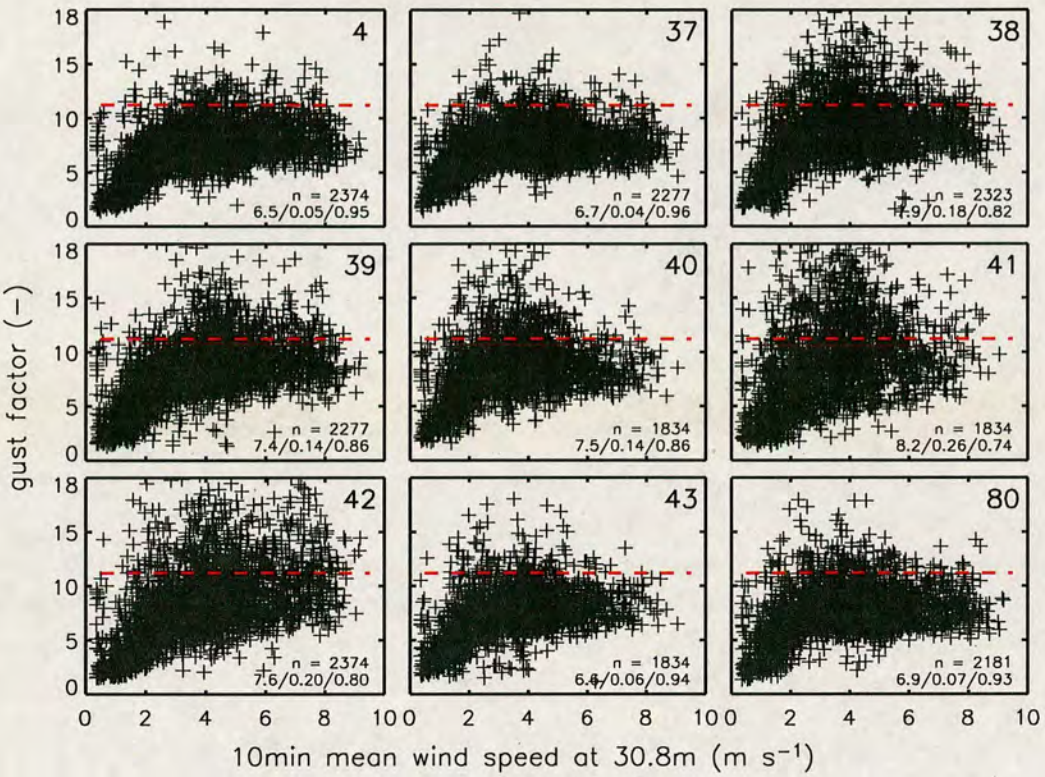

Figure 2.7: Plots of the gust factor for the nine experimental trees as function of wind speed. The red dashed line represents the value calculated by ForestGALES (10.1). The three values in the lower right-hand corner of each plot are the overall mean and the relative fraction of values exceeding and undercutting the ForestGALES value. n is the number of data points for each plot.

2.4.3 Wind loading per tree

ForestGALES assumes that the atmospheric shear stress (τ) is partitioned equally onto the individual trees of the stand and that the zero plane displacement (d) is the acting height of the force. The bulk of momentum absorption takes part in the upper part of the canopy, which leads to very low wind speeds in the trunk space. To take this into account the gaps between the trees (see Fig. 2.1) were filled artificially. The projected area a tree occupies is calculated by a Voronoi algorithm using the coordinates of the trees (Aurenhammer and Klein, 2000). The derived polygons cover the area in which every point is closer to the subject tree than to any other tree. The polygons leave no unaccounted space, so that the complete ground area is apportioned onto the trees. Figure 2.8 shows the Voronoi polygons for the nine experimental trees. The areas are listed

in Table 2.3.

The assumption that the shear stress portioning is scaled by the projected occupied area can be tested with the data from this experiment. Rearranging of Equation 2.4 gives:

$$\tau_{calc,i} = \frac{M_{mean,i}}{A_{Voronoi,i} \cdot d} \tag{2.15}$$

where $\tau_{calc,i}$ ($\mathrm{N\,m^{-2}}$) is the atmospheric shear stress apportioned to tree i, M_{mean} ($\mathrm{N\,m}$) is the measured mean turning moment, $A_{Voronoi,i}$ ($\mathrm{m^2}$) is the projected crown area, and d (m) is the zero plane displacement. All terms in the above equation were measured in this field study.

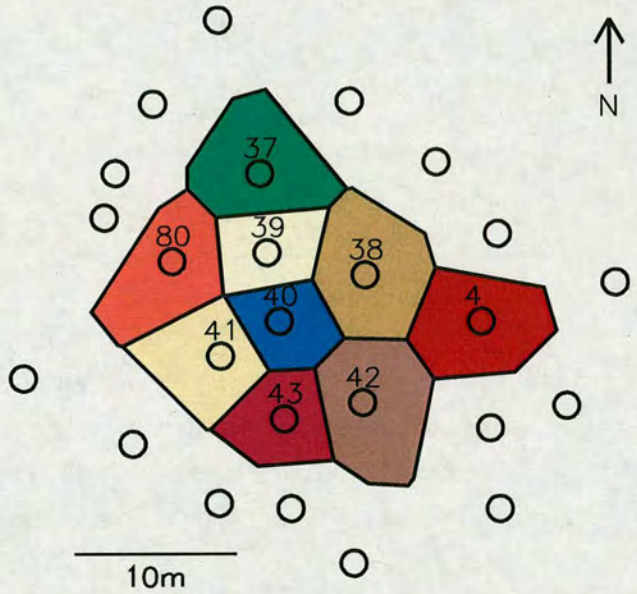

Figure 2.8: Projected occupied areas of the nine experimental trees calculated by the Voronoi algorithm. Circles indicate tree positions.

One of the windiest hours for which measurements are available was in the early morning of the 24$^{\mathrm{th}}$ of August 2005 between 3 and 4 am. Hourly mean wind speed and shear stress at canopy top were $6.7\,\mathrm{m\,s^{-1}}$ and $4.9\,\mathrm{N\,m^{-2}}$, respectively. The zero plane displacement was estimated to be at $18.7\,\mathrm{m}$ ($0.7\,\mathrm{z/h_C}$). For three trees (38,41,42) the ratio of calculated and measured shear stress is below unity. Only for tree 39 the value matches exactly unity. For the remaining five trees (4,37,40,43,80) the values are higher than one. The ratio of calculated and

measured shear stress is in the range 0.2 to 2.9. These values indicate that tree 4 has to withstand 10 times more shear stress per unit crown area than tree 42. The high variability of the ratios shows that the crown area cannot be assumed to be the only scaling factor when it comes to the partitioning of shear stress.

Table 2.3: Projected crown area calculated by the Voronoi algorithm ($A_{Voronoi}$), calculated shear stress per crown area (τ_{calc}), and fraction of calculated and measured shear stress for one windy hour (24.Aug.2005 3–4am; hourly mean wind speed at 30.8 m was 6.7 m s^{-1} and measured shear stress was 4.9 N m^{-2}).

ID	$A_{Voronoi}$ (m^2)	τ_{calc} (N m^{-2})	τ_{calc}/τ_{meas} (-)
4	46.2	14.0	2.9
37	49.0	5.8	1.2
38	50.0	4.2	0.9
39	28.9	4.9	1.0
40	26.6	6.3	1.3
41	38.1	2.6	0.5
42	51.1	1.1	0.2
43	31.0	10.5	2.2
80	43.8	9.4	1.9

Since the sonic anemometer was very close to the canopy top it is questionable whether the measured momentum flux is representative for the constant flux layer above the canopy. The estimation of the zero plane displacement also includes an error. To avoid this, the comparison can be normalised by calculating the fraction of the trees individual shear stress per crown area value over the sum of the collective:

$$\tau_{fraction,i} = \frac{\frac{M_{mean,i}}{A_{Voronoi,i}}}{\sum_{i=1}^{n=9} \frac{M_{mean,i}}{A_{Voronoi,i}}} \tag{2.16}$$

where i is the individual index for the nine experimental trees and n is the number of experimental trees. In contrast to Equation 2.15, this equation does not require turbulence data. Since sonic data are only available for measurements after the 23$^{\mathrm{rd}}$ of August, a bigger data pool is available for this analysis. The only restriction is that for the time interval in question data for all of the nine trees have to be available.

The results for all time intervals with a wind speed higher than $3\,\mathrm{m\,s^{-1}}$ are presented in Figure 2.9. If it was true that the amount of absorbed momentum is only scaled by crown area then all nine trees should have the same value ($1/9 = 0.\overline{1}$). The ranking is similar to the one in Table 2.3. Tree 4 has values greater than all other trees by more than 0.05, followed by trees 80, 37, 43, and 38. Those trees are ranked as the five tallest in the sample.

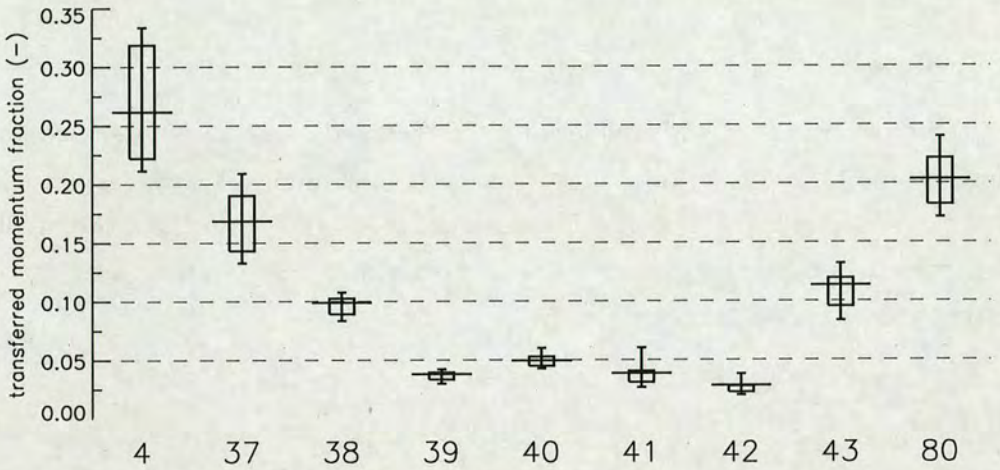

Figure 2.9: Comparison of the relative hourly mean shear stress partitioning (horizontal lines) onto the nine experimental trees. The boxes and vertical lines represent the $25^{\mathrm{th}}/75^{\mathrm{th}}$ and $10^{\mathrm{th}}/90^{\mathrm{th}}$ percentiles (n = 324).

2.4.4 Wind profile method

An alternative to the *roughness method* is the *wind profile method*, which is implemented into the HWIND model (Peltola et al., 1997; Gardiner et al., 2000; Blennow and Sallnäs, 2004). This approach calculates the wind loading from the frontal crown area, the wind profile, and a streamlining function. The general drag formula is:

$$F_D = \rho \cdot \int_0^z C_D(z) \cdot A(z) \cdot u(z)^2 \, dz \tag{2.17}$$

where ρ ($1.226\,\mathrm{kg\,m^{-3}}$) is air density, C_D ($-$) the dimensionless drag coefficient, A ($\mathrm{m^2}$) frontal crown area, u ($\mathrm{m\,s^{-1}}$) horizontal wind speed, and z (m) is height above ground. The drag coefficient was calculated as:

$$C_D = n \cdot u^{-s} \tag{2.18}$$

where n and s are the parameters from a wind tunnel study conducted by Mayhead (1973a). The values for n and s are 2.35 and 0.51, respectively.

The turning moment at the base of the tree is the integral of the drag multiplied by the height:

$$M = \int_0^z F_D(z) \cdot z \, dz \tag{2.19}$$

The crown of the trees is modelled to be diamond shaped with its maximum radius at 0.3 times of the total crown length (Pretzsch et al., 2002). The radius at the crown base is 0.6 fold the maximum radius. Figure 2.10 shows the profiles of the horizontal wind speed, the frontal crown area, the calculated drag, and corresponding turning moment.

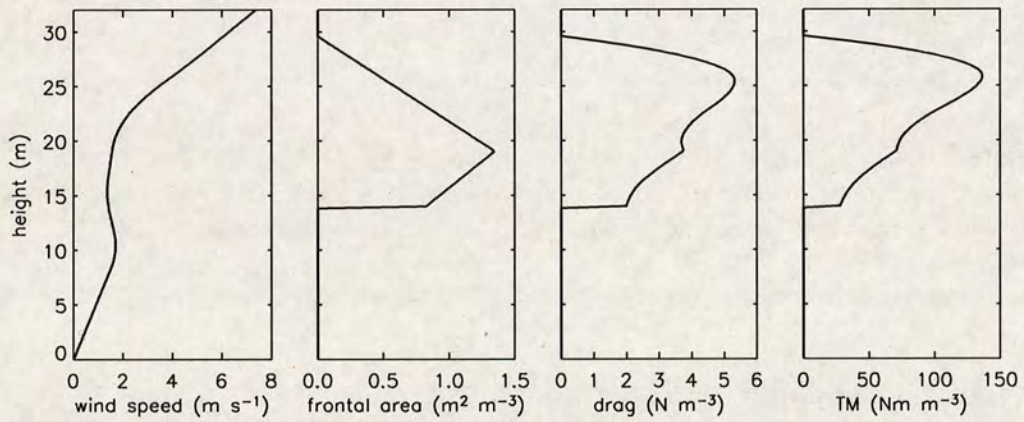

Figure 2.10: Application of the wind profile method for tree 4 for the 24.Aug.2005 (3–4 am). Plots from left to right: Wind profile, frontal crown area, drag, and turning moment.

A comparison of modelled and measured turning moments for one hour is shown in Figure 2.11. Four of the sample trees (41,39,40,38) are well predicted by the model. For the taller trees (37,43,80,4) the models performance is not that good. In three out of the four cases the model overpredicts the turning moment and in case of tree 4 the model underestimates the value. Reasons for this might be the distance between the 30 m mast and the experimental trees. The wind measurements do not necessarily represent the force that the instrumented trees

experience. The meteorological mast was a tilt up type tower. For reasons of practicability the mast was erected on an extraction track. Naturally the stand and canopy density at this spot is lower than the average of the stand, hence the wind might penetrate deeper into the canopy. This might explain some of the discrepancy between the modelled values and the measurements.

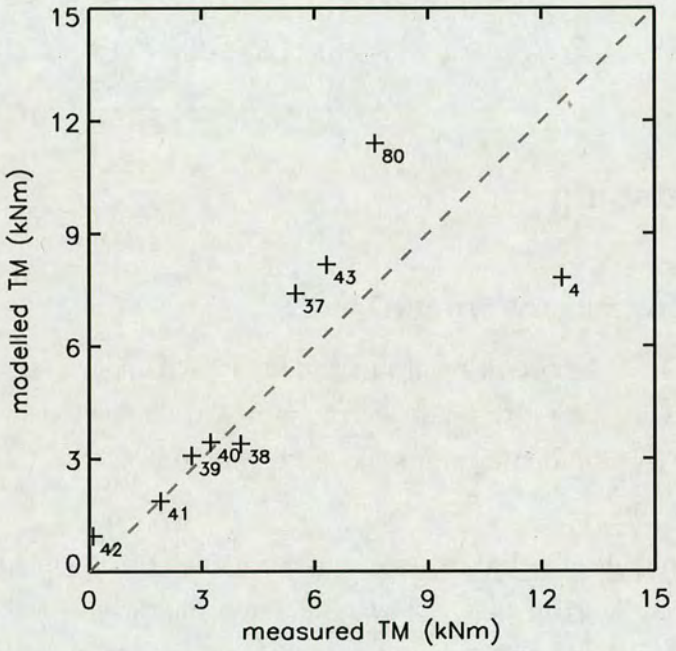

Figure 2.11: Calculated versus modelled hourly mean turning moments for the hour 3–4 am on the 24.Aug.2005. Hourly mean wind speed at 30.8 m was 6.7 m s^{-1}.

2.4.5 Sensitivity of parameters

For estimating the sensitivity of some input parameters, their values were changed by ±10 % (see Tab. 2.4). The model is most sensitive to changes in height and *dbh*. If either of these parameters is changed by 10 % from the original value the predicted critical wind speed deviates by ±3 m s^{-1}. Changing of the spacing and gustfactor results in smaller changes in critical wind speed.

Table 2.4: Sensitivity analysis on the changes in predicted critical wind speed for changes of 10 % for several ForestGALES parameters.

Parameter	change (%)	critical wind speed ($m\,s^{-1}$)
h_{100}	+10	11
h_{100}	−10	16
dbh	+10	16
dbh	−10	11
D	+10	14
D	−10	13
GF	+10	13
GF	−10	14

2.5 Discussion

2.5.1 Performance of ForestGALES

ForestGALES predicts the return period for wind damage for the experimental stand in Clocaenog Forest to be less than one year. The fact that there has been no observation of wind damage for almost a decade proves that these calculations are too pessimistic.

The two Weibull distributions, the one from the DAMS calculations and the other one from the 10 m mast, show differences in the low wind speed range up to $12\,m\,s^{-1}$. Above this value the two distributions are very close. In the wind speed classes that are considered to be near the critical wind speed the differences are very small. The relative differences become minimal at $18.4\,m\,s^{-1}$. Both distributions suggest that the predicted critical wind speed of $14\,m\,s^{-1}$, which corresponds to $20.5\,m\,s^{-1}$ at the 10 m mast, is exceeded frequently. The stand recently withstood two severe gale events without suffering any damage. However, the regression analysis between the 10 m mast and the 30 m mast suggest that the critical wind speed was not quite exceeded during either of the events. Nevertheless the wind speed distributions suggest that the critical wind speed of the stand is underestimated.

The mean gust factor measured for the nine experimental trees was 7.3. In contrast to the ForestGALES value, which predicts a value of 10.1 (a deviation of 28 %). Setting the GF to 7.3 in the ForestGALES model results in a critical wind speed of $17.7\,m\,s^{-1}$. However, for the nine experimental trees the calculated gust

factors cover the range of 6.5 (ID: 37) to 8.2 (ID: 41), i.e. 89 % and 112 % of the mean value. This suggests that the gust factor cannot be assumed to be identical for all trees in the stand. At the same time the gust factor measurements for each tree show large scatter. All in all it seems as if the gust factor is very variable in time and difficult to estimate. Due to the way the gust factor is implemented into the ForestGALES model such deviations do have a significant impact on the predictions of the critical wind speed.

One of the major assumptions of the model is that all of the trees have the same properties and are therefore exposed to the same amount of drag. Gardiner (1995) measured very similar turning moments of three trees in a field experiment. The stand in his field study was 12 m tall (median) with the tallest tree around 15 m. For the Clocaenog stand these values are 24.5 m and 34.2 m, respectively. Due to the advanced maturation of the stand the differences in tree properties are much more pronounced compared to the Gardiner (1995) stand. The taller trees are more exposed to the wind. The diversity in tree properties impedes the validity of the roughness method. From a forest manager's point of view, the experimental stand might not look irregular. But in terms of shear partitioning, which is relevant for wind-tree interactions, it is rather variable.

The characteristics of tree 39 match almost perfectly those of the average tree in the stand for which ForestGALES performs its calculations. For the example calculations for the shear stress partitioning on the 24^{th} of August the fraction of calculated and measured shear stress is unity, which indicates a perfect prediction. However, there is no obvious physical explanation for this and the agreement seems to be coincidental. In direct comparison with the other trees much less than the average shear stress is partitioned onto tree 39. In fact only tree 42 has a lower value. In terms of shear stress partitioning tree 39 is below average and does not act like the average tree. Reasons for this might be the sheltered position behind a dominant tree (80) for the prevailing wind direction.

Although the wind profile method was not fully tested, it seems as if it is not in any way superior to the roughness method. Finer adjustment of the parameters involved would probably increase the overall agreement of modelled and measured values. However, the much higher turning moments that tree 4 experiences in comparison to the other tall trees (37,43,80) cannot be explained just by differences in tree properties such as canopy area. It is more likely that the individual wind profiles for the group of trees differ. The fact that tree 4 is located next to an extraction track that creates a gap, points in this direction. Hence,

the profile method would need to be adapted in a way that allows adjustment of the wind profile for each individual tree.

2.5.2 Wind risk for experimental stand

As mentioned before ForestGALES calculates the critical wind speed for this experimental stand to be $14\,\mathrm{m\,s^{-1}}$. The values for overturning and breaking are $15.2\,\mathrm{m\,s^{-1}}$ and $14.1\,\mathrm{m\,s^{-1}}$. Those values change if we adjust the mean tree height to the true value, since the equation for calculating the mean height does not result in the correct value. By adjusting the values in the model the critical wind speed for overturning becomes $15.3\,\mathrm{m\,s^{-1}}$ and the one for breaking $14.4\,\mathrm{m\,s^{-1}}$. The differences compared to the original values are rather small and do not explain the too pessimistic estimate of the model.

More significant changes are caused by adjusting the gust factor to 7.3 instead of 10.1. For this scenario the critical wind speeds are $17.7\,\mathrm{m\,s^{-1}}$ and $16.7\,\mathrm{m\,s^{-1}}$. Those distinct differences emphasise the impact of the gust factor on the calculations of the critical wind speed. However, the wind speed distribution from the 10 m mast suggests that an hourly mean wind speed at the canopy top of $16.7\,\mathrm{m\,s^{-1}}$ ($24.5\,\mathrm{m\,s^{-1}}$ at the 10 m mast) is still exceeded every year. Therefore it seems as if this value is still too pessimistic.

The adjustment of the mean height and the gust factor causes an increase of the critical wind speed value and seems to be more realistic.

2.6 Conclusions

This is the first time that several modules of the ForestGALES model have been validated independently using the data from a single field study. The results suggest that the stand is more stable than predicted by the ForestGALES model. Especially the modelled gust factor deviates from the field measurements. Its overestimation increases the wind induced turning moment in the model. The ForestGALES model was designed for even aged regular stands. Although the Clocaenog stand is even aged it is highly irregular from an aerodynamic point of view. The turning moment the nine experimental trees are exposed to differs by one order of magnitude. Therefore the model assumption that the atmospheric shear stress is distributed equally onto the individuals of the stand does not hold. In direct comparison the taller trees have to withstand significantly higher drag

than the smaller ones. Most of the momentum transfer takes place in the upper part of the canopy, so that smaller trees are exposed to much less drag.

The data analysis from the Clocaenog field experiment highlights the demand for modifications in the ForestGALES model to make it work with irregular stand structures as they occur under low impact silvicultural systems. The wind-tree interaction appears to be more complex than they are in regular stands. More field data are needed for a better understanding and parametrisation of the relevant processes.

Acknowledgement

Many thanks to Arne Pommerening and Jens Haufe (University of Wales, Bangor) for granting permission to conduct the experiment in one of the experimental plots of the Tyfiant Coed project and for providing the detailed stand data set. The performance of the measuring system can only be described as awesome. This achievement would have been out of reach had it not been for the three chaps from the workshop at the Northern Research Station: Dave Brooks, John Strachan, and Jim Nicholl. Their help, advice, encouragement, and patient in explaining technical things is much appreciated.

Gathering all the equipment for this experiment was challenging and the fact that the preparation fell at a time of financial 'depression' did not make it any easier. Roland Vogt from the University of Bale, Switzerland, kindly helped out by lending an industrial PC, which was used for data storage until we got our hands on one on ebay.

I also like to thank Carl Foster and the team from the Technical Support Unit in Talybont, Wales, who helped lowering and erecting the meteorological mast several times. Shaun Mochan climbed up the trees for the tree pulling procedures and operated the winch during the mast erecting. The opportunity to fall back on such practical skilled people was a blessing.

The wind speed time series for Rhyl were kindly provided by the UK Meteorological Office.

References

Aurenhammer F and Klein R, 2000: *Voronoi Diagrams*, chap. Handbook of Computational Geometry, pp. 201–290. North-Holland, Amsterdam, Netherlands.

Bell PD, Quine CP, and Wright JA, 1995: The use of digital terrain models to calculate windiness scores for the Windthrow Hazard Classification. *Scottish Forestry*, 49, 217–225.

Blackburn GRA, 1997: *The Growth and Mechanical Response of Trees to Wind Loading*. PhD, University of Manchester.

Blennow K and Sallnäs O, 2004: WINDA - a system of models for assessing the probability of wind damage to forest stands within a landscape. *Ecological Modelling*, 175, 87–99.

Busby J, 1965: Studies on the stability of conifer stands. *Scottish Forestry*, 19, 86–102.

Cucchi V, Meredieu C, Stokes A, de Coligny F, Suárez J, and Gardiner BA, 2005: Modelling the windthrow risk for simulated stands of Maritime pine (*Pinus pinaster* Ait.). *Forest Ecology and Management*, 213, 184–196.

Derrick A, 1992: Wind energy conversation. In Clayton B, ed., *14th British wind energy association conference*, pp. 259–265.

Dunham R, Gardiner B, Quine C, and Suárez J, 2000: *ForestGALES - A PC-based wind risk model for British forests*. Forestry Commission, Edinburgh, UK.

Dupont S and Brunet Y, 2008: Edge flow and canopy structure: A large-eddy simulation study. *Boundary-Layer Meteorology*, 126, 51–71.

Edwards P and Christie J, 1981: Yield models for forest management. FC Booklet 48, Forestry Commission, Edinburgh, UK.

EFI, 2007: The storm "Kyrill" and its effect on European forests. `http://www.efi.int/portal/news___events/press_releases/?id=8`.

Fraser AI, 1964: Wind tunnel and other related studies on coniferous trees and tree crops. *Scottish Forestry*, 18, 84–92.

Gardiner B, Byrne K, Hale S, Kamimura K, Mitchell SJ, Peltola H, and Ruel JC, 2008: A review of mechanistic modelling of wind damage risk to forests. *Forestry*, 81, 447–463.

Gardiner B, Marshall B, Achim A, Belcher R, and Wood C, 2005: The stability of different silvicultural systems: A wind tunnel investigation. *Forestry*, 78, 471–484.

Gardiner B, Peltola H, and Kellomäki S, 2000: Comparison of two models for predicting the critical wind speeds required to damage coniferous trees. *Ecological Modelling*, 129, 1–23.

Gardiner B, Suárez J, Achim A, Hale S, and Nicoll BC, 2004: *ForestGALES. A PC-based wind risk model for British forests*. Forestry Commission, Edinburgh.

Gardiner BA, 1994: Wind and wind forces in a plantation spruce forest. *Boundary-Layer Meteorology*, 67, 161–186.

Gardiner BA, 1995: The interactions of wind and tree movement in forest canopies. In Coutts MP and Grace J, eds., *Wind and Trees*, chap. 2, pp. 41–59. Cambridge Univ. Press.

Gardiner BA, Stacey GR, Belcher RE, and Wood CJ, 1997: Field and wind tunnel assessments of the implications of respacing and thinning for tree stability. *Forestry*, 70, 233–252.

Green SR, Grace J, and Hutchings NJ, 1995: Observations of turbulent airflow in three stands of widely spaced Sitka spruce. *Agricultural and Forest Meteorology*, 74, 205–225.

Hale SE, Levy PE, and Gardiner BA, 2004: Trade-offs between seedling growth, thinning and stand stability in Sitka spruce stands: A modelling analysis. *Forest Ecology and Management*, 187, 105–115.

Kamimura K and Shiraishi N, 2007: A review of strategies for wind damage assessment in Japanese forests. *Journal of Forest Research*, 12, 162–176.

Kruijt B, Malhi Y, Lloyd J, Nobre AD, Miranda AC, Pereira MGP, Culf A, and Grace J, 2000: Turbulence statistics above and within two Amazon rain forest canopies. *Boundary-Layer Meteorology*, 94, 297–331.

Mason WL and Kerr G, 2004: Transforming even-aged conifer stands to continuous cover management. Information Note 40, Forestry Commission, Edinburgh.

Mayhead GJ, 1973a: Some drag coefficients for British forest trees derived from wind-tunnel studies. *Agricultural Meteorology*, 12, 123–130.

Mayhead GJ, 1973b: Sway periods of forest trees. *Scottish Forestry*, 27, 19–23.

Miller KF, 1985: Windthrow hazard classification. Leaflet 85, Forestry Commission.

Mitchell SJ, 1995: The windthrow triangle: A relative windthrow hazard assessment procedure for forest managers. *The Forestry Chronicle*, 71, 446–450.

Moore J and Quine CP, 2000: A comparison of the relative risk of wind damage to planted forests in Border Forest Park, Great Britain, and the Central North Island, New Zealand. *Forest Ecology and Management*, 135, 345–353.

Moore JR, Gardiner BA, Blackburn GRA, Brickman A, and Maguire DA, 2005: An inexpensive instrument to measure the dynamic response of standing trees to wind loading. *Agricultural and Forest Meteorology*, 132, 78–83.

Morse AP, Gardiner BA, and Marshall BJ, 2002: Mechanisms controlling turbulence development across a forest edge. *Boundary-Layer Meteorology*, 103, 227–251.

Nicoll BC, Gardiner BA, Rayner B, and Peace AJ, 2006: Anchorage of coniferous trees in relation to species, soil type, and rooting depth. *Canadian Journal of Forest Research*, 36, 1871–1883.

Peltola H and Kellomäki S, 1993: A mechanistic model for calculating windthrow and stem breakage of Scots pines at stand edge. *Silva Fennica*, 27, 99–111.

Peltola H, Kellomäki S, Väisänen H, and Ikonen VP, 1999: A mechanistic model for assessing the risk of wind and snow damage to single trees and stands of Scots pine, Norway spruce, and birch. *Canadian Journal of Forest Research*, 29, 647–661.

Peltola H, Nykänen ML, and Kellomäki S, 1997: Model computations on the critical combination of snow loading and windspeed for snow damage of Scots pine, Norway spruce and birch sp. at stand edge. *Forest Ecology and Management*, 95, 229–241.

Pommerening A and Murphy S, 2004: A review of the history, definitions and methods of continuous cover forestry with special attention to afforestation and restocking. *Forestry*, 77, 27–44.

Pretzsch H, Biber P, and Ďurský J, 2002: The single tree-based stand simulator SILVA: Construction, application and evaluation. *Forest Ecology and Management*, 162, 3–21.

Quine CP, 2000: Estimation of mean wind climate and probability of strong winds for wind risk assessment. *Forestry*, 73, 247–258.

Quine CP and Bell PD, 1998: Monitoring of windthrow occurrence and progression in spruce forests in Britain. *Forestry*, 71, 87–97.

Quine CP and White IMS, 1994: Using the relationship between rate of tatter and topographic variables to predict site windiness in upland Britain. *Forestry*, 67, 245–256.

Raupach MR, 1994: Simplified expressions for vegetation roughness length and zero-plane displacement as functions of canopy height and area index. *Boundary-Layer Meteorology*, 71, 211–216.

Raupach MR, Finnigan JJ, and Brunet Y, 1996: Coherent eddies and turbulence in vegetation canopies: The mixing-layer analogy. *Boundary-Layer Meteorology*, 78, 351–382.

Ruel JC, Quine C, Meunier S, and Suárez J, 2000: Estimating windthrow risk in balsam fir stands with the ForestGALES model. *The Forestry Chronicle*, 76, 329–337.

SMHI, 2005: Januaristormen 2005 [The January 2005 windstorm]. Faktablad 25, Sveriges Meteorolgiska och Hydrologiska Institut, SE-601Norrköping, Sweden.

Suárez JC, Gardiner BA, and Quine CP, 1999: A comparison of three methods for predicting wind speeds in complex terrain. *Meteorological Applications*, 6, 329–342.

Thom AS, 1971: Momentum absorption by vegetation. *Quarterly Journal of the Royal Meteorological Society*, 97, 414–428.

Troen I and Petersen E, 1989: *European Wind Atlas*. Risø National Laboratory, Roskilde.

UK Meteorological Office, 2006: Midas land surface stations data (1853-current), [internet]. British Atmospheric Data Centre. Available from `http://badc.nerc.ac.uk/data/ukmo-midas`.

Yang B, Shaw RH, and Paw U KT, 2006: Wind loading on trees across a forest edge: A large eddy simulation. *Agricultural and Forest Meteorology*, 141, 133–146.

Chapter 3

Critical wind speed estimates for individual trees from a field experiment

Abstract

Simultaneous measurements of wind speed and turning moment of a group of nine adjacent mature Sitka spruce trees were used for analysing the wind and tree interaction. A quadratic model was fitted to the data of turning moment and wind speed near the canopy top.

Predicted absolute mean turning moments for the nine trees were highly correlated with dbh^3 ($r = 0.98$) and stem weight ($r = 0.97$), which themselves are estimators for breaking and overturning. Predicted mean wind speeds for tree breaking are not correlated with individual tree properties. However, correlation of the predicted mean wind speeds for overturning suggest that dominant trees are at higher risk of tree failure.

For the experimental trees, dbh is the best estimator for predicting both the absolute turning moment and the risk of wind damage.

3.1 Introduction

Individual trees in a forest stand can differ significantly from each other regarding their properties, even in even-aged mono-cultures. Differences are the result of lifelong competition for resources including light, water, and nutrition (Oliver and Larson, 1990). At the same time mechanical stimulation is known to affect plant growth (Metzger, 1893; Stokes et al., 1995; Telewski, 1995; Stokes et al., 1997; Cleugh et al., 1998). Plant response to mechanical stimulation is termed *thigmomorphogenesis* after Jaffe (1973). In his experiments he showed that plants that were rubbed daily showed reduced height growth and increased

stem diameters, that resulted in higher rigidity of the plant stem. Since the main mechanical stimulus in natural conditions is the loading exerted by the wind, differences in tree growth are pronounced where sheltered and non-sheltered conditions are found in close proximity (James et al., 1994).

Forest canopies are very efficient in terms of wind energy absorption. The vast majority of momentum is absorbed in the upper part of the canopy (Baldocchi and Hutchison, 1987). Hence the drag that two neighbouring trees experience can be very different, due to differences in their height. Small suppressed trees benefit from a sheltered environment, that is created for them by their taller neighbours, which absorb most of the wind energy. Increased height growth goes hand in hand with diameter growth. Taller individuals in a stand have also bigger trunks and higher root mass (Levy et al., 2004) and therefore higher stiffness and improved anchorage (Nicoll et al., 2006).

This poses the question as to which individuals are the most vulnerable in a forest stand. Does the higher amount of biomass of the dominant trees fully compensate for the increased wind exposure? Or does their dominant and favourable position come at the cost of higher risk of failure. Do small trees accept the risk of mechanical failure and invest more biomass into height growth to reach higher light levels?

The vast majority of work in the literature, which dealt with the inter-stand variability of wind damage is based on post-damage surveys (e.g. Everham III and Brokaw, 1996; Coates, 1997; Evans et al., 2007). The disadvantage of such surveys is that the 'true' critical wind speed is unknown. Only the results of the wind damage process can be interpreted but not the process itself. Imagine that only one tree fails during a storm event for some reason. This will cause a sudden increase in wind loading inside the canopy, since the wind can penetrate deeper into the stand, which can trigger a chain reaction. This kind of wind damage causes street wise patterns of wind damage (e.g. Lines, 1953; Gardiner and Quine, 1994). At the same time not all tree failure can be accounted for by wind damage per se. In particular smaller trees are often damaged by falling bigger trees, and may bias the analysis (Peterson, 2004). Only in rare occasions wind speed measurements are available for above the forest during a destructive storm event (Oliver and Mayhead, 1974). Wind speed information is usually taken from the nearest weather station or is estimated from models (e.g. Lanquaye-Opoku and Mitchell, 2005). This procedure does not allow an accurate estimate of the stands critical wind speed at which damage occurs. The wind speed during a gale event

gradually builds up to a maximum. As no time information for tree failure is generally available, the only interpretation that post-damage surveys allow is that the threshold of wind damage was exceeded.

This chapter aims to estimate the critical wind speed at which tree damage will occur from simultaneously measured time series of wind speed and turning moment. A quadratic model is fitted to the data and the relationships are used to investigate whether a single tree property is able to explain the susceptibility of an individual tree to wind damage.

3.2 Material and methods

3.2.1 Experimental site

The field survey took place in a pure Sitka spruce (*Picea sitchensis* (Bong.) Carr.) stand in Clocaenog Forest, Wales (53°07′40″ N, 3°42′96″ W, 395 m a.s.l.) in 2005. Density of the stand was 292 trees ha^{-1}, mean height was 26.7 m, average diameter at breast height (*dbh*) was 35.8 cm, and mean slenderness (*h:dbh*) 76 (values calculated from measurements taken in 2002). For the four crown classes the slenderness values were 80±12 for dominant, 75±9 for co-dominant, 76±10 for subdominant, and 76±9 for suppressed trees. Each crown class contained 25 % of the total number of trees, where the trees were ranked by *dbh*. The last thinning of the stand was carried out in 1999, six years before this field survey. Urban et al. (1994) estimated the time scale for full adaptation to a stand intervention to be in the range of 5 to 10 years.

For the field survey nine adjacent trees were chosen as experimental trees which were approximately arranged in a 3×3 array (see Fig. 3.1). The nine trees cover a wide range of properties and all crown classes except the 'subdominant' are represented by the sample (see Tab. 3.1).

3.2.2 Tree failure moments

Tree failure can be distinguished into two main categories, breaking and overturning. The required turning moments for the two types are named breaking moment (M_{break} in Nm) and overturning moment (M_{over} in Nm). The trees critical moment (M_{crit} in Nm) is defined as the lower of these two values. Since no permission was granted for destructive treepulling tests of the experimental

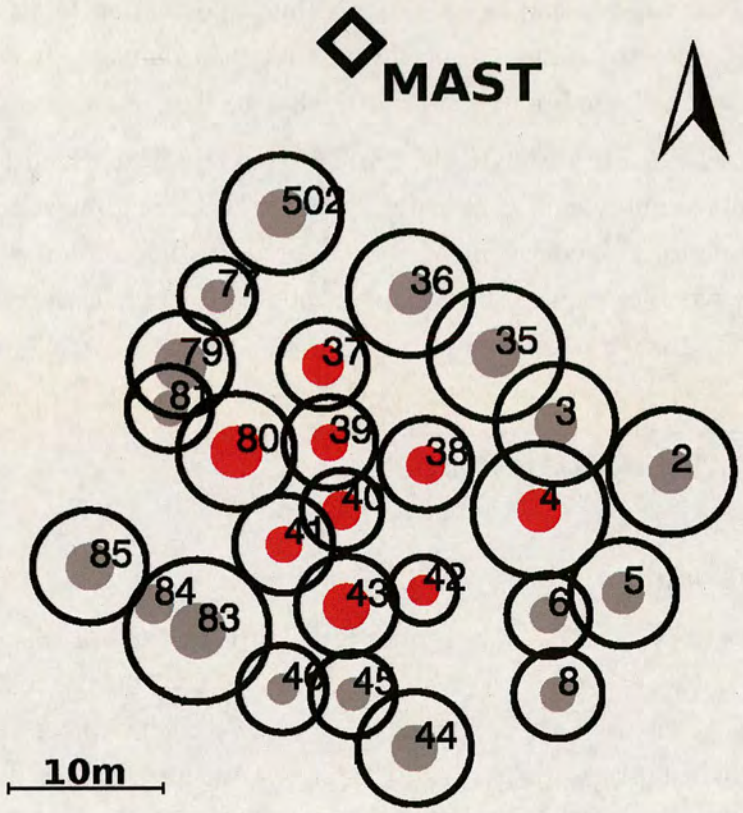

Figure 3.1: Map showing the nine experimental trees (red) and their direct neighbours (grey). The black circles indicate the average crown radii. Note that the meteorological mast was located inside the forest stand. Since the experimental trees were located at the edge of the plot, the coordinates of the trees adjacent to the mast were not measured.

trees, these moments were calculated from tree properties and relationships from the literature. The breaking moment of the individual tree was calculated as (Gardiner et al., 2000):

$$M_{break} = \frac{\pi}{32} \cdot MOR \cdot diam^3_{\text{at base}} \tag{3.1}$$

where MOR (3.4×10^7 Pa) is the modulus of rupture (Lavers, 1969) and $diam_{\text{at base}}$ (m) is the tree's base diameter calculated as function of dbh and tree height (h) (Gardiner, 1992):

$$diam_{\text{at base}} = \frac{dbh}{((h - 1.3)/h)^{0.6}} \tag{3.2}$$

The overturning moment (M_{over}) is calculated as a function of stem weight:

$$M_{over} = c_{reg} \cdot SW \tag{3.3}$$

where SW (kg) is the tree's fresh stem weight and c_{reg} ($\mathrm{N\,m\,kg^{-1}}$) an empirical species and soil specific regression coefficient, which was estimated from more than 2,000 treepulling tests (Fraser and Gardiner, 1967; Nicoll et al., 2006). For c_{reg} a value of $162\,\mathrm{N\,kg^{-1}}$ was used, which is the one for Sitka spruce growing on *'Gleyed mineral soils'* and with a rooting depth of 40–80 cm (Nicoll et al., 2006). The stem volume was modeled using individual tree height, *dbh*, and age using a model which was derived for British Sitka spruce trees assuming a density of $850\,\mathrm{kg\,m^{-3}}$ (Lavers, 1969). The stem weight of three of the experimental trees exceed the maximum stem weight, that had been used for the model in the original publication (Nicoll et al., 2006).

The estimated breaking and overturning moments for the nine experimental trees are listed in Table 3.1 (see also Fig. 3.2). The pairs appear similar for six out of the nine trees and differences are less than 5 %. The similarity of breaking and overturning moments has been described in the literature (Petty and Worrell, 1981; Cremer et al., 1982), which suggests that the development of roots and stem is balanced (Dunham and Cameron, 2000). For the three heaviest trees (4,43,80) the differences are more pronounced (26 %, 9 %, 15 %). For tree 39 and 42 the overturning moment is higher than the breaking moment. For the seven other trees the overturning moment is lower than the breaking moment. The fact that from the predictions more trees are likely to overturn rather than break is in agreement with post damage observations in nearby stands from the years 2005 and 2007 where more trees were overturned than snapped (Jens Haufe, personal communication).

3.2.3 Wind measurements

The wind profile in the forest was measured with eight cup anemometers (NRG#40, NRG Systems, US) mounted onto a 30 m mast (TallTower, NRG Systems, US), which was located about 30 m north from the experimental trees. Wind direction was measured at 27 and 15 m above ground using wind vanes

Table 3.1: Properties of the experimental trees in Clocaenog Forest. Values in parentheses give the normalised rank from all trees in the experimental plot based on measurements in 2002. The total number of trees in the stand is 292. (ID: tree number, dbh: diameter at breast height, h: tree height, cr-base: height of crown base, cr-class: crown class, M_{break}: breaking moment, M_{over}: overturning moment, M_{crit}: critical moment)

ID	dbh (cm)	h (m)	h:dbh (-)	stem weight (kg)	cr-base (m)	cr-class	M_{break} (kNm)	M_{over} (kNm)	M_{crit} (kNm)
4	59.8 (1.00)	29.6 (0.89)	49.5 (1.00)	2989	13.9	dom	774	484	484
37	42.2 (0.82)	31.1 (0.96)	73.7 (0.54)	1651	16.0	dom	270	267	267
38	38.9 (0.69)	27.3 (0.60)	70.2 (0.71)	1220	17.2	co-dom	214	197	196
39	35.4 (0.51)	26.9 (0.53)	76.0 (0.45)	1008	15.5	co-dom	161	163	161
40	37.6 (0.63)	28.0 (0.72)	74.5 (0.51)	1181	15.5	co-dom	193	191	191
41	34.0 (0.41)	24.3 (0.13)	71.5 (0.65)	834	15.8	surp	144	135	135
42	28.5 (0.08)	22.8 (0.04)	80.0 (0.30)	558	15.2	surp	85	90	85
43	47.2 (0.96)	30.5 (0.94)	64.6 (0.88)	1987	19.5	dom	379	321	321
80	54.5 (0.99)	31.9 (0.98)	58.6 (0.97)	2735	16.0	dom	582	443	443

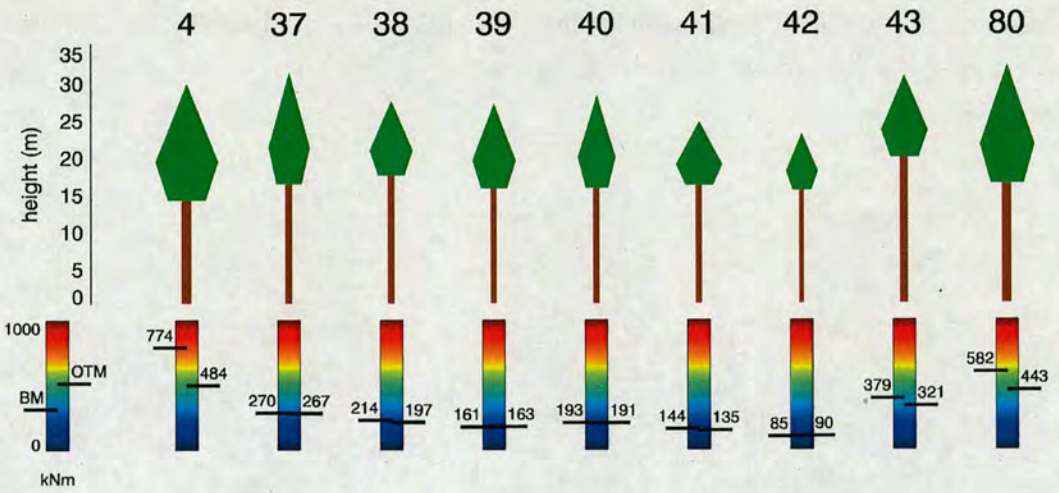

Figure 3.2: Scaled illustration of the nine experimental trees for the purpose of comparison. The numbers next to the colourbars are the breaking (left hand side) and overturning moments (right hand side).

(NRG#200P, NRG Systems, US). The upper four cup anemometers were logged every 3 s using a 21X data logger (Campbell Scientific, Logan, US). The lower four cup anemometers were logged by a Holtech logger (Durham, UK) once a minute.

3.2.4 Measurement of turning moment

The turning moments the experimental trees experienced were measured with strain transducers screwed into the trees at about 1.3 m height (Blackburn, 1997; Moore et al., 2005). Every tree was equipped with two strain transducers, which were arranged orthogonally to allow measurements in the xy-plane. Each strain transducer was calibrated individually by pulling the tree in the two directions in alignment with the position of the instruments on the trees. This provides calibration coefficients which allow calculation of the turning moments from the strain transducer signal. The time resolution of the measurements was 4 Hz.

3.2.5 Data treatment

The relationship between wind speed and turning moment was calculated on 10 min time intervals. The 3 s wind speed measurements at 30.8 m were averaged and the absolute maximum of the corresponding turning moment time series was extracted for each of the nine trees. An example of a 60 min long time series of

wind speed and turning moment is shown in Figure 3.3 and illustrates how the wind speed and turning moment values were extracted for the analysis of the wind tree interaction.

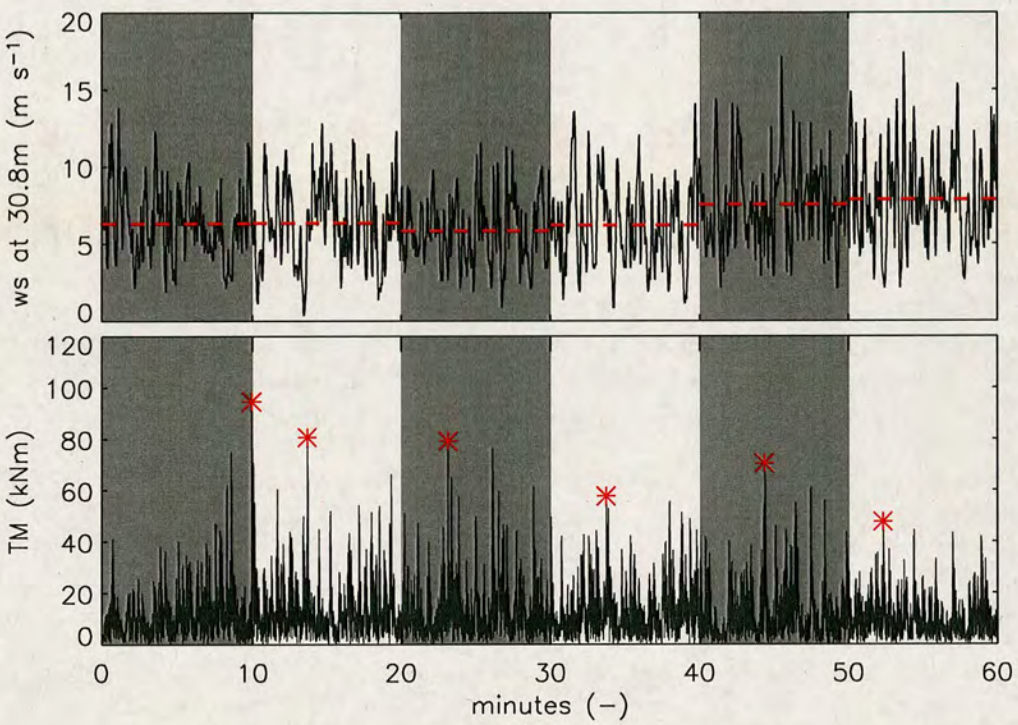

Figure 3.3: Time series of wind speed at 30.8 m (upper) and turning moment of tree 4 (lower) (date: 24.Aug.2005, 3–4 am). Dashed red lines are the 10 min average wind speed and the red asterisks represent the 10 min maximum turning moments which were extracted from the time series for further analysis.

Gardiner (1995) pointed out that the occurrence of coherent structures (gusts) coincides with the maxima in time series of turning moments. However, for this field study a linear relationship between 3 s gust speed and 10 min wind speed was observed, which allows a simple scaling between those two values (see Fig. 3.4). The meteorological tower was located ca. 30 m away from the centre of the nine experimental trees. Due to the limited spatial extent of coherent structures we cannot be sure that the maximum wind speeds at the meteorological tower are exactly the same as those that the trees were exposed to. Hence the 10 min mean wind speed is assumed to be a more robust parameter for the analysis of the wind and tree interaction.

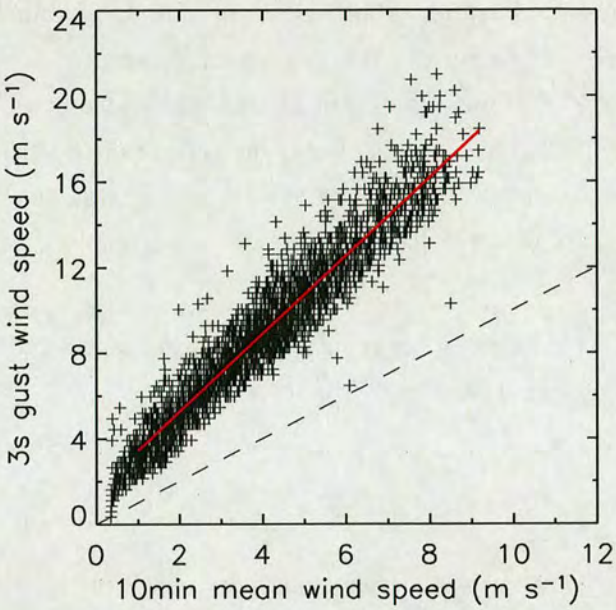

Figure 3.4: 3 s gust speed at 30.8 m height plotted versus 10 min mean wind speed the red line is the best fit of a linear regression model ($f(x) = x \cdot 1.82 + 1.61$, $R^2 = 0.91$, $n = 2743$).

3.2.6 Wind loading on individual trees

The turning moment at the tree base is composed of two components. One component results from the drag on the tree crown due to the wind (M_{drag}). The other component results from the overhanging crown mass as the tree top deflects and the centre of mass is moved from its rest position ($M_{\text{crown mass}}$). The total turning moment at the tree base is the sum of these two components:

$$M = M_{\text{drag}} + M_{\text{crown mass}} \tag{3.4}$$

For modelling purposes, the crown mass is often regarded as a single point mass located at the center of the canopy (Fraser and Gardiner, 1967). Hence its contribution to the total turning moment can be calculated as:

$$M_{\text{crown mass}} = \frac{1}{2} h \cdot g \cdot m_{\text{crown}} \cdot x_{\text{center of canopy}} \tag{3.5}$$

where h (m) is tree height, g ($9.81\,\text{m}\,\text{s}^{-2}$) is the gravitational constant, m_{crown} (kg) is the crown weight and $x_{\text{center of canopy}}$ (m) is the horizontal stem displacement at the center of the canopy. Except for the displacement (x) all terms in the above

equation are constant. Gardiner (1992) gives an analytical solution for the static tree bending, which only requires a 'load parameter' as input. Displacement at the center of the canopy is a linear function of this 'load parameter'. In comparison to the drag induced turning moment, the contribution of the crown mass is small and in the range of 5 % to 10 % of the total turning moment (Gardiner et al., 1997). Therefore it is feasabile to describe the stem displacement as a function of the drag.

For the analysis of the M_{drag} term a simplified form of the general drag formula was used. The drag formula in its original form is:

$$M_{drag} = \rho \cdot \int_0^z C_D(z) \cdot A(z) \cdot u(z)^2 \, dz \tag{3.6}$$

where ρ ($1.226\,\text{kg}\,\text{m}^{-3}$) is air density, C_D ($-$) the drag coefficient, A (m^2) is frontal crown area, u ($\text{m}\,\text{s}^{-1}$) horizontal wind speed, and z (m) height above ground. Unlike rigid obstacles, trees are flexible and streamline in high winds (Mayhead, 1973; Rudnicki et al., 2004). Hence crown area and drag coefficients themselves are functions of wind speed. However, several wind tunnel studies showed a linear relationship between drag and a single squared reference wind speed (Gillies et al., 2002; Vollsinger et al., 2005). The data from this experiment suggest the same relationship holds for at least the range of wind speeds for which measurements are available. Since the above wind tunnel studies exceeded the maximum wind speed from this field experiment, it seems reasonable to assume this relationship to be valid over a wider range.

Neglecting the drag coefficient and changes in projected crown area M_{drag} can be described with a quadratic model approach:

$$M_{drag} = b \cdot u^2 \tag{3.7}$$

where M_{drag} (kNm) is the drag induced turning moment at the tree base and u ($\text{m}\,\text{s}^{-1}$) is a reference horizontal wind speed. From the discussion above, it can be concluded that the crown mass term is proportional to the drag, since it accounts for most of the turning moment at the tree base. Hence, Equation 3.7 can also be used to describe the total turning moment (M) at the tree base:

$$M = \underbrace{b \cdot u^2}_{M_{\text{drag}}} + \underbrace{c \cdot u^2}_{M_{\text{crown mass}}} = a \cdot u^2 \tag{3.8}$$

where the parameter a incorporates the effects of drag and crown mass.

By inverting Equation 3.8 the wind speed can be calculated as function of turning moment (M). Inserting the estimated turning moments for breaking and overturning from Table 3.1 gives the possibility to calculate the corresponding wind speeds:

$$u = \sqrt{\frac{M}{a}}. \tag{3.9}$$

This simple modelling approach neglects some major aspects of the wind and tree interaction such as the streamlining of the trees in high wind and the leaf area profile. However, the most severe simplification is probably the fact that this approach ignores the dynamic behaviour of the tree. Trees can be described as harmonic damped oscillators (Holbo et al., 1980; Mayer, 1987). Their response to wind loading near their eigenfrequency can be 10 fold higher than at other frequencies (Kerzenmacher and Gardiner, 1998; Moore, 2002). Most of the deviations from the model fits are probably due to the dynamic nature of the wind and tree interaction.

3.3 Results

3.3.1 Model fitting

The 10 min mean wind speed at 30.8 m was used as independent variable for the model. Preliminary data analysis showed that wind direction had an influence on the model. Therefore analysis was limited to the wind sector 180 ° to 270 °, which contained 62 % to 69 % of the available data for the trees and represent the prevailing wind direction. For the identification of outliers a linear regression analysis was performed of the $\log_{10}-$transformed turning moment and the squared wind speed. An outlier was identified if the data point deviated more than 0.5 from the regression line in the log-transformed representation. Due to more scatter than for the other trees for tree 41 more than 8 % of the data were removed in this step. For the other eight trees no more than 3 % of the data were rejected for analysis (mean: 1.4 %).

The models were fitted using a least square approach. The data points and the fitted models for the nine experimental trees are shown in Figure 3.5.

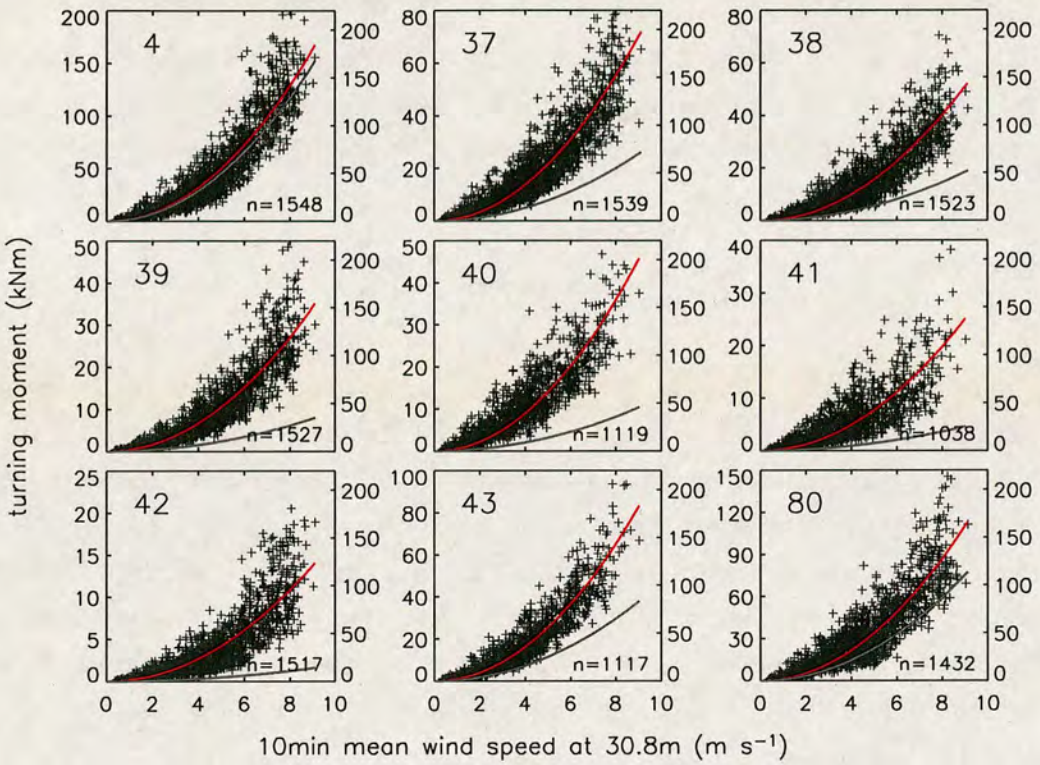

Figure 3.5: Measured 10 min maximum turning moment versus mean wind speed at 30.8 m height for the nine experimental trees. n is the number of data points used for the analysis. The red lines are the best fit of a quadratic model ($f(u) = a \cdot u^2$). The grey lines are identical to the red ones, except that they refer to the y-axis on the right hand side of the plots, which is the same for all plots and allows direct comparison of the models. Data points and red lines refer to the y-axis on the left hand side, which is adjusted for each graph.

For all of the nine models more than 1,000 data points were available for curve fitting. The differences in the total number of data points are due to some equipment failure during one of the field visits. The ratio of explained to unexplained variance (R^2) is for eight out of the nine models higher than 0.75. An exception is tree 41, for which R^2 is just 0.59. The standard error of the model parameter was estimated via the bootstrap technique with a resample size of 10,000. The statistical characteristics of the nine models are summarised in Table 3.2. The high values for the coefficient of determination (R^2) confirms that the model is able to explain most of the variation.

Although the coefficients of determination are high, the data still show a considerable amount of scatter around the model fit. Figure 3.6 is a boxplot

Table 3.2: Model parameter (a) of the quadratic models ($M = a \cdot u^2$) in Figure 3.5. Standard errors for a are given in parentheses and were estimated using the bootstrap technique with 10,000 repetitions. R^2 is the coefficient of determination.

ID	n	a (SE)	R^2
4	1548	2.015 (0.062)	0.84
37	1539	0.863 (0.027)	0.81
38	1523	0.627 (0.046)	0.78
39	1527	0.423 (0.029)	0.81
40	1119	0.561 (0.025)	0.75
41	1038	0.300 (0.036)	0.59
42	1517	0.170 (0.009)	0.75
43	1117	1.020 (0.049)	0.86
80	1432	1.357 (0.054)	0.77

representation of the residuals for the wind speed class 7–8 m s^{-1}. The residuals are normalised by the trees critical moment. Although the limits for the 1st and 3rd quartile are for no tree higher than 5 %, there are still values that exceed 15 %. The variation of the turning moments has to be kept in mind when critical wind speeds are discussed later in the chapter. The discussion will focus on the predicted critical mean wind speed.

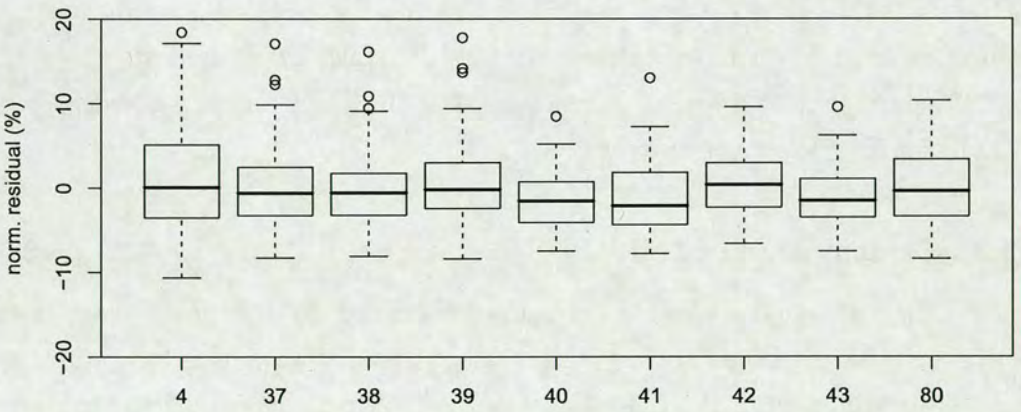

Figure 3.6: Normalised residuals ($(M-\hat{M})/M_{crit}$) for the wind speed class 7–8 m s^{-1} for the nine experimental trees. Horizontal lines indicate the median. Boxes cover the 1st and 3rd quartile. Vertical bars extend 1.5 times the interquartile range to either side of the boxes. Open symbols represent data values that exceed this range.

3.3.2 Turning moment as function of tree characteristics

In Figure 3.7 from the model fits estimated mean turning moments are plotted versus the tree characteristics from Table 3.1. The reference wind speed was set to $8\,\mathrm{m\,s^{-1}}$ at 30.8 m. All five plots indicate that bigger trees - in terms of either *dbh* or height - experience higher turning moments than smaller ones. However, the two parameters are not independent. Pearson and Kendall's rank correlation coefficients for the relationships between *dbh* and tree height are 0.80 and 0.72, respectively.

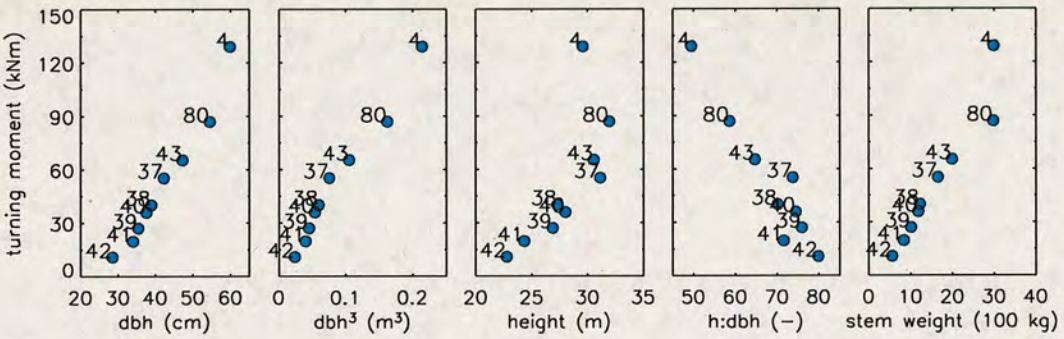

Figure 3.7: Predicted mean turning moments for the experimental trees in Clocaenog Forest for a reference wind speed of $8\,\mathrm{m\,s^{-1}}$ at 30.8 m height calculated from the models.

Kendall's rank correlation coefficients (τ) for the predicted mean turning moments and the two independent variables *dbh* (also dbh^3) and stem weight are 1.0, which indicates a perfect ranking. For the height and slenderness τ is 0.72 and -0.78, respectively.

3.3.3 Critical wind speed

The highest 10 min mean wind speed measured in the field survey was $9.1\,\mathrm{m\,s^{-1}}$. The predicted corresponding mean turning moments for this wind speed is in average 24.5 % (range: 16.4 % - 34.5 %) of the critical moments of the trees. Therefore, the models need to be extrapolated over a wide range to predict critical wind speeds, making the estimates susceptible to errors. For the purpose of inter tree comparison, the predicted mean turning moments are normalised by the tree's critical moment ($\hat{M}/M_{crit}$) from Table 3.1. This allows the representation of all nine models in a single plot (see Fig. 3.8). The critical wind speed is reached, when the curves reach unity.

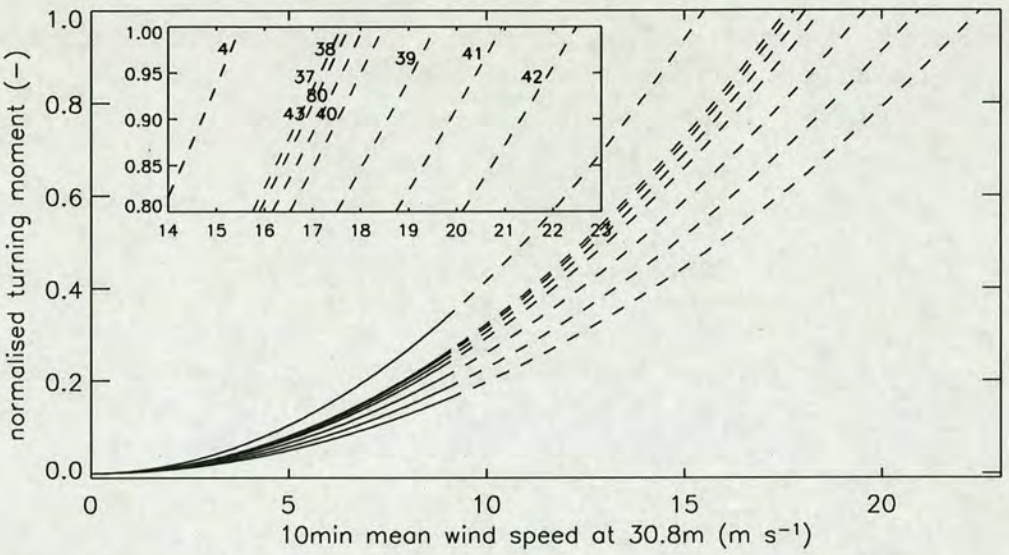

Figure 3.8: Summary of the best fits of the wind turning moment relationships from Figure 3.5. The y-axis is the normalised turning moment ($\hat{M}/M_{crit}$). The solid lines go up to $9.1\,\mathrm{m\,s^{-1}}$, the range which is covered by measurements. Dashed lines indicate extrapolated values. The small figure is a 'blow-up' of the bigger plot for the purpose of clarification. Numbers are the tree IDs.

Estimated mean critical wind speeds for breaking, overturning, and general tree failure (critical turning moment) are $19.8\,\mathrm{m\,s^{-1}}$, $18.8\,\mathrm{m\,s^{-1}}$, and $18.7\,\mathrm{m\,s^{-1}}$. The standard deviations for the three values are $1.56\,\mathrm{m\,s^{-1}}$, $2.20\,\mathrm{m\,s^{-1}}$, $2.06\,\mathrm{m\,s^{-1}}$, indicating that the values for the breaking moments are more similar than for the two other. Tree 4 has the lowest critical wind speed ($15.5\,\mathrm{m\,s^{-1}}$) and tree 42 the highest ($22.5\,\mathrm{m\,s^{-1}}$). From Figure 3.8 the nine trees can be divided into three different groups. The first group consists of five trees (37,38,40,43,80), which all have very similar critical wind speeds within an interval of $0.9\,\mathrm{m\,s^{-1}}$ ($17.6\,\mathrm{m\,s^{-1}}$ to $18.5\,\mathrm{m\,s^{-1}}$). Tree 4, the tree with the lowest slenderness value in the sample, is separated from this group and has a lower critical wind speed. To the right of the group of five individuals are trees 39, 41, 42. Their critical wind speeds are $19.6\,\mathrm{m\,s^{-1}}$, $20.9\,\mathrm{m\,s^{-1}}$, $22.5\,\mathrm{m\,s^{-1}}$. These three trees are the shortest of the group of the nine experimental trees (39: 26.9 m, 41: 24.3 m, 39: 22.8 m)

In Figure 3.9 the predicted mean wind speeds for the three moments (breakage, overturning, critical) are plotted versus several tree characteristics. The predicted critical mean wind speeds for breaking are not significantly correlated with any tree property. Absolute correlation coefficients for the breaking moment are in the

Table 3.3: Predicted wind speeds for breaking (u_{break}), overturning (u_{over}), and tree failure (u_{crit}) derived from the model calculations.

ID	u_{break} ($m\,s^{-1}$)	u_{over} ($m\,s^{-1}$)	u_{crit} ($m\,s^{-1}$)
4	19.6	15.5	15.5
37	17.7	17.6	17.6
38	18.5	17.8	17.8
39	19.6	19.7	19.6
40	18.6	18.5	18.5
41	21.7	20.9	20.9
42	22.5	23.1	22.5
43	19.3	17.8	17.8
80	20.7	18.1	18.1
mean	19.8	18.8	18.7
SD	1.56	2.20	2.06

range 0.06 to 0.33. The fact that the predicted mean turning moment increases linearly with dbh^3 as described above, results in similar wind speeds for breaking for the nine trees. At the same time the standard deviation of the predicted mean wind speed for breaking is small compared to the estimates for the overturning wind speeds.

For the relationships between the predicted critical wind speeds or overturning wind speeds the absolute correlation coefficients are higher than they are for u_{break}. The absolute value for the relationship between u_{crit} and stem weight is 0.81. All correlation coefficients, except those for slenderness, have negative values, what indicates that bigger and taller trees are at higher risk of failure than small trees.

All calculated correlation coefficients are listed in Table 3.4. Since dbh^3 and stem weight are linearly related to the breaking and overturning moment, the Pearson correlation coefficient was calculated for these variables. For the three other parameters Kendall's rank correlation coefficient was calculated, since these parameters are not linearly correlated with the breaking or overturning moment.

3.4 Discussion

The absolute turning moments experienced by the nine experimental trees are very different. For a reference wind speed of $8\,m\,s^{-1}$ at 30.8 m, tree 4 has to

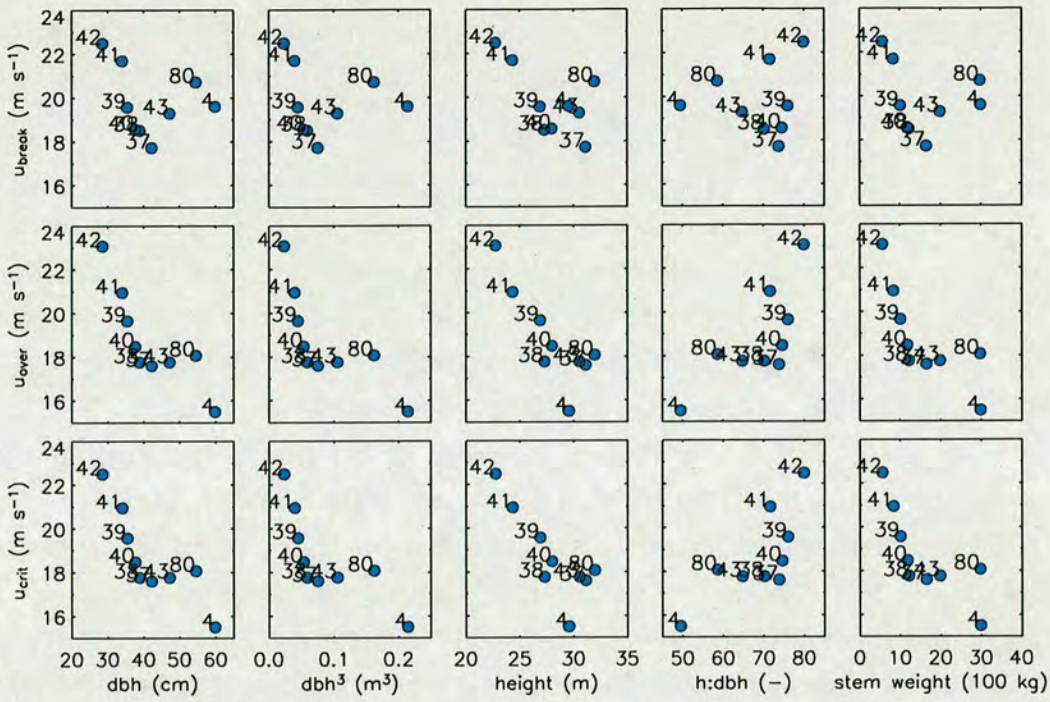

Figure 3.9: Predicted 10 min mean wind speed at 30.8 m for breaking (u_{break}), overturning (u_{over}), and general tree failure (u_{crit}) plotted versus individual tree properties (dbh, dbh^3, height, slenderness, and stem weight).

Table 3.4: Pearson (r) and Kendall's rank correlation (τ) coefficients for the plots in Figure 3.9.

parameter	type	u_{break}	u_{over}	u_{crit}
dbh	τ	-0.28	-0.72	-0.72
dbh^3	r	-0.15	-0.76	-0.78
height	τ	-0.33	-0.56	-0.56
h:dbh	τ	0.06	0.50	0.50
stem weight	r	-0.25	-0.80	-0.81

withstand 129 kNm at the tree base. For the same wind speed tree 42, experiences only 11 kNm, which is less than 10 % of the value for tree 4. These huge differences are caused by differences in exposure and the fact that a vast amount of wind energy is absorbed in the upper parts of the canopy. Tree 4 is a dominant tree, which overtops its adjacent neighbours. Since the tree is taller the cantilever arm of the wind drag is longer compared to a smaller tree, which also increases the turning moment at the tree base. The smaller trees in the sample benefit from a sheltered wind environment, which is due to the wind energy absorption

in the upper parts of the canopy (Baldocchi and Hutchison, 1987). Within the number of experimental trees, the tallest one (80: 31.9 m) exceeds the smallest one (42: 22.8 m) by more than 9 m.

The turning moments for a reference wind speed appear to scale with tree properties which determine the rigidity and anchorage of the tree. Resistance to breakage increases linearly with dbh^3 and the anchorage does so as function of stem weight. The Pearson correlation coefficients for the two relationships *M vs. dbh*^{3} and *M vs. stemweight* in Figure 3.7 are 0.98 and 0.97, respectively. The linear scaling with dbh^3 as an independent parameter indicates that the strain ($\Delta L/L$) at the outer surface is similar for all nine trees. The uniform stress hypothesis states that trees grow to even out the stress for all parts of the tree by allocating biomass in areas that experience higher stress than average (Mattheck, 1990, 1991). The results from this study suggest that this principle is not only applicable for the parts of a single tree but also for adjacent trees in a stand. The last thinning of the stand was conducted 6 years before this field survey. This time frame is long enough for the individual tree to adapt to the new wind exposure conditions (Urban et al., 1994).

The linear scaling shows that there is a balance between exposure to wind loading and resistance to wind damage. The highest calculated critical turning moment for tree 4 (484 kNm) is 5.7 times higher than the lowest one in the sample for tree 42 (85 kNm). However, the big difference makes it hard to imagine that tree 42 would survive if it was one of the tallest members of the stand. Tree 4 already experiences a turning moment of 85 kNm at a wind speed of 6.5 m s^{-1}. This underlines the fact that the survival of smaller trees depends on the presence of taller neighbours, which create a sheltered environment for them. The removal of the dominant trees would leave the stand in a very vulnerable state. A nearby stand in which the frame trees (dominant trees) were removed by mistake suffered from significant wind damage during two gale events in 2005 and 2007 (Haufe, 2007).

For the predicted mean wind speed required to overturn the trees, all absolute values of the correlation coefficients exceed or are equal to 0.68. The fitted models estimate lower critical wind speeds for bigger trees, in terms of *dbh* or height. The results suggest that, in general, bigger trees are at a higher risk of wind damage, which is in agreement with results from Peterson (2004). However, the three tallest trees (4,43,80) exceeded the maximum stem weight of the treepulling data base that was used for modelling the stem weight - overturning moment

relationship (Nicoll et al., 2006). The fact that the estimated breaking moment of tree 4 is 1.6 fold higher than the overturning moment contradicts observations, that these two values are usually similar (Somerville, 1979; Petty and Worrell, 1981; Gardiner et al., 2000). On the other hand Byrne and Mitchell (2007) found a linear relationship between overturning moment and stem weight for Western hemlock (*Tsuga heterophylla* (Raf.) Sarg.), which had stem weight up to almost 3000 kg. There is no obvious reason why the relationship should change for higher stem weight for Sitka spruce as long as the rooting depth is not restricted due to for example a high water table. However, without information from destructive tree pulling tests, this problem cannot be examined in any more detail.

The analysis showed that *dbh* is the best estimator for predicting absolute experienced turning moment and for estimating the risk of wind damage for the experimental trees. The correlation coefficients for *dbh* are higher than they are for slenderness, which is a common parameter for estimating the stability of stands (Cremer et al., 1982; Blackburn and Petty, 1988; Valinger et al., 1993).

3.5 Conclusions

The wind and turning moment relationship for nine mature Sitka spruce trees were analysed with data from a field experiment. The data were used to fit quadratic models for the relationship between wind speed and turning moment, which except for one tree, exceeded 0.75 for the R^2 value.

The measured turning moment increases linearly with the breaking and overturning moments over the whole range of tree properties. However, trees which are exposed to higher wind loading and hence higher turning moments compensate for this by higher resistance. Therefore the differences in experienced turning moment are much more pronounced than they are for the predicted critical wind speeds.

The predicted wind speeds for breaking were only weakly correlated with any of the tested tree properties. For the overturning moment and the critical turning moment the correlation coefficients were higher. For the estimators *dbh*, height, and stem weight, the correlation coefficients are negative, while they are positive for slenderness. This indicates that dominant and co-dominant trees have the highest risk of failure by overturning.

dbh or its derived parameter dbh^3, had the best correlation for predicting the

absolute experienced turning moment and the critical wind speed for trees within the range of tested estimators.

Acknowledgement

The field study took place in an experimental plot established by Arne Pommerening and Jens Haufe from the University of Wales, Bangor. Many people helped in setting up this experiment. Special thanks go to Shaun Mochan, Alexis Achim, and the Technical Support Unit in Talybont, Wales.

References

Baldocchi DD and Hutchison BA, 1987: Turbulence in an almond orchard: Vertical variations in turbulent statistics. *Boundary-Layer Meteorology*, 40, 127–146.

Blackburn GRA, 1997: *The Growth and Mechanical Response of Trees to Wind Loading*. PhD, University of Manchester.

Blackburn P and Petty JA, 1988: Theoretical calculations of the influence of spacing on stand stability. *Forestry*, 61, 235–244.

Byrne KE and Mitchell SJ, 2007: Overturning resistance of western redcedar and western hemlock in mixed-species stands in coastal British Columbia. *Canadian Journal of Forest Research*, 37, 931–939.

Cleugh HA, Miller JM, and Böhm M, 1998: Direct mechanical effects of wind on crops. *Agroforestry Systems*, 41, 85–112.

Coates KD, 1997: Windthrow damage 2 years after partial cutting at the Date Creek silvicultural systems study in the interior cedar-hemlock forests of northwestern British Columbia. *Canadian Journal of Forest Research*, 27, 1695–1701.

Cremer KW, Borough CF, McKinnell FH, and Carter PR, 1982: Effects of stocking and thinning on wind damage in plantations. *New Zealand Journal of Forestry Science*, 12, 244–268.

Dunham RA and Cameron AD, 2000: Crown, stem and wood properties of wind-damaged and undamaged Sitka spruce. *Forest Ecology and Management*, 135, 73–81.

Evans AM, Camp AE, Tyrrell ML, and Riely CC, 2007: Biotic and abiotic influences on wind disturbance in forests of NW Pennsylvania, USA. *Forest Ecology and Management*, 245, 44–53.

Everham III EM and Brokaw NVL, 1996: Forest damage and recovery from catastrophic wind. *The Botanical Review*, 62, 113–185.

Fraser AI and Gardiner JBH, 1967: Rooting and stability in Sitka spruce. Bulletin 40, Forestry Commission.

Gardiner B, Peltola H, and Kellomäki S, 2000: Comparison of two models for predicting the critical wind speeds required to damage coniferous trees. *Ecological Modelling*, 129, 1–23.

Gardiner BA, 1992: Mathematical modelling of the static and dynamic characteristics of plantation trees. In Franke J and Roeder A, eds., *Mathematical modelling of forest ecosystems*, pp. 40–61. J.D. Sauerländer's Verlag, Frankfurt a. M.

Gardiner BA, 1995: The interactions of wind and tree movement in forest canopies. In Coutts MP and Grace J, eds., *Wind and Trees*, chap. 2, pp. 41–59. Cambridge Univ. Press.

Gardiner BA and Quine CP, 1994: Wind damage to forests. *Biomimetics*, 2, 139–147.

Gardiner BA, Stacey GR, Belcher RE, and Wood CJ, 1997: Field and wind tunnel assessments of the implications of respacing and thinning for tree stability. *Forestry*, 70, 233–252.

Gillies JA, Nickling WG, and King J, 2002: Drag coefficient and plant form response to wind speed in three plant species: Burning Bush (*Euonymus alatus*), Colorado Blue Spruce (*Picea pungens* Glauca.), and Fountain Grass (*Pennisetum setaceum*). *Journal of Geophysical Research - Atmospheres*, 107, 4760–4774.

Haufe J, 2007: Sticking your head out – the social status of trees and wind risk – a case study from Clocaenog Forest. Newsletter 26, CCFG.

Holbo HR, Corbett TC, and Horton PJ, 1980: Aeromechanical behavior of selected Douglas-fir. *Agricultural Meteorology*, 21, 81–91.

Jaffe M, 1973: Thigmomorphogenesis: The response of plant growth and development to mechanical stimulation. *Planta*, 114, 143–157.

James JC, Grace J, and Hoad SP, 1994: Growth and photosynthesis of *Pinus sylvestris* at its altitudinal limit in Scotland. *The Journal of Ecology*, 82, 297–306.

Kerzenmacher T and Gardiner B, 1998: A mathematical model to describe the dynamic response of a spruce tree to the wind. *Trees*, 12, 385–394.

Lanquaye-Opoku N and Mitchell SJ, 2005: Portability of stand-level empirical windthrow risk models. *Forest Ecology and Management*, 216, 134–148.

Lavers GM, 1969: The strength properties of timbers. Tech. Rep. 50, Forestry Commission, Edinburgh.

Levy P, Hale S, and Nicoll B, 2004: Biomass expansion factors and root : shoot ratios for coniferous tree species in Great Britain. *Forestry*, 77, 421-430.

Lines R, 1953: The Scottish gale damage. *Irish Forestry*, 10, 3–15.

Mattheck C, 1990: Why they grow, how they grow: The mechanics of trees. *Arboricultural Journal*, 14, 1–17.

Mattheck C, 1991: *Trees: The mechanical design*. Springer-Verlag, Berlin, Germany.

Mayer H, 1987: Wind-induced tree sways. *Trees*, 1, 195–206.

Mayhead GJ, 1973: Some drag coefficients for British forest trees derived from wind-tunnel studies. *Agricultural Meteorology*, 12, 123–130.

Metzger C, 1893: Der Wind als maßgebender Faktor für das Wachstum der Bäume. *Mündener Forstliche Hefte*, 3, 35–86.

Moore JR, 2002: *Mechanical behaviour of coniferous trees subjected to wind loading*. Ph.D. thesis, Oregon State University, Corvallis.

Moore JR, Gardiner BA, Blackburn GRA, Brickman A, and Maguire DA, 2005: An inexpensive instrument to measure the dynamic response of standing trees to wind loading. *Agricultural and Forest Meteorology*, 132, 78–83.

Nicoll BC, Gardiner BA, Rayner B, and Peace AJ, 2006: Anchorage of coniferous trees in relation to species, soil type, and rooting depth. *Canadian Journal of Forest Research*, 36, 1871–1883.

Oliver CD and Larson BC, 1990: *Forest stand dynamics*. John Wiley & Sons Inc, New York.

Oliver H and Mayhead GJ, 1974: Wind measurements in a pine forest during a destructive gale. *Forestry*, 47, 185–195.

Peterson CJ, 2004: Within-stand variation in windthrow in southern boreal forests of Minnesota: Is it predictable? *Canadian Journal of Forest Research*, 34, 365–375.

Petty JA and Worrell R, 1981: Stability of coniferous tree stems in relation to damage by snow. *Forestry*, 54, 115–128.

Rudnicki M, Mitchell SJ, and Novak MD, 2004: Wind tunnel measurements of crown streamlining and drag relationships for three conifer species. *Canadian Journal of Forest Research*, 34, 666–676.

Somerville A, 1979: Root anchorage and root morphology of *Pinus radiata* on a range of ripping treatments. *New Zealand Journal of Forest Science*, 9, 294–315.

Stokes A, Fitter A, and Coutts M, 1995: Responses of young trees to wind and shading: Effects on root architecture. *Journal of Experimental Botany*, 46, 1139–1146.

Stokes A, Nicoll B, Coutts M, and Fitter A, 1997: Responses of young Sitka spruce clones to mechanical perturbation and nutrition: Effects on biomass allocation, root development, and resistance to bending. *Canadian Journal of Forest Research*, 27, 1049–1057.

Telewski F, 1995: Wind-induced physiological and developmental responses in trees. In Coutts MP and Grace J, eds., *Wind and Trees*, chap. 14, pp. 237–263. Cambridge Univ. Press, Cambridge.

Urban ST, Lieffers VJ, and MacDonald SE, 1994: Release in radial growth in the trunk and structural roots of white spruce as measured by dendrochronology. *Canadian Journal of Forest Research*, 24, 1550–1556.

Valinger E, Lundquist L, and Bondesson L, 1993: Assessing the risk of snow and wind damage from tree physical characteristics. *Forestry*, 66, 249–260.

Vollsinger S, Mitchell SJ, Byrne KE, Novak MD, and Rudnicki M, 2005: Wind tunnel measurements of crown streamlining and drag relationships for several hardwood species. *Canadian Journal of Forest Research*, 35, 1238–1249.

Chapter 4

Competition indices as a measure for individual wind loading

Abstract

The wind loading experienced by a tree in a forest stand is influenced by its relative position in the stand. Most of the energy is absorbed in the upper parts of the forest canopy. Hence the dominant trees create a sheltered environment for the smaller ones.

Wind risk models like ForestGALES are at the moment not able to account for any differences in tree properties, because every tree in the stand is considered to have the same properties. With the advent of low impact silviculture systems, which create irregular stand structures, new approaches need to be found.

Simultaneous measurements of wind speed and turning moment were undertaken in an even-aged Sitka spruce plantation forest. The data are used to test the performance of several competition indices in explaining differences in wind loading between nine neighbouring trees.

Results show that the competition indices are able to explain a lot of the variance in wind loading, and indices with high input requirements do not perform better than the simpler ones. The data for two of the trees showed an increased turning moment, when the wind was blowing from a direction with lower competition. However, the amount of data was not sufficient for parametrisation of the impact of gaps.

4.1 Introduction

The drag a solitary tree has to withstand is a function of the wind profile, crown area, and drag coefficient. In a forest the relationship is affected by the presence of neighbouring trees which influence the wind profile and possibly

increase the damping due to crown clashing (Rudnicki et al., 2003, 2008). Therefore a dominant tree has to withstand higher wind loading compared to a suppressed one, which benefits from the shelter provided by its taller neighbours. This is compensated for by higher stiffness and better root anchorage, which increase the resistance to wind damage (Nicoll and Ray, 1996).

This level of complexity is currently not accounted for in wind risk models, because wind-tree interactions are modelled at the stand level scale rather than at the individual tree scale (Gardiner et al., 2000). The models treat each tree in the same way assuming that their properties are equal. Hence every tree in the stand is exposed to the same drag, has the same critical turning moment and therefore the same risk of damage by the wind. As foresters in Britain are encouraged to manage more stands under low impact silvicultural systems, this will increase the number of irregular stands, and creates a demand for predicting the response of trees on an individual tree level (Rojo and Orois, 2005).

The hypothesis for this chapter is that competition indices are a suitable tool to predict wind loading at an individual tree level. Such indices are often used in growth models (Courbaud et al. (2001); Pretzsch et al. (2002); Stadt et al. (2007); Schröder et al. (2007)). A correlation between competition indices and wind loading would allow a straight forward linking of growth and wind risk models. At the same time it would allow the simulation of different forest management practises and their impact on the risk of wind damage. Following this, the approach could then be used to identify best management practise. This is of particular importance in Britain, where the transformation of regular into irregular stands is a major goal for forestry (Mason, 2002). This aim can only be achieved by creating a light regime at the forest floor, which allows the establishment of natural regeneration. Therefore thinning is inevitable, which at least in the short term can compromise the stability of the stand (Page et al., 2001; Hale et al., 2004).

4.2 Material and methods

4.2.1 Site characteristics

The field experiment was conducted from May until November 2005 in a pure Sitka spruce (*Picea sitchensis* (Bong.) Carr.) stand in Clocaenog Forest, North Wales (53°07′40″N, 3°42′96″W, 395 m a.s.l.). The stand was established as a row

mixture of Sitka spruce and Scots pine (*Pinus sylvestris* L.) or lodgepole pine (*Pinus contorta* Dougl. ex Loud.) in 1951 and was thinned three times since (1975, 1993, and 1999).

Stand density was 292 trees ha^{-1} and basal area was 30.8 m^2 ha^{-1} (2002). The floor is amply covered by about 10 year old natural regeneration. The current state of the stand can be seen as starting point of a successful transformation towards an irregular stand structure (Schütz, 2001).

4.2.2 Tree characteristics

In total nine trees were chosen as experimental trees, which were arranged in a 3×3 array. Due to the maturity of the stand the nine trees differ widely regarding their properties. The height of the tallest tree (80: 31.9 m) exceeds the smallest one (42: 22.8 m) by more than 9 m. For each tree the crown radius was measured by going from the trunk to the crown edge at different angles. A stick was placed vertically beneath the crown edge. For each point the angle and distance to the trunk was measured. The average crown radius was calculated as the radius of a circle with the same area as the measured polygon. For the competition indices the neighbouring trees have to be defined. To do this the tree positions were used to create a Voronoi mosaic. Trees are considered as neighbours if they share the same side of one of the polygons. Table 4.1 lists the properties of the nine experimental trees as well as their neighbours.

Table 4.1: Mensurational and positional data for the nine experimental trees. Measurements were taken in 2005. (h: height, dbh: diameter at breast height, cr-rad: average crown radius, cr-class: crown class)

ID	h (m)	dbh (cm)	cr-rad (m)	neighbours (ID)	cr-class
4	29.6	59.8	4.2	[2,3,5,6,38,42]	dom
37	31.1	42.2	2.8	[36,38,39,77,79,80,502]	dom
38	27.3	38.9	2.9	[3,4,35,36,37,39,40,42]	co-dom
39	26.9	35.4	2.9	[37,38,40,41,80]	co-dom
40	28.0	37.6	2.5	[38,39,41,42,43]	co-dom
41	24.3	34.0	3.1	[39,40,43,46,80,83,84]	surp
42	22.8	28.5	2.1	[4,6,8,38,40,43,44,45]	surp
43	30.5	47.2	3.1	[40,41,42,45,46]	dom
80	31.9	54.5	3.6	[37,39,41,79,81,84,85]	dom

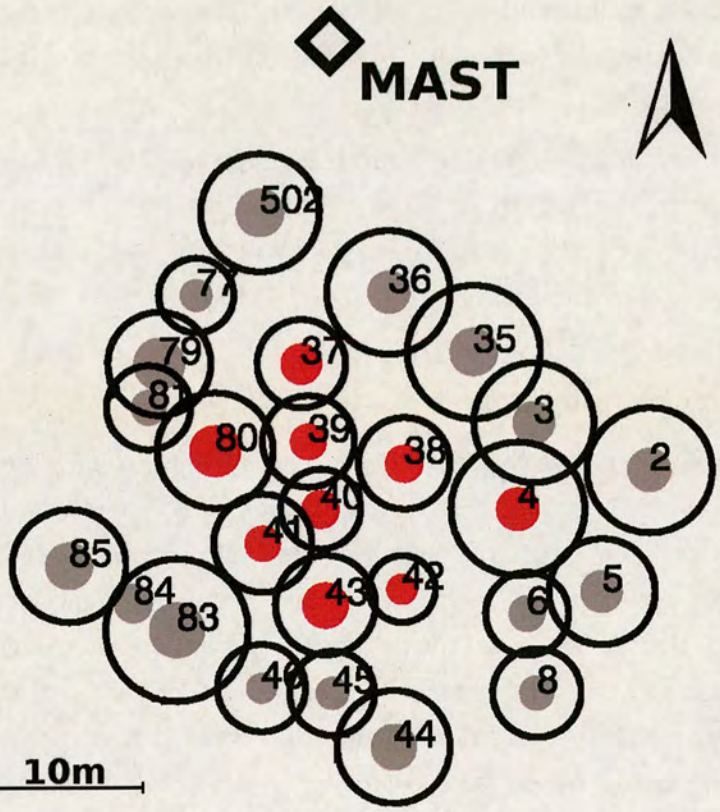

Figure 4.1: Map showing the nine experimental trees (red circles) and their direct neighbours (grey circles). The black circles represent the crown radii. Note that the meteorological mast was located inside the forest stand. Because the experimental trees were located at the edge of the plot, the coordinates of the trees around the mast are unknown.

4.2.3 Instrumentation

General

No mains was available at the site. Because the logging system was relatively power demanding, the decision was made that it would only be switched on when a gale event was expected. In total more than 400 hours of data were gathered between May and November 2005. The measured maximum hourly mean wind speed was $8.3\,\mathrm{m\,s^{-1}}$. All available hourly data values are shown in Figure 4.2.

Wind measurements

A 30 m tall mast (TallTower, NRG Systems, US) was erected in the forest in proximity to the nine experimental trees (see Fig. 4.1). The mast was equipped

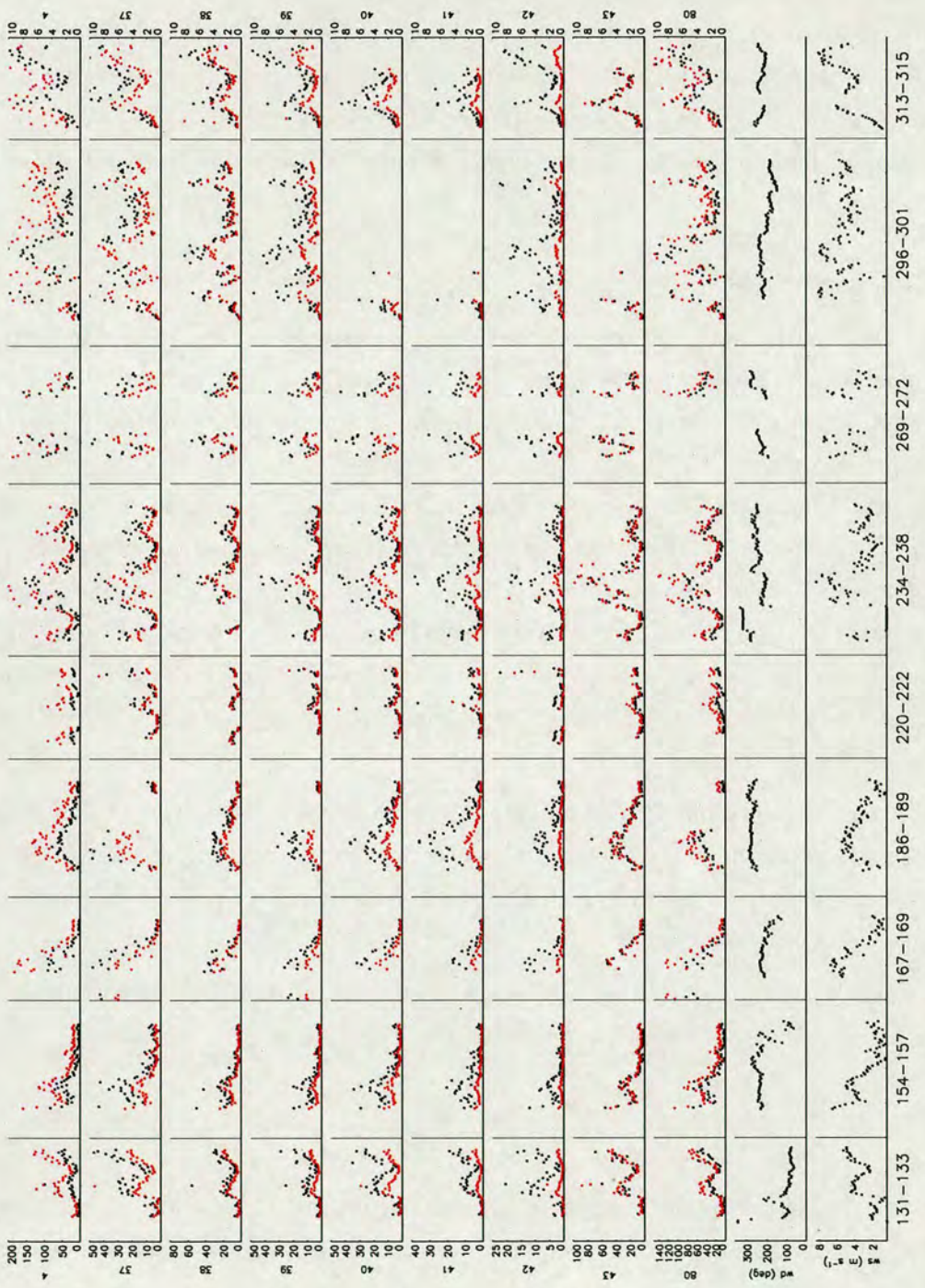

Figure 4.2: Time series of all available hourly maximum (y-axis on the left hand side, black dots) and mean (y-axis on the right hand side, red dots) turning moments in kNm for the nine experimental trees. The scaling of the ordinates varies between plots. The two bottom graphs are mean wind direction (wd) at 27.0 m and hourly mean wind speed at 30.8 m height (ws). The time series are not continuous. The numbers at the bottom indicate the julian day 2005 for each section separated by vertical lines.

with eight cup anemometers (heights (m): 5, 10, 15, 18, 21, 24, 27, 30.8; NRG#40, NRG Systems, US) and two wind vanes (heights (m): 15, 27; NRG#200P, NRG Systems, US). The four upper cup anemometers and the wind vanes were logged every 3 s using a 21X data logger (Campbell Scientific, Logan, US). The lower four cup anemometers were logged once a minute by another data logger (Holtech, Durham, UK).

Turning moments

The wind induced turning moments were measured on nine trees using strain transducers (Blackburn, 1997; Moore et al., 2005). Each experimental tree was equipped with two strain transducers, which were screwed orthogonally into the trunk at about 1.3 m height. To achieve sufficient resolution the two strain gauges of each transducer were incorporated into a Wheatstone bridge, which was completed with two precision resistors (348 Ω). The signal was measured using a differential channel of a CR10 data logger (Campbell Scientific, Logan, US) at 4 Hz. The data loggers were programmed to use an excitation of 2.5 V and to use the highest possible resolution (0.33 μ V). All CR10s were part of a RS485 network. An industrial PC provided data storage, which stored all raw data as plain text files.

From the formulas by Moore and Maguire (2004) the eigenfrequencies of the nine experimental trees are calculated to be in the range 0.24 to 0.33 Hz (mean: 0.28 Hz). This means that a single sway circle is covered by about 16 measurements.

Tree bending causes a change in distance between the two points where the strain transducer is screwed into the trunk. The definition of strain is:

$$\varepsilon = \frac{\Delta L}{L} \tag{4.1}$$

where ΔL (m) is the change in distance and L (m) the total distance between the attachment points. The bending causes a change in electrical resistance of the active strain gauge, which can be measured as voltage across two legs of a Wheatstone bridge. The measured strain is linearly correlated to the wind induced turning moment. To be able to relate the strain signal to the turning moment it is necessary to calibrate each strain transducer individually by stepwise pulling of the experimental trees into two directions while measuring the applied force using a load cell (Model 616, Tedea Huntleigh, US). The applied turning

moment is calculated as:

$$M = F \cdot cos(\alpha) \cdot h \tag{4.2}$$

where F (N) is the applied force measured by a load cell, α (°) the rope angle, and h (m) the height of the anchor point on the experimental tree. For all strain transducers a linear relationship between turning moment and signal output was measured. The slope of the regression line was used as calibration coefficient. For a more extensive description of the calibration procedure see Appendix A.

4.2.4 Turning moment coefficient

Drag (F_D) is defined as the force exerted by a fluid on an object and is calculated as:

$$F_D = \rho \cdot \int_0^z C_D(z) \cdot A(z) \cdot u(z)^2 \, dz \tag{4.3}$$

where ρ ($1.226\,\mathrm{kg\,m^{-3}}$) is air density, C_D ($-$) is the dimensionless drag coefficient, A ($\mathrm{m^2}$) is the projected crown area, u ($\mathrm{m\,s^{-1}}$) is the horizontal wind speed, and z (m) is height above ground. In contrast to buildings trees cannot be considered as rigid obstacles with a constant projected area. Trees streamline in the wind and therefore C_D and A themselves are functions of wind speed (Mayhead, 1973; Rudnicki et al., 2004). However, as a simplification of Equation 4.3 the drag can be described as a function of a reference wind speed where:

$$F_D \propto u^2 \tag{4.4}$$

If in a next step it is assumed that the drag acts as a point load then the drag is also proportional to the turning moment a tree experiences. Hence the turning moment is proportional to squared wind speed:

$$M \propto u^2 \tag{4.5}$$

The data from this field study show that the suggested relationship is valid for the wind speed range of the experiment. The simplifications allow us to calculate the **T**urning **M**oment **C**oefficient (TMC in kg) for each experimental tree, which

is defined as fraction of experienced turning moment and squared wind speed at 30.8 m height:

$$TMC = \frac{M}{u^2_{30.8m}} \tag{4.6}$$

A graphical illustration of the TMC is the slope of the regression line of the measured turning moments plotted against the squared horizontal wind speed as it is shown in Figure 4.3.

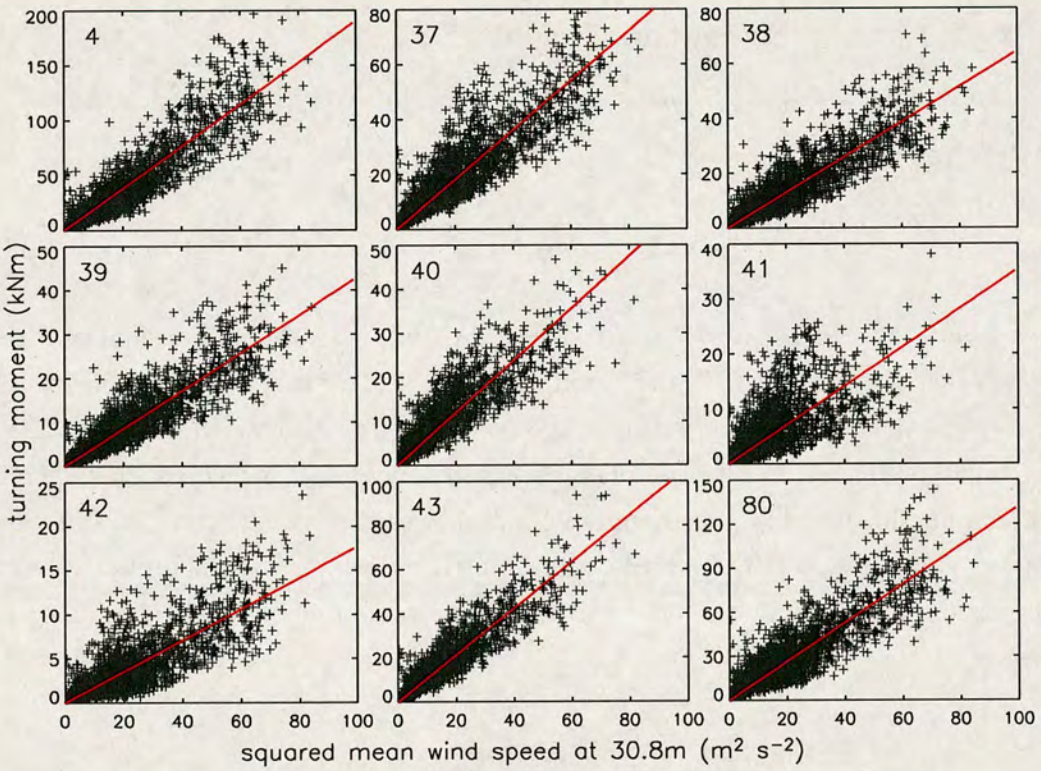

Figure 4.3: Maximum turning moments of 10 min time intervals plotted versus squared mean wind speed at 30.8 m. Note that the scales of the ordinate vary. The red lines are the best fit of a linear regression.

The calculated TMCs are listed in Table 4.2. Taller and therefore more exposed trees (ID: 4,37,43,80) have higher values than more suppressed trees.

Table 4.2: Turning moment coefficient (TMC), Pearson correlation coefficient (r), and number of data points used for the regression analysis.

ID	TMC (kg)	r	n
4	1.91	0.91	2338
37	0.90	0.88	2228
38	0.64	0.89	2295
39	0.43	0.89	2236
40	0.60	0.87	1798
41	0.35	0.68	1782
42	0.18	0.82	2336
43	1.06	0.91	1797
80	1.32	0.87	2146

4.2.5 Competition indices

Trees within a forest stand find themself in permanent competition for resources like light and nutrients. Availability of these resources has an impact on the photosynthetic rate, which itself governs biomass production and growth rate. Since dominant trees are more exposed to light and have increased total leaf area, they can photosynthesise more.

A coarse qualitative approach is the subdivision of the trees into four crown classes (1) dominant, (2) co-dominant, (3) subdominant, and (4) suppressed. A finer and non-discrete quantification can be achieved using distant dependent competition indices, which take the relation of tree properties of a subject tree and its neighbours into consideration. Many different indices have been developed, with differing data demands. A wide range of indices, which require just tree position and one additional tree characteristic (e.g. diameter at breast height, height), have been used and gave satisfying results for describing crown properties (e.g Rouvinen and Kuuluvainen, 1997). Good correlation has been found between competition indices and individual tree growth (e.g. Stadt et al., 2007; Mailly et al., 2003). Hence such approaches are often used as basis for growth simulators (e.g. Pretzsch et al., 2002).

For all the used indices a neighbour of the subject tree is defined as a tree, which shares a side of the Voronoi mosaic with the subject tree. Tree positions are used for the determination of the polygons (Aurenhammer and Klein, 2000).

h:dbh - slenderness

The height to diameter at breast height ratio (*h:dbh*) - also called slenderness - does not take tree position into account. Thus it is called a distance independent index. Several authors used the ratio at the stand level as a measure of stability (Wonn and O'Hara, 2001; Kenk and Guehne, 2001). Stands with lower ratios are regarded as more stable. Achim et al. (2005) used a similar approach to rate the stability of Canadian balsam fir (*Abies balsamea* (L.) Mill.) stands.

Indices by Rouvinen and Kuuluvainen, 1997

Rouvinen and Kuuluvainen (1997) compared the performance of several competition indices to describe crown properties of natural mature Scots pine trees in Finland. Here their indices numbered 10 to 12 are used, which are defined in the appendix of their article.

These three indices only require *dbh*, tree height of the neighbouring trees, and distance to the neighbours what makes these indices distance-dependant. The equations for the three indices are:

$$CI_{10} = \sum_{i=1}^{n} \frac{\frac{dbh_j}{dbh_i}}{dist_{ij}} \tag{4.7}$$

$$CI_{11} = \sum_{i=1}^{n} \frac{\frac{dbh_j}{dbh_i}}{dist_{ij}^{\,2}} \tag{4.8}$$

$$CI_{12} = \sum_{i=1}^{n} \frac{\left(\frac{dbh_j}{dbh_i}\right)^2}{dist_{ij}} \tag{4.9}$$

where *dbh* (m) is diameter at breast height, i and j represent neighbour and subject tree, respectively. $dist_{ij}$ (m) is the distance between subject and objective tree. The impact of all neighbours is accounted for by summing the individual values up over the number of neighbours (n).

Hegyi Index

The method of distant dependent competition indices was developed by Hegyi (1974). The formula we use here is:

$$CI_{\text{Hegyi}} = \sum_{i=1}^{n} \frac{(\frac{cr_j}{cr_i})^{1.3}}{dist_{ij}^{0.4}} \tag{4.10}$$

where cr (m) is the average crown radius and $dist_{ij}$ (m) the horizontal distance between subject tree and competitor. The index is the sum of the values calculated for each neighbour.

Schütz-Index, 1989

Competition in mixed species stands is more complicated compared to monocultures, because the crown shape of the species differ. Schütz (1989) developed a competition index which uses crown dimension to take this into account. This index is the most demanding in terms of data requirements:

$$CI_{\text{Schütz}} = \sum_{i=1}^{n} 0.5 - \frac{dist_{ij} - (cr_j + cr_i)}{(cr_j + cr_i)} + 0.65 \cdot \frac{h_i - h_j}{dist_{ij}} \tag{4.11}$$

where n is the number of neighbours, h (m) is tree height, $dist_{ij}$ (m) is the distance between subject tree and competitor, and cr (m) is the mean crown radius. A difference of 1 m in tree height between two trees has the same impact as a decrease of the horizontal distance between those two trees of 1.5 m. The equation is applied for every neighbour and the sum over all competitors is the value of the competition index. A neighbouring tree is only considered as competitor if the calculated value is greater than zero.

Table 4.3: Competition indices for the nine experimental trees. For description see text.

ID	h:dbh	CI_{10}	CI_{11}	CI_{12}	CI_{Hegyi}	$CI_{\text{Schütz}}$
4	49.4	0.55	0.08	0.37	1.85	2.01
37	73.7	0.91	0.13	0.92	3.80	0.66
38	70.1	1.11	0.15	1.26	4.16	2.81
39	75.9	1.07	0.20	1.28	2.61	3.59
40	74.5	0.92	0.18	1.43	3.01	1.91
41	71.6	1.33	0.22	1.75	3.03	5.46
42	79.9	1.51	0.21	2.31	5.65	4.58
43	64.7	0.60	0.11	0.41	1.98	0.14
80	58.6	0.68	0.10	0.48	2.18	0.68

4.2.6 Modified competition index

Wind is a vector and is therefore not just determined by its absolute value but also by direction. Taking this into consideration for the calculation of competition indices means, that the tree position in relation to the wind direction should be taken into consideration. Neighbouring trees, which are located on the leeward side of the subject tree, do not have a sheltering effect on the subject tree. At the same time it seems sensible to weight neighbours which line up with the wind direction higher than those, whose angle deviates from the wind direction. Here the deviation from the wind direction is weighted in an interval from zero to unity for the interval [0:90] degrees using a cosine function.

The mathematical expression for the modified Schütz index looks like:

$$CI_{\text{Schütz}} = \sum_{i=1}^{n} I(wd) \cdot \left(0.5 - \frac{dist_{ij} - (cr_j + cr_i)}{(cr_j + cr_i)} + 0.65 \cdot \frac{h_i - h_j}{dist_{ij}}\right) \tag{4.12}$$

$$I(wd) = \begin{cases} 0 & if \quad |\text{angle} - \text{wd}| \geq 90, \\ cos(angle - wd) & if \quad |\text{angle} - \text{wd}| < 90. \end{cases}$$

where wd (°) is wind direction and $angle$ (°) is the angle between competitor and objective tree. For an illustration see Figure 4.4

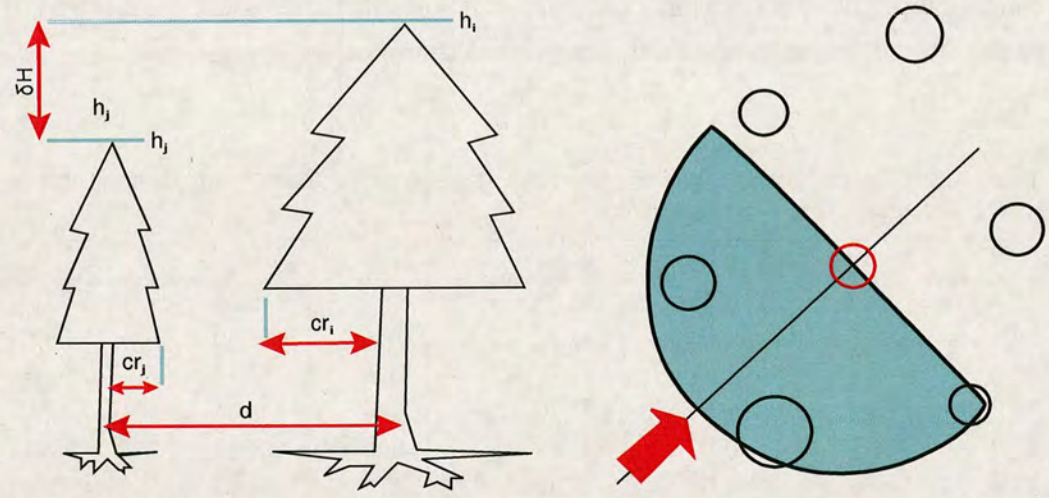

Figure 4.4: Illustration of the Schütz index (left hand side) and schematic explanation of the modified Schütz Index (right hand side). Only trees located within the half circle are considered as neighbours. The red thick arrow in the lower left corner indicates the wind direction.

4.2.7 Thinning scenarios

The maintenance of an irregular stand structure requires regular thinning to create a light regime at the forest floor which encourages the establishment and survival of natural regeneration (Hale, 2003; Hale et al., 2004). For the experimental stand three different thinning scenarios were simulated. For the purpose of comparison the removed basal area is the same for the three scenarios. The basal area, which is removed during one thinning operation is 20 % of the original value (30.8 m^2). The three scenarios differ in the way the harvested trees are selected. In the sections below the three scenarios are briefly described.

From above

The thinning scenario *from above* targets the tallest trees in the stand. All trees are ranked by height and the tallest tree is removed. This is iterated until the target basal area is reached. Neighbours of any harvested tree are preserved from cutting to avoid the creation of bigger gaps. 40 trees need to be harvested to reach the target basal area.

From below

In the *from below* scenario the smallest trees in the stand are removed. As in the scenario *from above* adjacent trees are supposed to remain in the stand. However, due to the smaller diameters of the harvested trees more trees need to be removed and it is not possible to meet the basal area target without removing adjacent trees. This thinning scenario removes 74 trees.

Neutral

The *neutral* scenario has the aim to remove the same percentage of trees in every *dbh*-class (3 cm bin size). Again no adjacent trees were removed. This is the only scenario which contains a certain degree of randomness. The trees are not ranked in any way before the first tree is chosen. For every step only the *dbh*-class is defined from which a tree is chosen. The tree which is harvested from this class is selected randomly after making sure that none of its neighbours has already been removed. The number of trees that is harvested to reach the 20 % target is 60.

For every tree in the stand the critical turning moment is calculated using the formulas, which are implemented in the ForestGALES model (Dunham et al., 2000; Gardiner et al., 2000). The critical turning moment is the lower of the two values breaking and overturning moment. At the same time the competition

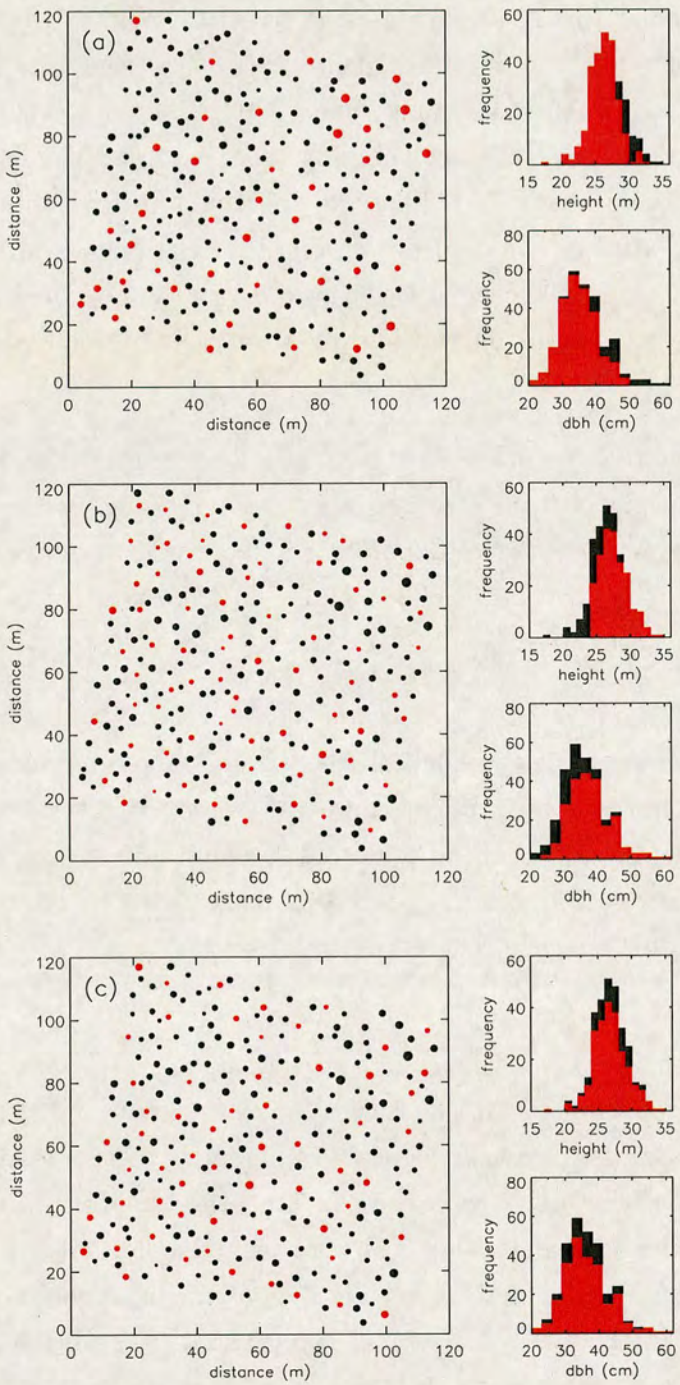

Figure 4.5: Thinning scenarios for the Clocaenog stand (a) from above, (b) from below, and (c) neutral. Circles represent the trees and are scaled by dbh. Red circles represent trees that are harvested. The bar plots on the right hand side are the distributions of height and dbh before (black) and after (red) thinning. The bin size is 1 m and 3 cm, respectively.

indices for all of the trees in the stand are calculated and the critical wind speeds (u_{crit}) are estimated from the relationship between TMC and critical turning moment (M_{crit}), where TMC is calculated as a function of a competition index. The critical wind speed for the trees of the stand are calculated as:

$$u_{crit} = \sqrt{\frac{M_{crit}}{TMC}} \quad \text{where} \quad TMC = f(CI) \tag{4.13}$$

4.3 Results

4.3.1 TMC versus competition indices

In Figure 4.6 the TMCs are plotted against six competition indices. As expected the competition indices are negatively correlated with TMC. All coefficients of correlation (see Tab. 4.4) have a magnitude greater than 0.6 indicating that the indices explain most of the variance. The best data fitting is achieved for the simplest index (*h:dbh*). Because this index is not distant dependent, the removal of an adjacent tree would not cause a change in competition and the regression model would not predict a higher TMC. Therefore we regard the *h:dbh* ratio more as a result of the competition process and adaptive growth of the tree rather than an independent variable itself.

In five of the six plots in Figure 4.6 tree 4 is an outlier. Tree 4 is the most dominant tree in the sample and its measured TMC is in all cases higher than the modelled one. In four out of six cases the correlation coefficients increase when tree 4 is removed from the analysis (see Tab. 4.4).

4.3.2 Impact of wind direction on TMC

The influence of wind direction on the turning moment coefficient is tested for trees 4 and 37. The calculated modified Schütz indices for the two trees show variation, when it is plotted as a function of direction (see Fig. 4.7). Two wind sectors of 40° width were chosen for comparison. The first sector is [240:280] degrees and the second one covers the sector [150:190] degrees. The centres of the two sectors are aligned perpendicularly. Most gale events at the experimental

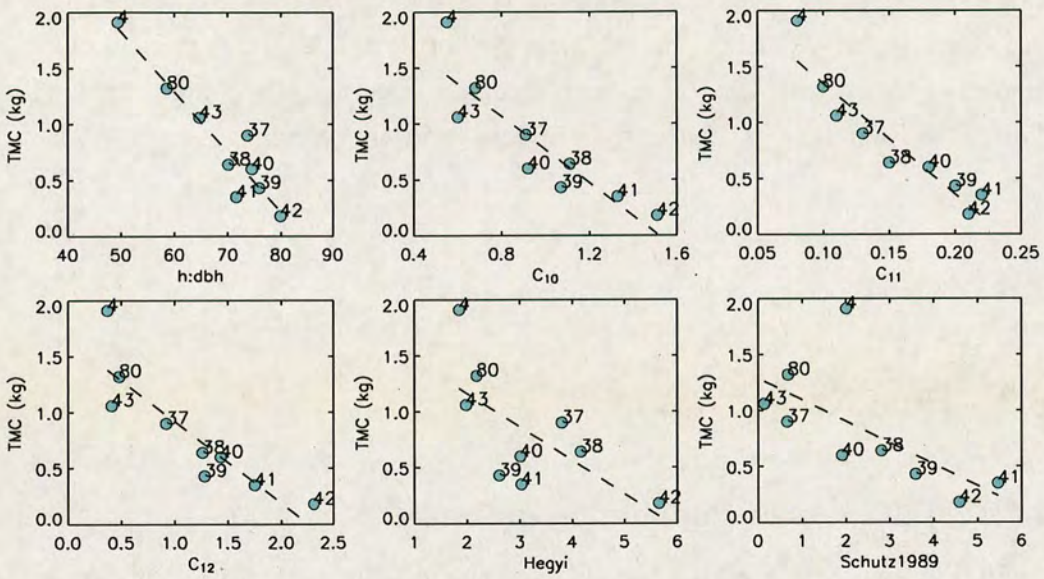

Figure 4.6: Turning moment coefficients (TMC) plotted against the six competition indices. The dashed lines represent the best fit of a linear regression.

site come from a south-westerly to westerly direction, which is also the overall prevailing wind direction. The high values for the southerly sector belong to a single gale event. Due to the lack of gale events from other directions the comparison is limited to these two wind sectors.

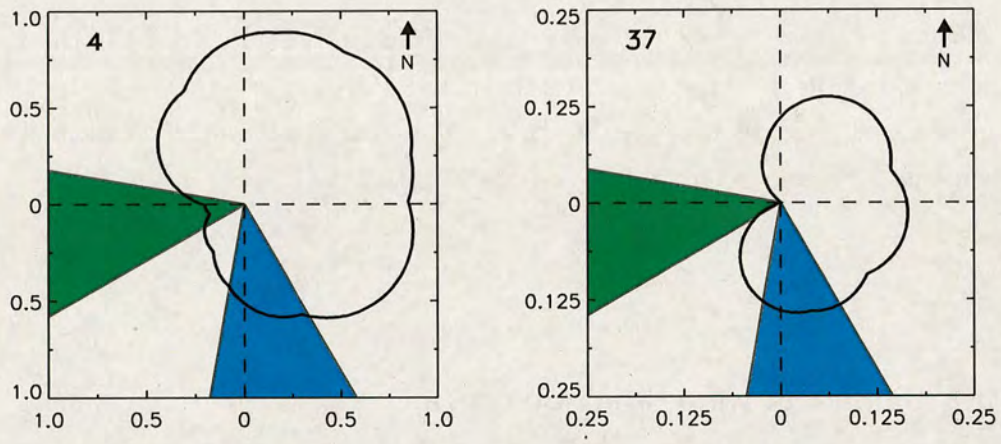

Figure 4.7: Polar plot of the modified Schütz index for tree 4 and tree 37. The green areas represent the wind sector [240:280] and the blue areas the wind sector [150:190] degrees. These are the two sectors, which are used for the regression analysis in Figure 4.8 and Table 4.5.

The sitemap in Figure 4.1 shows gaps in westerly direction for tree 4 and

Table 4.4: Correlation coefficient and root mean square errors (RMSE) for the six plots in Figure 4.6. The coefficients are calculated for data sets *with* and *without* tree 4.

CI	all trees		without ID 4	
	r	RMSE	r	RMSE
h:dbh	-0.95	0.17	-0.88	0.32
CI_{10}	-0.89	0.23	-0.92	0.41
CI_{11}	-0.94	0.18	-0.96	0.37
CI_{12}	-0.89	0.24	-0.94	0.34
CI_{Hegyi}	-0.68	0.38	-0.63	0.34
$CI_{Schütz}$	-0.65	0.39	-0.89	0.40

tree 37. In this direction competition is reduced for both trees as it can be seen in Figure 4.7. Since for the modified Schütz index fewer trees are considered as competitors, the absolute values are lower than the ones in Table 4.3. Two tall neighbouring trees (5: 27.8 m, 6: 27.4 m) result in higher competition for the southerly wind direction compared to the westerly one for tree 4. The neighbours (77: 21.6 m, 79: 28.6 m) in westerly direction of tree 37 are smaller than tree 37, which results in very low competition for this direction.

The analysis of the two data pools results in two different regression lines, which are shown in Figure 4.8. The slopes of the regression lines are for both trees higher if the wind is coming from a westerly direction (green line). If the wind is blowing from a westerly direction the trees experience higher turning moment for the same wind speed compared to the southerly direction (blue line). The results of the regression analysis are summarised in Table 4.5.

4.3.3 Impact of thinning on stability

Crown area data are only available for the nine experimental trees and their direct neighbours. Therefore it was not possible to use either the *Hegyi*-Index or the *Schütz*-Index. As the distant independent index *h:dbh* ratio does not change after a thinning it was also disregarded. Therefore the three indices (C_{10}, C_{11}, C_{12}) from the work of Rouvinen and Kuuluvainen (1997) were used. Only the result of index C_{10} are presented here. This index has been chosen even though it does not have the highest coefficient of correlation. However the differences with C_{11} and C_{12} are not significant and due to the fact that the independent parameters are only used in a linear way makes it less prone to measurement error. All values of u_{crit} for individual trees were then calculated and frequency plots calculated

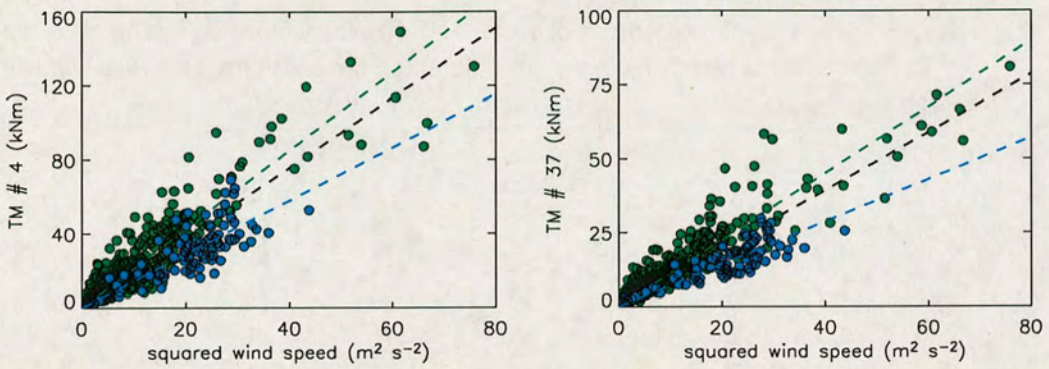

Figure 4.8: Turning moment plotted versus squared wind speed for tree 4 and tree 37. Green data points represent the wind sector [240:280] degrees and blue data points are for the wind sector [150:190] degrees. The green and blue lines represent the best fit of a linear regression for the two different wind sectors, whereas the black line is the best fit for all data points.

of the distribution of all the trees in the plots as a function of the class of critical wind speed. Due to some outliers values between the 10^{th} and 90^{th} percentile are used for analysis.

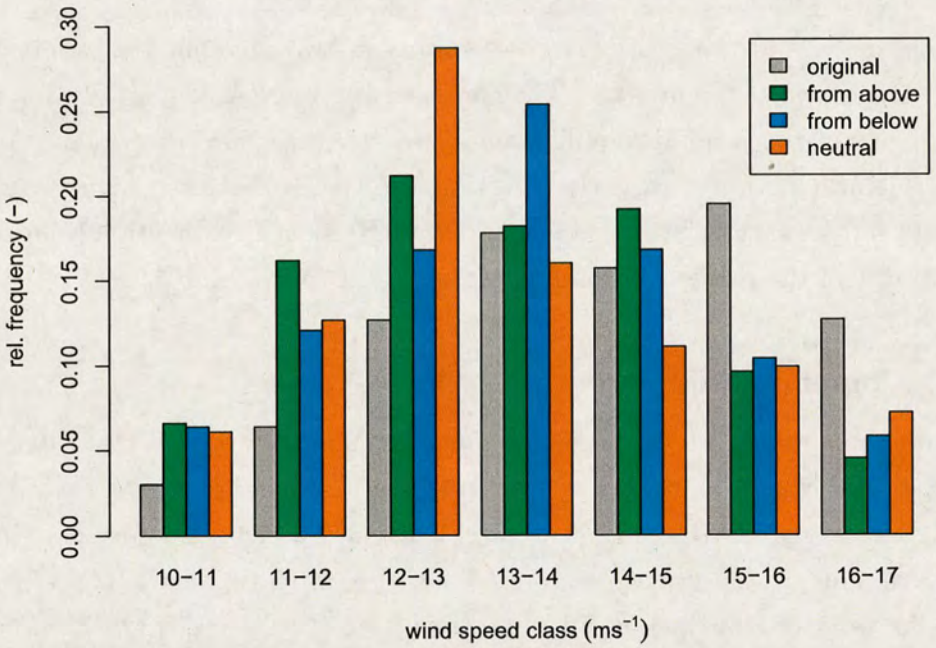

Figure 4.9: Distribution of calculated wind speeds causing tree failure in the range 10–17 m s^{-1} for the experimental stand in Clocaenog Forest before and after the application of the thinning scenarios.

Figure 4.9 shows that all three thinning scenarios leave a stand behind which

Table 4.5: Values for the regression analysis in Figure 4.8.

sector	A [240:280] (deg)	B [150:190] (deg)	$A \cup B$ [240:280] $\cup$ [150:190] (deg)
	Tree 4		
slope (SE)	2.12 (0.031)	1.44 (0.040)	1.89 (0.029)
r	0.91	0.93	0.89
SE	9.75	8.8	10.9
n	441	104	545
	Tree 37		
slope (SE)	1.12 (0.016)	0.71 (0.016)	0.98 (0.015)
r	0.92	0.95	0.89
SE	4.84	3.61	5.68
n	404	102	506

is less stable than the original one. For the original stand the critical wind speed class 15–16 $\mathrm{m\,s^{-1}}$ is the one with the highest number of members. The harvesting causes a shift of the median value to lower wind speed classes.

The change in frequency in the wind speed class 10–11 $\mathrm{m\,s^{-1}}$ is very similar for all three scenarios. About 3 % more trees are members of this wind speed class after the thinning compared to the stand before the thinning. The superiority of the *from below* scenario can be seen in the two next wind speed classes 11–12 $\mathrm{m\,s^{-1}}$ and 12–13 $\mathrm{m\,s^{-1}}$. In those two classes the *neutral* and *from above* scenario gain more trees than the *from below* scenario. The *neutral* scenario has the highest gain in the wind speed class 12–13 $\mathrm{m\,s^{-1}}$.

The three management scenarios and their influence on the critical wind speed are summarised in Table 4.6. The mean critical wind speeds for the three scenarios are similar. This is to some extend surprising. The reason for this is the fact that almost twice as many trees needs to be harvested for the *from below* scenario compared to the *from above* scenario. Due to the smaller numbers less trees are affected in the *from above* scenario. However, trees that are affected experience a bigger change of the competition index and hence a bigger change in wind loading. Hence the mean values in Table 4.6 give only limited information. The stability of a stand is better defined by its weakest members.

The differences for the *from below* scenario in comparison to the two others would have been more pronounced if no adjacent trees had been harvested. It is believed that a lower target basal area, which could have been achieved without

the removal of adjacent trees, would have resulted in more pronounced advantage of this scenario. However, the ranking of the mean critical wind speed is as expected. The *from below* scenario has the highest value, followed up by the *neutral* scenario. The *from above* scenario leaves the stand in the most vulnerable condition.

Table 4.6: Summary of the three thinning scenarios. Total basal area of the stand before thinning was 30.8 m^2. Calculated critical wind speed for the original stand is calculated as 14.6 $m\,s^{-1}$.

	from above	from below	neutral
BA removed (m^2)	6.31	6.17	6.25
BA removed (%)	20.5	20.1	20.3
trees removed	40	74	60
mean u_{crit} ($m\,s^{-1}$)	13.2	13.6	13.4
median u_{crit} ($m\,s^{-1}$)	13.2	13.5	13.0
SD u_{crit}	1.3	1.3	1.5

4.4 Discussion

The correlation coefficients for competition and TMC have all negative values. Lower competition is associated with higher TMCs, i.e. higher turning moment for a certain wind speed. The correlation coefficients for the indices that were used in this work are in the range of -0.63 to -0.96, which indicates that competition is able to explain a lot of the observed variance. The range of indices used suggest that more input data demanding indices do not perform better than simple ones. In fact the most data demanding indices ($CI_{\text{Schütz}}$ and CI_{Hegyi}), which both use crown information, have the lowest correlation coefficients. In this study average crown radius was used as a parameter. Thus irregularities in crown shape are not accounted for and might be an inappropriate simplification. But even an irregularly projected crown shape would not account for the fact that the crown is a three dimensional body. The complexity of the crown shape and the difficulties to measure it makes it an unfavourable and impractical parameter. Detailed and reliable crown information are difficult to collect from the ground without destructive sampling. Remote sensing data might deliver such data in the future but at the moment they are not widely available.

The analysis of two different wind sectors for tree 4 and tree 37 revealed that the TMC is also a function of wind direction. Taking this into consideration requires information about the positions of neighbouring trees in relation to the wind direction. Trees on the leeward site can be neglected, because they do not have any impact on the exposure of the tree. At the same time trees, which are in alignment with the prevailing wind direction, should be weighted more than those which are positioned at an angle from the wind direction. The equations and relationships used here should be considered as a suggestion. The data from this field study are not sufficient for a complete parametrisation.

Low competition in one direction can be caused by gaps. In case of tree 4 an extraction track skirts in westerly direction, which results in lower competition from this direction. This also has an impact on the wind loading and the TMC, which is bigger for the direction with lower competition. The same behaviour was observed for tree 37. Stacey et al. (1994) estimated that "a gap of 15 m (one tree height) doubles the turning moment". Because of their abrupt increase of wind loading for the upwind trees, creating gaps should be avoided by all means.

This is the first time that the turning moments of individual trees have been related to competition indices. Therefore it is not possible to make general conclusions and at the moment the results cannot necessarily be transferred to the conditions of other stands than the experimental one. Since the normal rotation period is less than the age of the Clocaenog stand and because clearfelling was until recently the standard management, the stand structure and the low stand density has to be considered as extraordinary for Britain. Due to the low stand density there is always space between neighbouring tree crowns and therefore it can be assumed that crown clashing is irrelevant for the analysis of the wind and tree interaction in this stand. The sitemap in Figure 4.1 suggests that some of the crowns overlap, but this is an artifact, caused by the projection of the maximum crown radii. A three dimensional view would show that there is always space between the crowns at all heights (see also fisheye photographs in Appendix B). It is known that crown clashing is an efficient way for trees to damp swaying and inhibits the occurrence of otherwise higher turning moments (Milne, 1991; Rudnicki et al., 2003). Hence, such a collective of trees can be much more stable than the individuals themselves would appear to be.

The three thinning scenarios create stands with different stability. The most stable stand is created by the *from below* scenario, followed by the *neutral* scenario and the *from above* scenario. For the calculations of critical wind speeds the

assumption is made that the intervention has no impact on the wind profile. This is only true to a certain degree, because the roughness of the underlying surface has an influence on the wind profile. The method used is restricted to thinning regimes that do not remove too much of the projected crown area, which changes the surface roughness, alters the wind profile, and changes turbulence characteristics.

4.5 Conclusions

Current wind risk models are not applicable to irregular stand structures such as occur in low impact management systems. These structured stands require new approaches for calculating wind risk, which take the exposure of individual trees into consideration.

Distant dependant competition indices explain much of the variance when they are used as independent variable to explain individual wind loading on trees. However, it seems as if even small gaps cause a rapid increase of wind loading, which has also been described in other studies (Fraser, 1964; Stacey et al., 1994). The sample size of this experiment is not big enough to parametrise the relationship between gap size and wind loading. More high resolution field data of tree response to wind loading are needed to do that.

The fact that competition indices are widely used in forest modelling and especially the fact that they are implemented in growth simulators is promising. Linking the two model types appear to be straight forward and the tree data from a growth simulator would allow an upscaling to stand level and predictions of wind risk through time as the stand matures.

Acknowledgement

The experimental plot was established by Arne Pommerening and Jens Haufe from the University of Wales, Bangor, who generously made the stand data available, which were used for the simulation of the thinning scenarios.

For erecting and lowering the meteorological mast I fell back on the support from the guys from the technical support unit in Talybont: Carl Foster, Brian Jones, Dai Evans, "Dickie", and Justin Chapbell. Thanks go also to Shaun Mochan, who operated the winch during the mast operations.

Building a reliable logging system from scratch with a tight budget was a big challenge and its realisation would have been impossible without the help from Dave Brooks, John Strachan, and Jim Nicholl from the workshop at the Northern Research Station. Their support is much appreciated.

References

Achim A, Ruel JC, and Gardiner BA, 2005: Evaluating the effect of precommercial thinning on the resistance of balsam fir to windthrow through experimentation, modelling, and development of simple indices. *Canadian Journal of Forest Research*, 35, 1844–1853.

Aurenhammer F and Klein R, 2000: *Voronoi Diagrams*, chap. Handbook of Computational Geometry, pp. 201–290. North-Holland, Amsterdam, Netherlands.

Blackburn GRA, 1997: *The Growth and Mechanical Response of Trees to Wind Loading*. PhD, University of Manchester.

Courbaud B, Goreaud F, Dreyfus P, and Bonnet F, 2001: Evaluating thinning strategies using a tree distance dependent growth model: Some examples based on the CAPSIS software "uneven-aged Spruce forests" module. *Forest Ecology and Management*, 145, 15–28.

Dunham R, Gardiner B, Quine C, and Suárez J, 2000: *ForestGALES - A PC-based wind risk model for British forests*. Forestry Commission, Edinburgh, UK.

Fraser AI, 1964: Wind tunnel and other related studies on coniferous trees and tree crops. *Scottish Forestry*, 18, 84–92.

Gardiner B, Peltola H, and Kellomäki S, 2000: Comparison of two models for predicting the critical wind speeds required to damage coniferous trees. *Ecological Modelling*, 129, 1–23.

Hale SE, 2003: The effect of thinning intensity on the below-canopy light environment in a Sitka spruce plantation. *Forest Ecology and Management*, 179, 341–349.

Hale SE, Levy PE, and Gardiner BA, 2004: Trade-offs between seedling growth, thinning and stand stability in Sitka spruce stands: A modelling analysis. *Forest Ecology and Management*, 187, 105–115.

Hegyi F, 1974: A simulation model for managing jack-pine stands. In Fries J, ed., *Growth Models for Tree and Stand Simulation*, pp. 74–90. Royal College of Forestry, Stockholm.

Kenk G and Guehne S, 2001: Management of transformation in central Europe. *Forest Ecology and Management*, 151, 107–119.

Mailly D, Turbis S, and Pothier D, 2003: Predicting basal area increment in a spatially explicit, individual tree model: A test of competition measures with black spruce. *Canadian Journal of Forest Research*, 33, 435–443.

Mason WL, 2002: Are irregular stands more windfirm? *Forestry*, 75, 347–355.

Mayhead GJ, 1973: Some drag coefficients for British forest trees derived from wind-tunnel studies. *Agricultural Meteorology*, 12, 123–130.

Milne R, 1991: Dynamics of swaying of *Picea sitchensis*. *Tree Physiology*, 9, 383–399.

Moore JR, Gardiner BA, Blackburn GRA, Brickman A, and Maguire DA, 2005: An inexpensive instrument to measure the dynamic response of standing trees to wind loading. *Agricultural and Forest Meteorology*, 132, 78–83.

Moore JR and Maguire DA, 2004: Natural sway frequencies and damping ratios of trees: Concepts, review and synthesis of previous studies. *Trees*, 18, 195–203.

Nicoll B and Ray D, 1996: Adaptive growth of tree root systems in response to wind action and site conditions. *Tree Physiology*, 16, 891–898.

Page L, Cameron AD, and Clarke GC, 2001: Influence of overstorey basal area on density and growth of advance regeneration of Sitka spruce in variably thinned stands. *Forest Ecology and Management*, 151, 25–35.

Pretzsch H, Biber P, and Ďurský J, 2002: The single tree-based stand simulator SILVA: Construction, application and evaluation. *Forest Ecology and Management*, 162, 3–21.

Rojo JMT and Orois SS, 2005: A decision support system for optimizing the conversion of rotation forest stands to continuous cover forest stands. *Forest Ecology and Management*, 207, 109–120.

Rouvinen S and Kuuluvainen T, 1997: Structure and asymmetry of tree crowns in relation to local competition in a natural mature Scots pine forest. *Canadian Journal of Forest Research*, 27, 890–902.

Rudnicki M, Lieffers VJ, and Silins U, 2003: Stand structure governs the crown collisions of lodgepole pine. *Canadian Journal of Forest Research*, 33, 1238–1244.

Rudnicki M, Meyer TH, Lieffers VJ, Silins U, and Webb VA, 2008: The periodic motion of lodgepole pine trees as affected by collisions with neighbors. *Trees*, 22, 475–482.

Rudnicki M, Mitchell SJ, and Novak MD, 2004: Wind tunnel measurements of crown streamlining and drag relationships for three conifer species. *Canadian Journal of Forest Research*, 34, 666–676.

Schröder J, Röhle H, Gerold D, and Münder K, 2007: Modeling individual-tree growth in stands under forest conversion in East Germany. *European Journal of Forest Research*, 126, 459–472.

Schütz JP, 1989: Zum Problem der Konkurrenz in Mischbeständen. *Schweizerische Zeitschrift für Forstwesen*, 140, 1069–1083.

Schütz JP, 2001: Opportunities and strategies of transforming regular forests to irregular forests. *Forest Ecology and Management*, 151, 87–94.

Stacey GR, Belcher RE, Wood CJ, and Gardiner BA, 1994: Wind flows and forces in a model spruce forest. *Boundary-Layer Meteorology*, 69, 311–334.

Stadt KJ, Huston C, Coates KD, Feng Z, Dale MR, and Lieffers VJ, 2007: Evaluation of competition and light estimation indices for predicting diameter growth in mature boreal mixed forests. *Annals of Forest Science*, 64, 477–490.

Wonn HT and O'Hara KL, 2001: Height:Diameter ratios and stability relationships for four northern Rocky Mountain tree species. *Western Journal of Applied Forestry*, 16, 87–94.

Chapter 5

Wind loading on trees in two nearby stands with different structure

Abstract

Irregular structured forests are believed to be more stable in terms of wind damage than regular ones. The simulation of several different silvicultural systems in the wind tunnel showed that trees of the overstorey have to withstand lower turning moments, if they have an understorey (Gardiner et al., 2005). To date this has not been confirmed in field experiments.

The results from a field experiment are presented, in which the wind profiles and turning moments of trees in two neighbouring stands with different structure were measured simultaneously. One stand had an understorey the other did not. The analysis of the measured turning moments, wind profiles, and turbulence characteristics are consistent with the hypothesis and suggest that more wind energy is absorbed by the trees without an understorey. The correlation coefficient (r_{uw}) and the values for the Eulerian length scales L_u/h_C and L_w/h_C are increased when the wind comes from a direction with an understorey, what indicates that coherent structures penetrate deeper into the forest. Direct comparison of measured turning moments show that a tree without an understorey experiences higher turning moments than a similar tree with an understorey.

The results are in agreement with the wind tunnel studies from Gardiner et al. (2005) and suggest that the overstorey crop benefits from an understorey in terms of wind loading and reduced wind risk.

5.1 Introduction

Timber production is not the only goal of British forestry. Non commercial services such as recreation, ecology, biodiversity, and aesthetic issues of forests

have increased in importance over the last decade (Mason et al., 1999) and are now for many forests more important than timber production. In Britain the traditional silvicultural system is clear-felling/restocking, which does not necessary ensure many of the mentioned benefits. Therefore British foresters are encouraged to manage their stands as 'continuous cover forests' (CCF) [1], where a canopy is maintained throughout the lifetime of the site, which is very different to normal clearfelling/restocking. In comparison to continental Europe, the British wind climate is much more severe (Troen and Petersen, 1989) and therefore wind damage is of major relevance to British forestry (Andersen, 1954; Rollinson, 1987; Gardiner and Quine, 1994). Due to a lack of experience with irregular stand structures, there are concerns as to whether irregular stands under CCF management could be less stable than regular ones.

Post damage surveys in the literature analysing the differences in wind damage for different stand structures are not consistent in their conclusions. Several studies conclude that irregular stands are more windfirm than regular ones (e.g. Dvorák et al., 2001). Other studies found no differences in susceptibility to wind damage for the two stand types (e.g. Schütz et al., 2006). However, no reference was found, stating that regular stands are more stable than irregular, which might explain the general believe in the benefit of an irregular structure. Many studies were carried out after very severe storm events. Miller (1985) states that the influence of the stand structure on the amount of wind damage vanishes in 'catastrophic' events, but has an influence in 'endemic' events, which have lower maximum wind speeds.

In many cases, the lower slenderness of the dominant trees in irregular stands compared to regular ones is identified as the most significant stand parameter for explaining differences in stability (Mason, 2002). For two trees with the same height and same mechanical wood properties but with different *dbh*, the one with the lower slenderness will have a higher breaking moment since the rigidity of the tree is determined mostly by the diameter of the stem. The stouter tree will also have higher stem mass and since the above ground mass is positively correlated with root mass (Cheng and Niklas, 2007) lower slenderness is believed to increase the anchorage of the tree, resulting in a higher resistance to overturning (Nicoll et al., 2006).

[1] "Continuous cover" is defined as the use of "silvicultural systems whereby the forest canopy is maintained at one or more levels without clear felling." Clearfelling is defined as the cutting-down of all trees on an area of more than 0.25 ha. (Pommerening and Murphy, 2004)

Other studies focused on the impact of stand structure on the turbulence. Exchange of momentum and any other scalar between the forest and the atmosphere is dominated by coherent structures which are typical for a mixing layer (Gao et al., 1989; Finnigan, 2000). The streamwise length scale of these structures is controlled by the shear length scale, which itself is governed by canopy characteristics, particularly the distribution of the leaf area (Raupach et al., 1996; Brunet and Irvine, 2000). More recent work in plant canopies suggest that the 'bending stiffness plays an important role in the frequency and wavelength selection for the coherent motion of the canopy' (Ghisalberti and Nepf, 2006; Py et al., 2006; de Langre, 2008). Marshall et al. (2002) found indications for this relationship in wind tunnel studies with model forests. Such a mechanism provides a link to the work described in the previous section. Trees with lower slenderness values have higher stiffness and smaller eigenfrequencies (Moore and Maguire, 2004).

Achieving the goals of CCF requires the presence of an understorey that will replace the overstorey when this is felled. One limiting growth factor for the understorey is the availability of light, which is governed by the canopy closure of the overstorey (Hale, 2003). Lower tree density promotes deeper penetration of the wind into the stand. An understorey introduces form drag and hence alters the turbulence. Gardiner et al. (2005) found in wind tunnel studies that the presence of an understorey reduced the loading of the trees of the overstorey, but could not give a satisfactory explanation for the underlying processes.

The difficulties in estimating the impact of forest management on the stability of a stand arise from the fact that any kind of intervention changes the growth conditions for the crop and the turbulence characteristics concurrently. Since wind damage is governed by the trade-off between resistance and wind imposed drag, it is difficult to separate these two different effects. This highlights the fact that management can make the difference between unstable and stable stands and possibly the difference between financial gain or loss.

This chapter focuses on a single aspect of stability, which is in what way does stand structure influence the risk of wind damage. The aim of this work is to analyse the wind and tree interaction of individual trees in two neighbouring stands, which differ in structure and represent two types of silvicultural management systems (clearfelling/restocking and group selection).

5.2 Material and methods

5.2.1 Study site

The experimental site was a stand of European larch (*Larix decidua* P. Mill.) in Kyloe Wood, Northumberland, England (55°32′ N, 1°99′ E, 120 m a.s.l.) planted in 1947 and about 25 m tall at the time of the field study (2006). The stocking density was approximately 119 trees ha^{-1}. At the location of the experiment two different stand structures were in close proximity with an identical overstorey. However, one of the stands had an understorey composed of a mixture of larch and Sitka spruce (*Picea sitchensis* (Bong.) Carr.), which was about 11 m tall. Next to this stand the same overstorey crop is present without any understorey at all. The differences are due to a forest management trial several years ago. Pigs, that were brought in, ate all the regeneration in the stand, which now has no understorey (Ian Robinson, personal communication).

Figure 5.1: The two photographs show the locations of the two meteorological masts, which are only 30 m apart. On the left hand side is the location *without* an understorey near Mast-I. On the right hand side is the location *with* an understorey near Mast-II. Both photographs point into westerly direction, which is the prevailing wind direction at this site.

The experimental site is in the south-west corner of the forest at the bottom of a hill, which extends to the east and provides shelter from this wind direction (see Fig. 5.2). The terrain slopes gently in a westerly direction, which is also the prevailing wind direction. The forest extends more than 200 m in this direction, which is assumed to be sufficient for the wind profile to adapt, so that the measurements are not affected by edge effects (Irvine et al., 1997).

The measurements started in March 2006 before bud burst of the larch. Bud

burst took place at the beginning of May and refoliation was completed by the middle of May. Thus data for the two different canopy conditions are available.

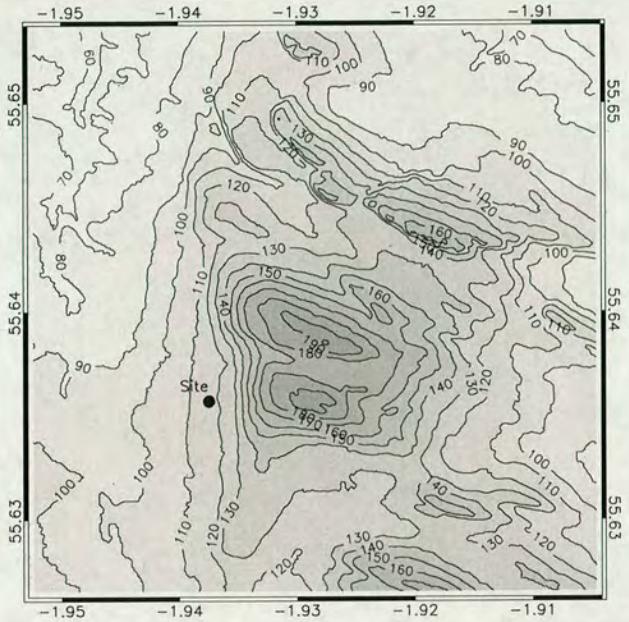

Figure 5.2: Contour map (3 km × 3 km) of the area of the experimental site. Isolines are in 10 m elevation steps.

5.2.2 Study trees

Nine trees were chosen as experimental trees. Six of them were part of the overstorey. These trees cover a height range of 20.5 to 27.6 m and a diameter at breast height (*dbh*) range of 33.7 to 40.6 cm. Four of the six trees were located near Mast-II at the location with an understorey (see Fig. 5.3). Whilst the other two study trees (101,102) were located near Mast-I, at the location with no understorey. In addition three trees from the understorey were monitored. These three trees were located near Mast-II. The mensurational data for the nine experimental trees are summarised in Table 5.1.

5.2.3 Wind and turbulence measurements

The experiment was designed to measure the wind-tree interaction with a high temporal resolution. Wind profiles were measured at two locations with eight

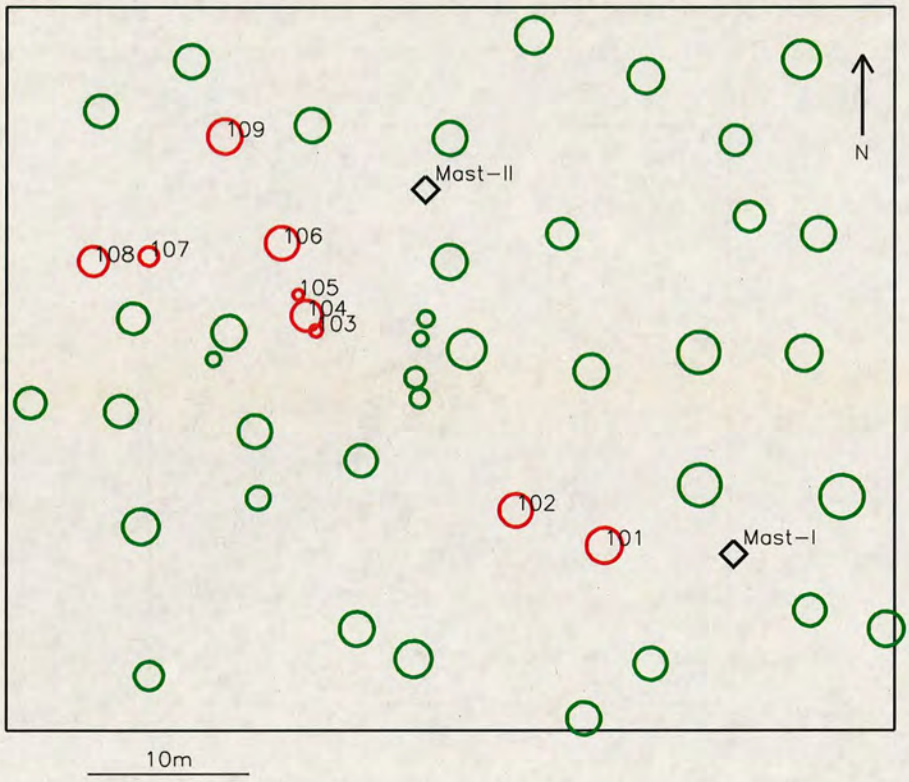

Figure 5.3: Map of the experimental site. Only the nine experimental and trees taller than 15 m are plotted. The grey polygon represents the area where an understorey is present. The red circles are the nine experimental trees.

cup anemometers (NRG#40, NRG systems, US). The measurement heights were 5 m, 10 m, 15 m, 18 m, 21 m, 24 m, 27 m, 30.8 m above the ground. Although the distance between the two masts was only 30 m, the stand structure differs. Mast-I is at a location where there is no understorey (see Fig. 5.3). The cup anemometers and wind vanes, that were mounted onto Mast-II, were logged every 3 seconds by a CR23X data logger (Campbell Scientific, Logan, US). The cup anemometers of Mast-I were logged every 3 seconds by a Gigalog8 (Audon Electronics, UK). In addition to the cup anemometers Mast-II carried two wind vanes (27 m, 15 m) and two Ultrasonic Anemometers (USA-1, METEK GmbH, Germany) at 16.0 and 29.8 m height for measuring atmospheric turbulence. The upper sonic was located above the canopy and the lower one within the canopy.

Due to its high power demand the sonics were only turned on, when a 3 second wind speed measurement of the uppermost (30.8 m) cup anemometer mounted on Mast-II exceeded 7 $m\,s^{-1}$. The sample frequency of the sonics was set to 10 Hz

Table 5.1: Properties of the nine experimental trees. No breaking moments were estimated for the two smallest trees, since their wood properties most likely differ from those of a mature tree. (ID: tree number, h: height, dbh: diameter at breast height, cr-base: height of crown base, M_{break}: breaking moment (estimated))

ID	Species	h (m)	dbh (cm)	cr-base (m)	M_{break} (kNm)
101	Larch	27.6	40.6	16.8	315
102	Larch	21.8	37.7	12.9	256
103	Sitka	8.7	13.7	2.0	-
104	Larch	22.4	35.2	13.8	208
105	Sitka	9.4	12.1	2.5	-
106	Larch	20.5	37.8	11.9	260
107	Sitka	11.3	21.4	3.0	40
108	Larch	21.0	33.7	13.6	183
109	Larch	21.5	39.8	11.9	302

and the transformed digital signal was stored on compact-flash cards as ASCII files using a couple of Gigalog8s (Audon Electronics, UK).

For a complete list of equipment and a schematic overview of the measuring system, please see Appendix C.

5.2.4 Measurements of turning moment

The turning moment of the nine experimental trees was measured at 4 Hz using strain gauges glued to aluminium callipers (strain transducers). Each experimental tree was equipped with two strain transducers screwed into the trees perpendicularly to each other at about 1.3 m height (Blackburn, 1997; Moore et al., 2005). A CR23X data logger (Campbell Scientific, Logan, US) was used to measure the signal. The number of differential channels on the logger panel was not sufficient for the number of strain transducers used. To increase the number of channels a relay multiplexer (AM416, Campbell Scientific, Logan, US) was used for some of the strain transducers. For final data storage a Gigalog8 (Audon Electronics, UK) was used. The CR23X streamed the data as RS232 signal to the Gigalog8, which stored the data as plain text on a compact flash card. All strain transducers, which were connected to the multiplexer, were powered by a separate regulated power supply. For the sake of energy conservation the multiplexed strain transducers were only switched on in periods of higher wind speed ($> 7\,\mathrm{m\,s^{-1}}$ at 30.8 m) and only when the battery voltage had not dropped

below a pre-defined threshold. Therefore the data pools for the nine trees do not match (see Fig. 5.4).

The signal output of the strain transducers is linear to the change in distance between the two points where the strain transducer is screwed into the tree. For calibration every single strain transducer was calibrated by stepwise pulling the tree while measuring the applied force with a S-type load cell (Model 616, Tedea Huntleigh, US). Each tree was pulled into two directions to calibrate the two gauges. A detailed description of the strain transducer measurements and the calibration procedure is given in Appendix A.

5.2.5 Data treatment

Strain data

The strain transducer measurements are not inert to temperature fluctuations. Although the arrangement of two strain gauges on the aluminium body is to compensate for temperature changes (Blackburn, 1997), the influence on the strain signal is visible as a wave with a 24 hr cycle due to the differences of thermal expansion of wood and aluminium. However, the strain data analysis was performed on only 10 or 60 minute time intervals. Due to the differences in the time scale a simple linear detrending of the raw strain signal was considered appropriate to filter out unwanted drift caused by temperature changes.

Sonic data

The meteorological masts used in this experiment were tilt up towers (TallTower, NRG Systems, US). Once the mast was erected there was no possibility to access the instruments. Therefore perfect horizontal alignment of the sonic anemometers was not possible. Flux measurements are sensitive to the choice of coordinate system (Finnigan, 2004) and hence to the rotation which is applied to the raw sonic data. The two most common rotation methods differ in the time frame that is considered. For the *double rotation*, the reference coordinate system is chosen in a way that the mean vertical wind component ($\overline{w}$) becomes zero for every time interval. Another method, known as *planar fit*, defines the reference xz-plane over longer time periods (Wilczak et al., 2001). In this method the plane is adjusted, so that the vertical wind speed component over a longer time and many intervals is minimal. In this case the mean vertical wind component for an individual interval in the sample can be different from zero.

Another second rotation is applied to the sonic data around its vertical axis.

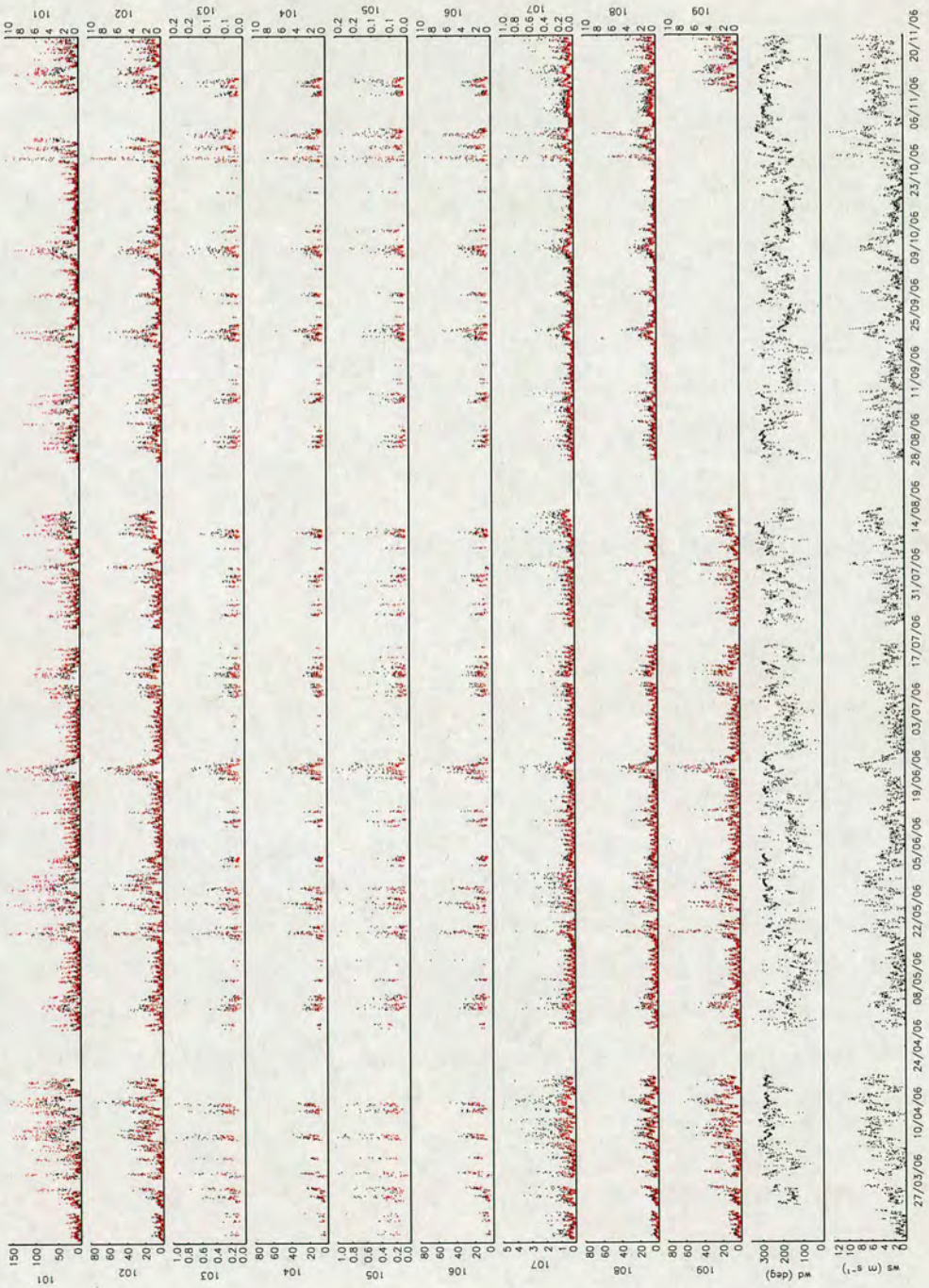

Figure 5.4: Time series of measured hourly maximum (y-axis on left hand side, black dots) and mean (y-axis on right hand side, red dots) turning moments in kNm for the nine study trees. The scale of the y-axis is adjusted for each plot. The two time series at the bottom are wind direction (wd) at 27.0 m and hourly mean wind speed at 30.8 m height (ws) measured at Mast-II.

The x-axis of the sonic is aligned into the direction of the mean wind, so that the mean lateral wind component becomes zero. This is common practise in the analysis of turbulence time series and allows for comparison with other studies.

For this study both rotation methods were tested. A comparison showed only small differences for the calculated turbulence characteristics and did not change the general picture. For the final analysis the *planar fit* method was used, because it should be more reliable and robust (Finnigan et al., 2003).

All turbulence characteristics were calculated from sets of 8192 data points, which is about 13 min. The time interval was chosen to speed up the fast Fourier transformation which works best for a number of data points which can be defined as 2^x (where x is an integer).

5.3 Results and discussion

5.3.1 General

The experiment was set up to allow the comparison of different data sets in order to assess the impact of the stand structure on the wind-tree interaction. First of all the two locations can be compared by analysing the wind profiles of the two masts and by comparing the experienced turning moments of the trees at the two locations. The position of the Mast-II, which carried the sonic anemometers, allows the comparison of two different wind sectores. Seen from the position of Mast-II only the sector spanning from north to west features understorey. All other directions lack an understorey. Therefore the impact of the understorey on the turbulence characteristics can be examined as well, by splitting the data pool up using wind direction (see Fig. 5.5).

5.3.2 Wind profiles

The sectorwise mean wind profiles for the two masts are shown in Figure 5.6. Due to the poor resolution of the cup anemometers in low wind speed the analysis was restricted to time periods in which the hourly mean wind speed at 30.8 m exceeded $3\,\mathrm{m\,s^{-1}}$. The shelter the site receives from easterly winds means that the data pool for these wind directions is very small. The wind speeds in the trunk space at the two locations are very low. In comparison, the wind speeds at Mast-I are higher than they are at Mast-II. The second wind speed maximum

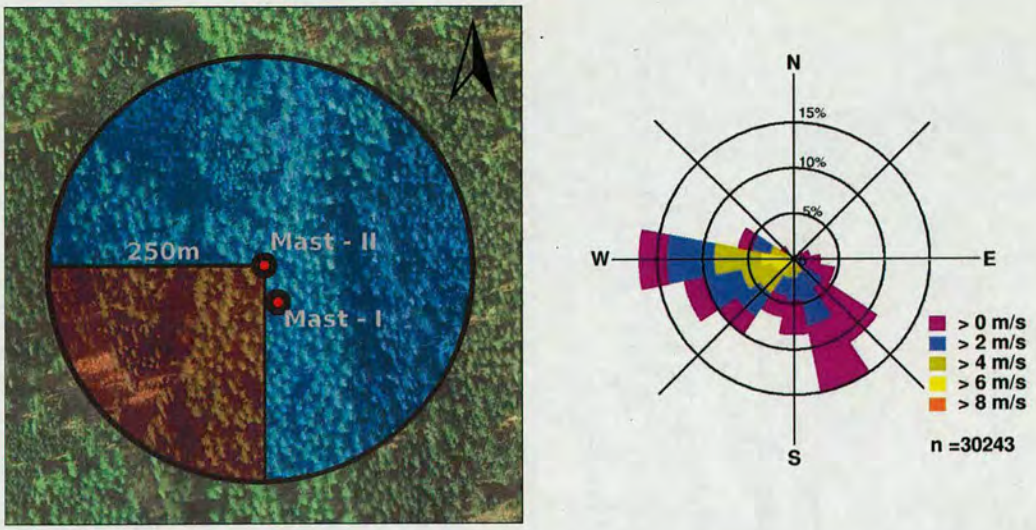

Figure 5.5: The two wind sectors which are considered to represent different stand structures. Wind blowing over the red sector [180:270] represents a stand *with* an understorey and the blue sector is *without* an understorey. Wind rose for the time period of the experiment. The data for the wind rose were measured at Mast-II and relates to the wind speed measurements at 30.8 m height and the wind direction measurements at 27 m.

in the trunk space is also more pronounced at Mast-I. For the Mast-II a second wind speed maximum is only recognised for the sectors W to NNW.

The inflection point of the wind profile - defined as the height of maximum shear - is higher at Mast-I. This indicates that the wind in-forces more drag on the canopy in higher parts. Since the turning moment is calculated as the integral of force over height this should result in higher turning moments.

The differences between the normalised wind profiles at the two locations are plotted in Figure 5.7. The differences are most pronounced at heights 21 m and 18 m for westerly directions. For those heights higher wind speeds were measured at Mast-II. This indicates that less momentum has been absorbed by the canopy and has been transferred into tree motion.

5.3.3 Momentum absorption

For this experiment two sonic anemometers were available. Both sonics were mounted onto Mast-II at 29.8 m and 16.0 m. The surrounding trees were about 23.5 m tall. Hence the upper sonic was located several meters above the canopy ($1.27\,z/h_C$). The lower sonic was located within the canopy ($0.68\,z/h_C$), a few meters above the average crown base at 13.2 m ($0.56\,z/h_C$) and also some meters

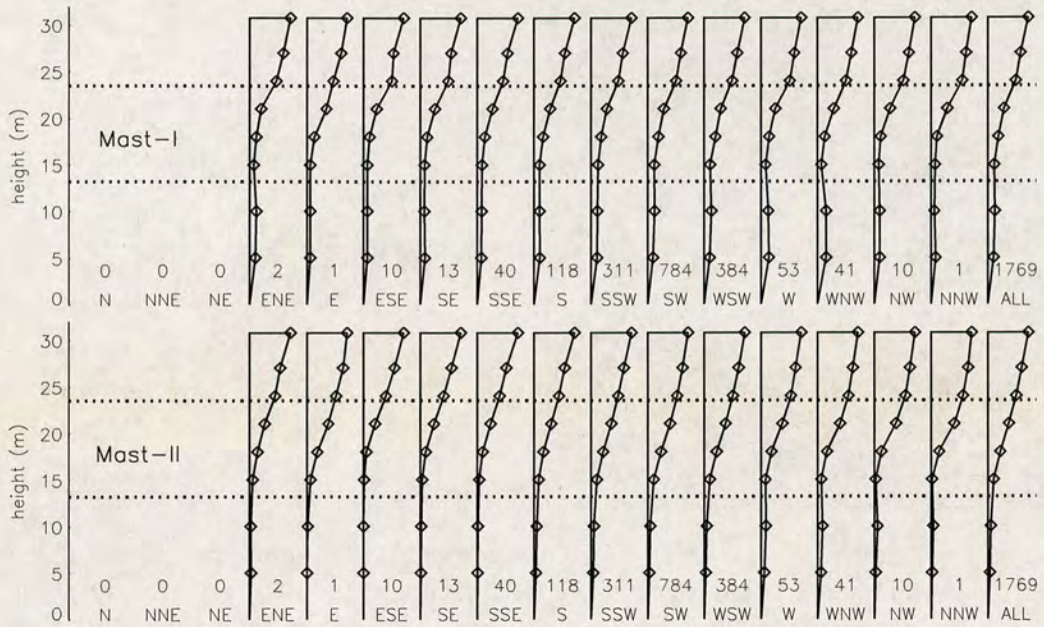

Figure 5.6: Normalised average hourly wind profiles for 22.5 ° wide sectors. The number at the bottom of each plot is the number of hours used. Only data after bud burst (May–November) were used. Hours with mean wind speeds lower than $3\,m\,s^{-1}$ at 30.8 m were rejected from analysis. The dashed lines indicate the extension of the overstorey canopy.

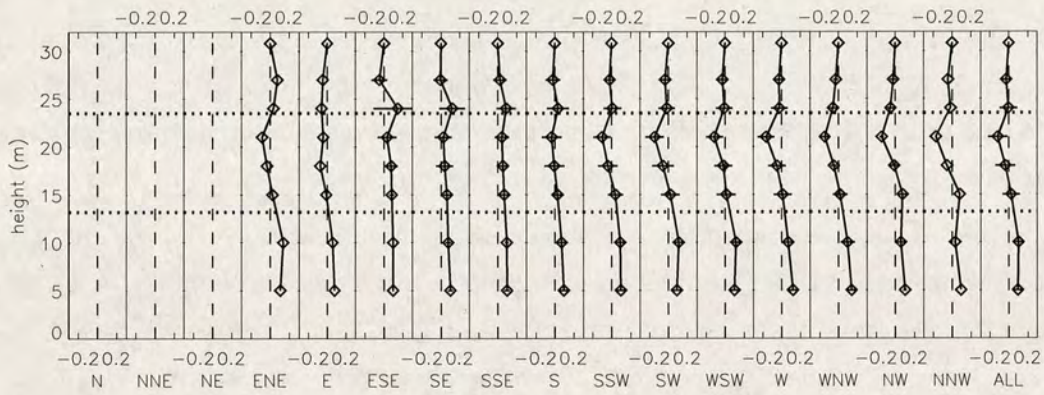

Figure 5.7: Differences of the normalised wind profiles (Mast-I - Mast-II) from Figure 5.6. The horizontal lines are standard deviations. Due to small sample sizes for some wind sectors the calculation of the standard deviation was not always possible.

above the understorey.

The difference in momentum flux ($\overline{u'w'}$) at the two sonic heights is a measure of the amount of momentum which has been absorbed over the height between

the two sonics and transferred into tree motion. For comparison the difference is scaled by the momentum flux at the upper sonic height, which represents the atmospheric stress above the forest.The relative momentum absorption (RMA) is calculated as:

$$RMA = \frac{\overline{u'w'}_{1.27\,z/h_C} - \overline{u'w'}_{0.68\,z/h_C}}{\overline{u'w'}_{1.27\,z/h_C}} \tag{5.1}$$

where u' and w' are the instantaneous deviations of the horizontal and vertical wind component and the overline indicates an average over a time period (here: 8192/10 seconds).

If the measured momentum fluxes at the two heights were equal *no* momentum was absorbed between the two heights and the value for RMA would approach zero. In contrast, if the momentum flux at the lower sonic height was to be zero, *all* momentum would have been absorbed by the canopy above the lower sonic height and the RMA becomes unity.

In Figure 5.8 the relative momentum absorption is plotted versus wind direction. The pattern of the data points suggest that less momentum is absorbed when the wind comes from southerly to westerly direction, which coincides with the area where there is an understorey. Values greater than unity indicate an upward momentum flux at the lower sonic height. Since the vertical momentum flux is caused by the shear stress of air layers, an upward momentum flux indicates an inversion of the normal wind profile in the trunk space of the forest. Hence a second wind speed maximum has to be present in the trunk space to cause an upward momentum flux. The occurrence of a second wind speed maximum is also recognisable in some of the wind profiles in Figure 5.6 and has also been described by several other authors (e.g. Shaw, 1977; Baldocchi and Meyers, 1988).

The momentum flux is related to the drag (F_D):

$$F_D = \frac{\overline{u'w'}}{z} dz \tag{5.2}$$

The drag of the plant canopy is a function of the frontal crown area. Before bud burst the crown area of the canopy is reduced. Hence the data points for this time period do line up at the lower margin of the data pool as it can be seen in Figure 5.8.

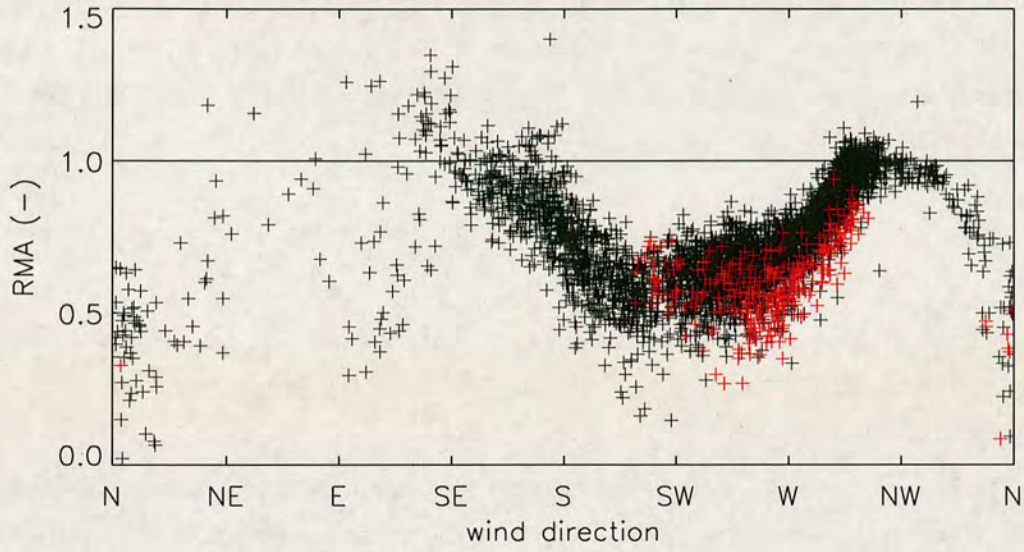

Figure 5.8: Relative momentum absorption (RMA) between the heights 29.8 m ($1.27\,z/h_C$) and 16.0 m ($0.68\,z/h_C$) calculated from the turbulence data from the two sonic anemometers at Mast-II (n = 3940). Red symbols represent data, that were measured before bud burst (March & April 2006, n = 352).

5.3.4 Turbulence characteristics

Since the sonics were only switched on if a 3 s wind speed measurement at 30.8 m height exceeded 7 m s^{-1}, all measurements represent neutral or near neutral conditions with $|((z-d)/L)| < 0.05$, where L is the Obukhov length ($L = -u_*^3/k\beta\overline{w'\Theta'}$).

For comparison, the same wind sectors as in the previous sections were chosen in order to analyse differences that might occur due to the presence of an understorey. Analysis is geared to the *'Family portrait'* of canopy flow statistics presented by Raupach et al. (1996). Since just one mast had sonic anemometers the analysis is tightened to single point statistics by applying Taylor's frozen turbulence hypothesis. The values for the turbulence characteristics are summarised in Table 5.2.

Turbulence characteristics are in good agreement with the values from Raupach et al. (1996) derived for a wide range of plant canopies, i.e. σ_u/u_* is about 1.8, σ_w/u_* about 1.1, r_{uw} about -0.5 at the level above the canopy and $|Sk_u|, |Sk_w|$ approximately 1 within the canopy.

In general the turbulence characteristics at the upper height are very similar for the two wind sectors. However, some differences are noticeable. The normalised standard deviation for the streamwise wind vector (σ_u/u_*) is higher, and streamwise (L_u/h_C) and vertical (L_w/h_C) Eulerian length scales are higher for the sector with an understorey. Since the Eulerian length scale is a measure of coherence in the turbulence, this suggests that the dominant size of the eddies is larger for this sector and that those eddies penetrate deeper into the canopy (Marshall et al., 2002). This is backed up by the wind profiles in Figure 5.6, that show higher shear stress at Mast-II near the canopy top for the wind sector with an understorey. Raupach et al. (1996) showed that the shear stress length scale at canopy top ($L_s = U(h_C)/U'(h_C)$) is the scaling parameter for the dominant eddy size.

For the lower sonic anemometer at $0.68\,z/h_C$ (about 2 m above the understorey) the differences for the two wind sectors are more pronounced than they are above the overstorey. The values for the normalised wind speed (u/u_{h_C}) and normalised momentum flux ($\overline{u'w'}/u_*^2$) are reduced for the wind sector without an understorey. At the same time the standard deviation and skewness of the streamwise wind vector (σ_u/u_* and Sk_u) are lower, whereas kurtoses are bigger (Kt_u, Kt_w). Differences of the correlation coefficient are also observed. For the sector with an understorey r_{uw} is -0.44 and only a little smaller than the value obtained at the upper sonic height (-0.46). For the sector without an understorey the correlation coefficients are -0.48 at $1.27\,z/h_C$ and -0.22 at $0.68\,z/h_C$, respectively.

In Figure 5.9 the values from Table 5.2 are plotted together with the profiles from a large eddy simulation (LES) performed by Dupont and Brunet (2008b). The cases that are shown are *"case 3, LAI=5"* and *"case 2, LAI=2"*, which are believed to represent best the two analysed wind sectores from this field survey. Both scenarios have the same leaf area distribution of the overstorey, but case 3 has an understorey, while case 2 has none.

5.3.5 Quadrant analysis

The joint probability distribution is a method of the conditional analysis (Lu and Willmarth, 1973) and is well established in the analysis of turbulence.

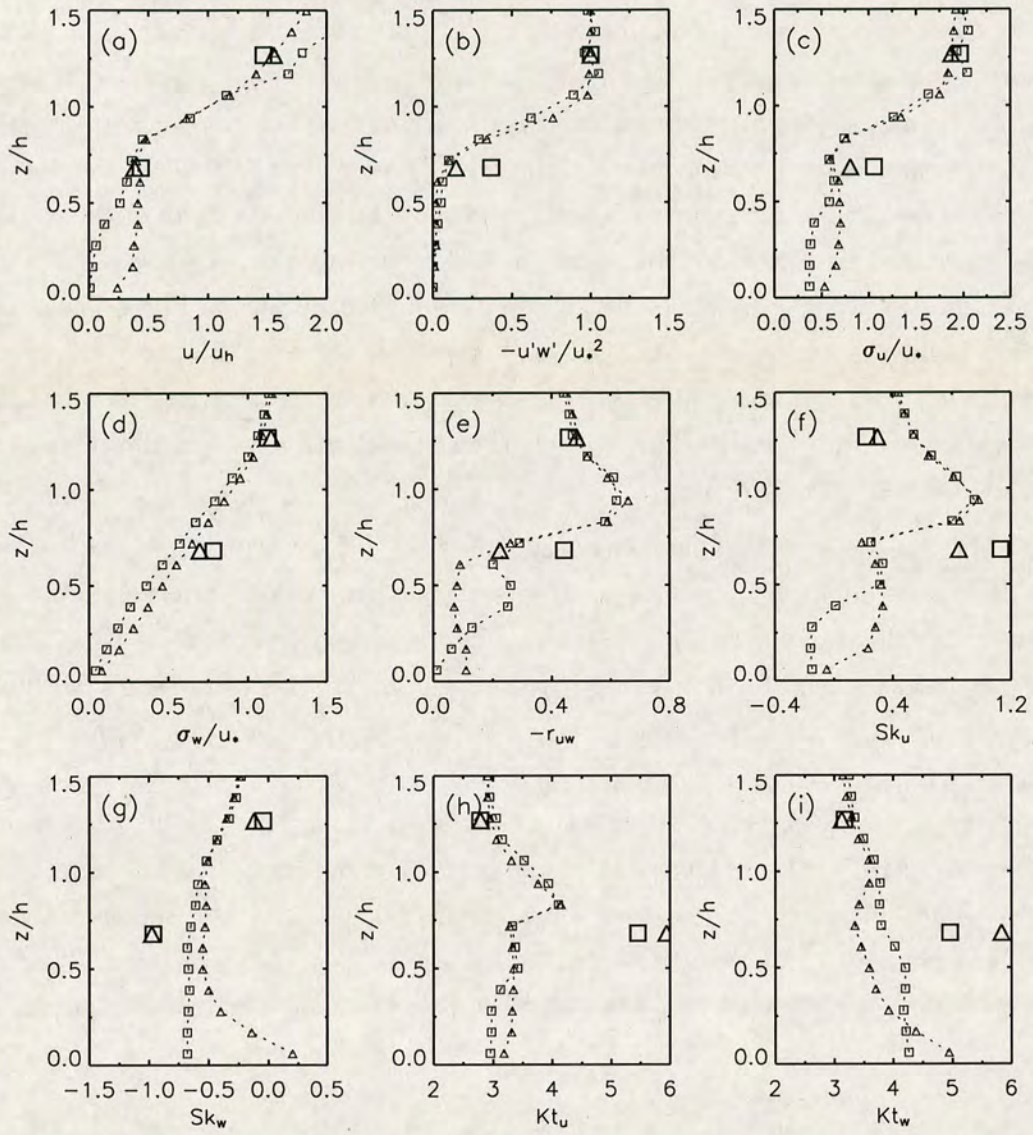

Figure 5.9: *Family portrait* of the turbulence at Mast-II. Plots of mean horizontal wind speed (a), momentum flux (b), coefficient of correlation (c), standard deviations of the horizontal (d) and vertical (e) wind component, skewness of the horizontal (f) and vertical (g) wind component, and kurtoses of the two wind components (h and i) for two heights. All values are normalised by either horizontal wind speed at canopy top (u_{h_C}) or friction velocity (u_*) at $1.27\,z/h_C$. □ values represent the wind sector with an understorey ([180:270], n = 1791). △ represents all other wind directions *except* the sector [180:270] (n = 1799). The profiles were derived from large eddy simulations carried out by Dupont and Brunet (2008b). The □ symbols represent *"case 3, LAI=5"* and △ represent *"case 2, LAI=2"* from the original publication.

Table 5.2: Turbulence characteristics for the two sonic heights and for two different wind sectors, whereas the one sector [180:270] features understorey and all other directions are associated with a stand structure without an understorey.

	$180 < wd < 270$ with understorey n = 1791		$180 > wd > 270$ without understorey n = 1799	
	$1.27\,z/h_C$	$0.68\,z/h_C$	$1.27\,z/h_C$	$0.68\,z/h_C$
u/u_h	1.46	0.44	1.55	0.38
$\overline{u'w'}/{u_*}^2$	1.00	0.37	1.00	0.15
σ_u/u_*	1.97	1.05	1.87	0.80
σ_w/u_*	1.12	0.78	1.14	0.70
r_{uw}	-0.46	-0.44	-0.48	-0.22
Sk_u	0.22	1.13	0.29	0.85
Sk_w	-0.04	-0.96	-0.12	-0.98
Kt_u	2.79	5.46	2.79	5.94
Kt_w	3.17	4.96	3.12	5.83
L_u/h_C	1.19	0.28	0.93	0.11
L_w/h_C	0.37	0.14	0.32	0.07

Regarding the momentum flux four sign combinations are possible. The naming of those four quadrants follows the one of Shaw et al. (1983):

1^{st} *quadrant* : $u' > 0, w' > 0$: outward interaction
2^{nd} *quadrant* : $u' < 0, w' > 0$: ejections or bursts
3^{rd} *quadrant* : $u' < 0, w' < 0$: inward interaction
4^{th} *quadrant* : $u' > 0, w' < 0$: sweeps or gusts

Events in the 1^{st} and 3^{rd} quadrant contribute to upward transport of momentum whereas the 2^{nd} and 4^{th} quadrant contribute to downward transport. If the turbulence was not organised and therefore completely random in a Gaussian manner, the joint probability distribution of the two parameters would be circular.

In Figure 5.10 the joint probability distributions of the normalised u and w components are shown. For the analysis the instantaneous wind speed fluctuations have been normalised by their standard deviations. The bin size for the histogram analysis was 0.2. The four plots show the distributions at the two sonic heights and again for the two different wind sectors. The plots at the height of the upper sonics are very similar. The distributions have a distinct elliptical

shape, which indicate that the momentum transfer is organised and dominated by ejection and sweep events. The time fractions for those two quadrants are 0.35 (2^{nd} quadrant) and 0.31 (4^{th} quadrant). The distributions for the two wind sectors are almost identical. This suggests that the understorey has no impact on the turbulence characteristics above the overstorey and that differences in the turbulence within the canopy are not due to differences in the turbulence above the forest.

In comparison to the plots at the height of the upper sonic, the ones at the lower height no longer show a distinct elliptical shape. This indicates that the signal of the strongest gusts has been attenuated by the overstorey and does not reach the lower sonic height. In contrast to the upper sonic height the two plots show differences for the two wind sectors. For the wind sector without an understorey the distribution is more circular shaped and therefore less organised compared to the wind sector with an understorey. This is in agreement with the profiles in Figure 5.9 that also show lower absolute correlation coefficients (r_{uw}) for the stand without an understorey indicating less organisation of the eddies for the stand without an understorey.

5.3.6 Wind loading on trees

For the analysis of the turning moment a quadratic model ($f(x) = a \cdot x^2$) was fitted to the 10 min mean wind speed and corresponding maximum turning moment data. For the model the wind speed data from the upper cup anemometer on Mast-II (30.8 m) was used as independent variable. The model was fitted with a least square approach. Standard errors were estimated from a bootstrap with 10,000 repetitions.

5.3.7 Tree comparison

The data in Table 5.1 show that the five trees 102, 104, 106, 108, and 109 are very similar regarding their heights. From this sample tree 102 is the only one, which is located at the spot with no understorey. Therefore the data from these five trees are suitable for a direct comparison of the measured turning moments to identify differences.

In Figure 5.12 the 10 min mean and maximum turning moment of the four

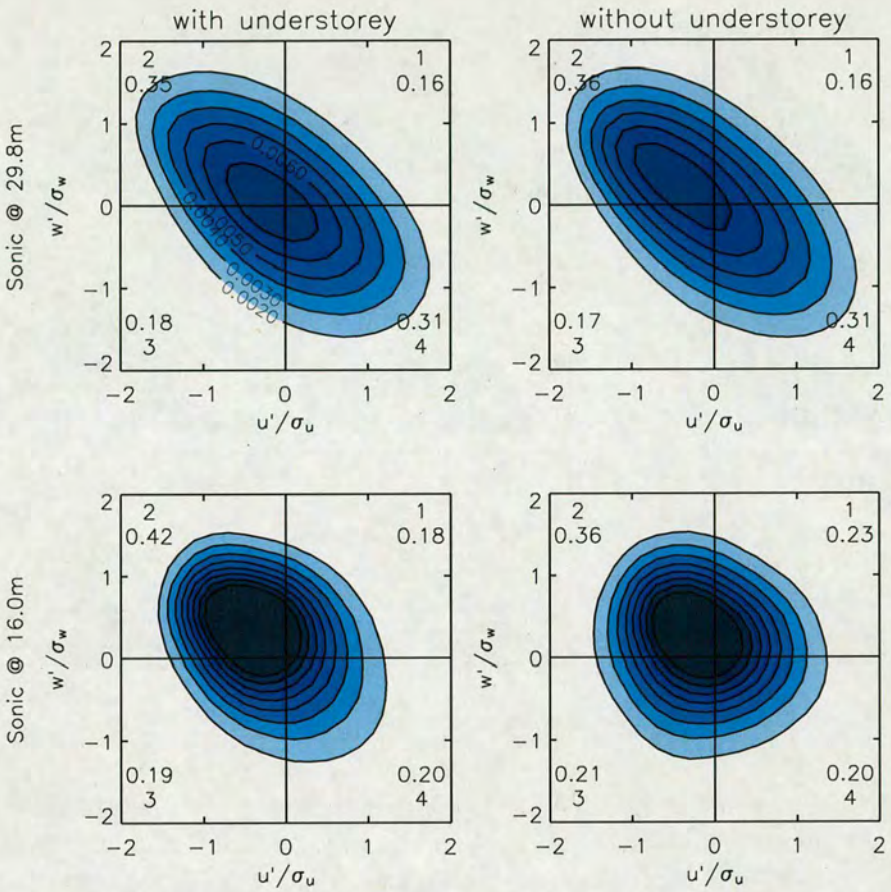

Figure 5.10: Joint probability distributions of the normalised instantaneous deviations of the horizontal (u) and vertical (w) wind components for the two sonic anemometers. The two columns represent two different wind sectors. Plots in the left column represent the wind sector [180:270] degrees, whereas the right column represents all directions *except* the wind sector [180:270] degrees. The numbers in the corners give the time fraction for each quadrant.

trees with an understorey are plotted against the values of tree 102. The majority of data points for the trees 104 and 106 lie below the 1:1 line, which indicates that tree 102 has to withstand higher turning moments. For tree 109 the data clouds spread around the 1:1 line showing that the turning moments tree 102 and 109 experience are very similar. The slope of the linear regression analysis is higher than unity indicating that in average tree 109 experiences higher turning moments. The slope parameter and correlation coefficients for all regression lines are given in Table 5.4.

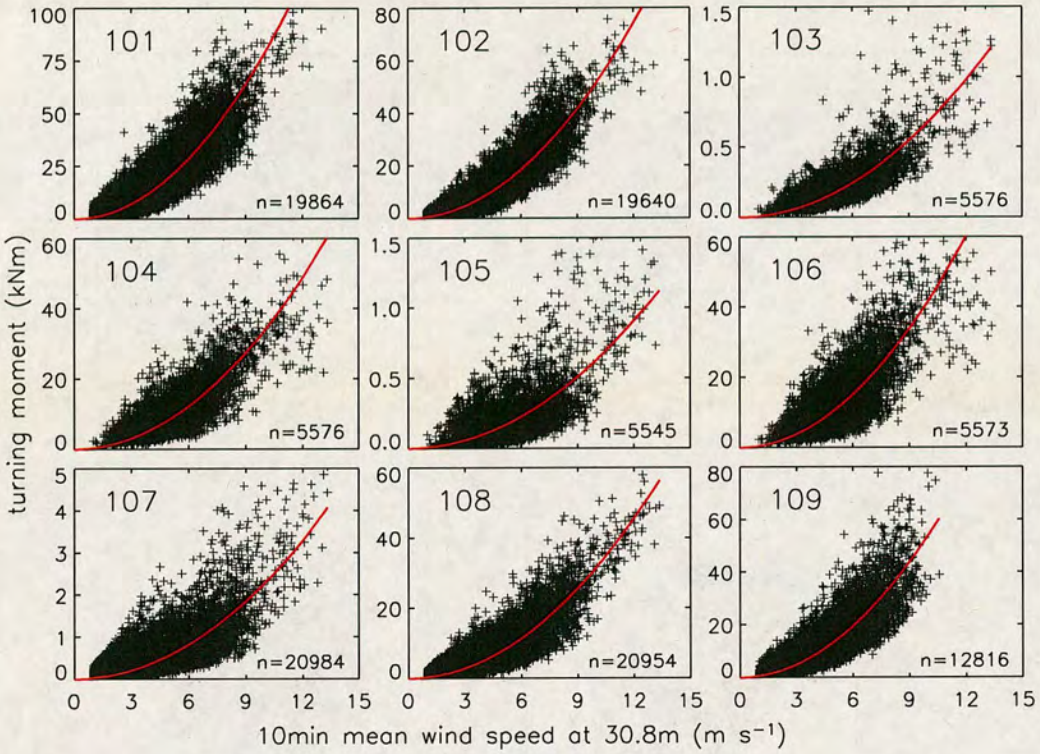

Figure 5.11: Experienced 10 min maximum turning moment of the nine experimental trees as a function of 10 min mean wind speed. The red lines are the best fit of a quadratic function ($f(x) = a \cdot x^2$). The parameters of the nine models are listed in Table 5.3. Only measurements after bud burst were used for the analysis. Note that the scaling of the ordinates varies between plots.

Table 5.3: Parameters of the quadratic models ($f(x) = a \cdot x^2$) in Figure 5.11 derived from bootstrapping with 10,000 repetitions. Standard error is given in parentheses.

ID	n	a (SE)	R^2
101	19865	0.790 (0.0218)	0.79
102	19641	0.516 (0.0147)	0.84
103	5577	0.007 (0.0044)	0.64
104	5577	0.339 (0.0157)	0.59
105	5446	0.006 (0.0008)	0.48
106	5574	0.418 (0.0193)	0.55
107	20985	0.023 (0.0024)	0.64
108	20955	0.317 (0.0162)	0.80
109	12817	0.542 (0.0224)	0.73

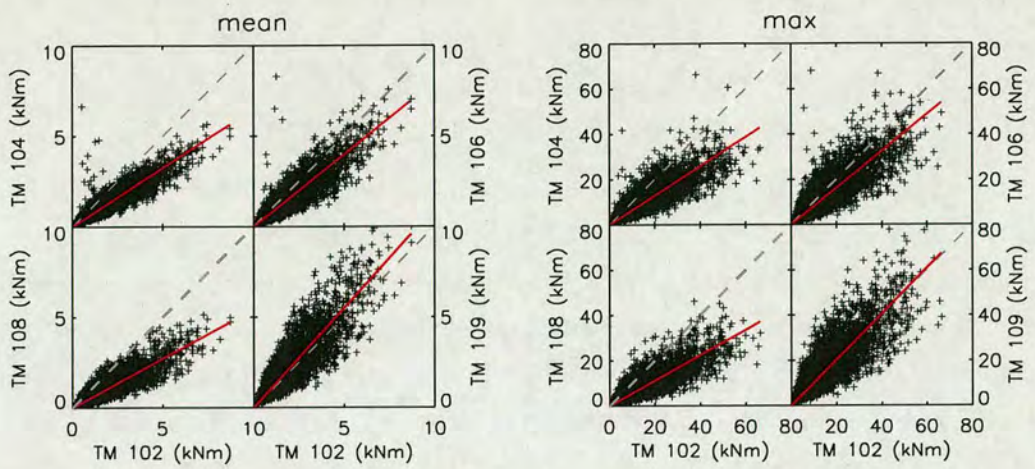

Figure 5.12: Scatter plots of simultaneously occurring mean (left) and maximum (right) turning moments of trees 104, 106, 108, and 109 plotted against the values for tree 102. Tree 102 was located in the area *without* understorey, while the four other trees were surrounded by understorey. The red line is the best fit of a linear regression.

Table 5.4: Statistics for the regression lines in Figure 5.12. (ID: tree identification, slope: slope of regression line, r: Pearson's correlation coefficient)

ID	mean (n=4176)		max (n=4172)	
	slope	r	slope	r
104	0.65	0.89	0.65	0.81
106	0.80	0.74	0.81	0.80
108	0.54	0.84	0.56	0.81
109	1.10	0.84	1.02	0.80
∅	0.77	0.83	0.76	0.81

The values of four regression lines are not enough to calculate higher statistical moments than the average. However, the average slope of the four linear regressions for the maximum turning moment is 0.77 (see Tab. 5.4) and this value is in good agreement with measurements from the wind tunnel. Gardiner et al. (2005) measured the wind loading of model trees in the wind tunnel, to examine the impact of different stand structures on the wind loading. The authors compare the bending moment coefficients of different stand layouts (see their Fig. 2b, p.476). The stand with an understorey from this experiment is described best

with the *Group Selection 200 mm trees*[2] from the wind tunnel experiment and the stand without an understorey is most similar to the *Uniform 50 % thinned 200 mm forest*[3]. The fraction of the two bending moment coefficients is 0.79, which is very similar to the value from this field study (0.77).

In plant physiology it is recognised that plants are able to adjust to environment conditions within their physiological limits. The acclimatisation to mechanical stimulation is known as *thigmomorphogenesis* and its impact on plant growth has been shown in many studies under field (e.g. Urban et al., 1994) and laboratory conditions (e.g. Ennos, 1997). Trees that are exposed to higher wind speeds and therefore higher turning moments show increased diameter growth. Ranking the four trees 104, 106, 108, and 109 using the slope from the linear regressions from Table 5.4 gives:

slope:	109	(1.02)	>	106	(0.81)	>	104	(0.65)	>	108	(0.58)
dbh (cm):	109	(39.8)	>	106	(37.8)	>	104	(35.2)	>	108	(33.7)
h (m):	104	(22.4)	>	109	(21.5)	>	108	(21.0)	>	106	(20.5)

The ranking by *dbh* results in the same order as the ranking by the slopes from Figure 5.12. Since rigidity is determined by the trunk diameter, this can be interpreted as an adaptation to different wind loading. This ordering does not work for tree height, so height is probably a poorer indicator of wind loading than *dbh*.

5.3.8 Critical wind speed

The turning moment at the tree base is only one component, that needs to be considered in the analysis of wind risk. The critical wind speed for tree failure is determinate by the resistance to failure (breaking or overturning). Therefore the plots in Figure 5.11 are only of limited use for predicting wind speeds of tree

[2] "... *Shelterwood/group selection.* The forest was constructed with equal numbers of trees of two heights (0.1 and 0.2 m) to simulate a canopy with an understorey, which will replace the high canopy after." (Gardiner et al., 2005, p.473)

[3] "... *Even-aged* Forest constructed out of only 0.2 m trees at a spacing of 0.0231 m (1874 trees m^{-2}) to simulate an even-aged stand of 15 m height and a spacing of 1.73 m. This is identical to the forest used in previous windtunnel experiments and therefore allows comparison with previously obtained results. This will be referred to as "EA" in the remainder of the text. Results for a similar forest from which 50 per cent of the trees were removed are also presented. These were measured and presented in Stacey et al. (1994). It will be referred to as "EA-50 per cent thinned". (Gardiner et al., 2005, p.473)

failure.

The assumption of the uniform stress hypothesis (Morgan and Cannell, 1994), allows the calculation of the breaking moment using the *dbh* and the species specific modulus of rupture (MOR) to calculate the stiffness of a trees trunk. The stiffness is linearly related to dbh^3.

The fitted model equations from Table 5.3 allow the calculation of the critical wind speed for breakage. For the inter-tree comparison the turning moments were normalised by the individual breaking moments from Table 5.1. The critical wind speed for a tree is reached when the value reaches unity. In Figure 5.13 the normalised model values for the six experimental trees of the overstorey are plotted versus the 10 min mean wind speed at Mast-II. This normalisation allows to compare all the six overstorey trees although tree 101 is significantly bigger than the rest. Estimated critical wind speeds cover the range of 19.5 to 24.4 m s^{-1}. Figure 5.13 shows that trees 101 and 102 without an understorey have the lowest predicted critical wind speeds.

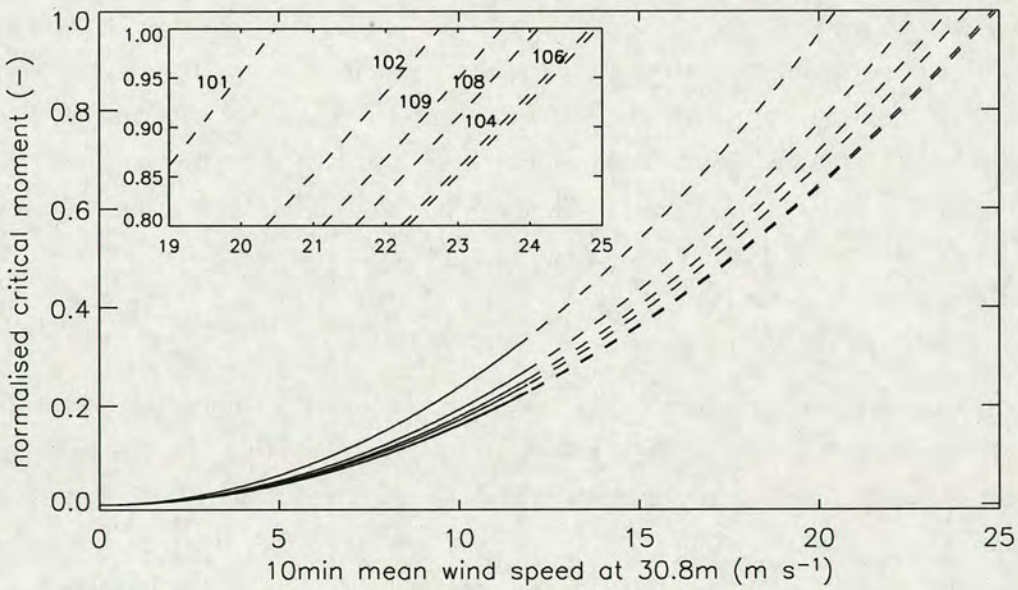

Figure 5.13: Normalised predicted mean turning moments ($\hat{M}/M_{break}$) versus 10 min mean wind speed measured on Mast-II at 30.8 m. The small plot inside is a 'blow up' from the bigger plot for the purpose of clarification.

5.3.9 Drag partitioning

In addition to the six trees from the overstorey, three trees from the understorey (103,105,107) were also monitored. All three trees were Sitka spruce. By comparing the time series in Figure 5.11 the differences in wind loading between overstorey and understorey become evident. The measured turning moments of the understorey trees are about a factor 100 smaller for trees 103 and 105 and still a factor 50 smaller for tree 107, which is taller than the two others. These huge differences underline the efficiency of energy absorption in the canopy of the overstorey and are in agreement with the wind profiles in Figures 5.6, which showed a strong attenuation of the wind profile in the overstorey canopy. This creates a relatively sheltered wind environment for the understorey. In addition to this the cantilever arm of the acting wind force is smaller due to the reduced height of the trees. These two factors result in very little turning moment at the base of the trees of the understorey. Another cause for the low turning moments might be the density of the understorey, which promotes crown interaction. Crown clashing is known to be a very efficient way of dissipating sway energy and inhibits the occurrence of high turning moments (Milne, 1991; Rudnicki et al., 2004). Gardiner et al. (2005) measured much higher ratios of extreme turning moments between overstorey and understorey. Their Figure 2b gives a ratio of 6-7, which is very different from what was measured in this experiment. A reason might be the much higher density of the understorey in the field experiment. The Shelterwood/group selection forest model "was constructed with equal numbers of trees of two heights" (Gardiner et al., 2005, p.473). The trees of the understorey were not mapped individually, but the ratio of the members of the understorey to the overstorey in the experimental stand is closer to 10:1 than 1:1 (see also the Photograph on the right hand side of Fig. 5.1).

If the irregular structure of the stand should be maintained in the future the removal of individuals from the overstorey is unavoidable. In this case the understorey will be suddenly exposed to higher wind speed. Since the trees are not provided with an opportunity to adapt to these wind speeds, this will inevitable result in a jump in the risk of wind damage for the stand. In comparison to common British plantations the stand density ($119\,\text{trees}\,\text{ha}^{-1}$) and the crown density are very low. This underlines the efficiency of energy absorption of the overstorey, which establishes a very sheltered environment for the understorey. Problems might occur if the trees, which make up the overstorey, are removed and the understorey is suddenly exposed to much higher wind loading which the

trees are not adapted to. This would increase the risk of wind damage. However, due to the efficiency of energy absorption a steadily stepwise increase of exposure seems almost impossible.

5.3.10 Interpretation of observations

In the previous sections the differences in the wind-tree interaction for the two stand types have been worked out. The analysis of wind speed, turbulence, and turning moment data are consistent and suggest that the experimental trees without an understorey are exposed to higher wind loading and have a higher risk of failure. The question is in what way does the presence of an understorey alter the turbulence structure so as to create this situation? Comparison of the turbulence characteristics showed that the eddy size is increased and that turbulence is more organised at the lower sonic level if the wind was coming from a direction with an understorey. At the same time a second wind speed maximum is observed at the location of Mast-I without an understorey, whereas its formation is inhibited at Mast-II due to the presence of an understorey. The existence of an inflection point in the trunk space could possibly promote the establishment of another mixing layer and could be the source of eddies, that are produced in the trunk space. For some time intervals RMA values greater than unity were observed, which can only be achieved by an upward momentum flux at the lower sonic level. The eddies from the lower mixing layer might impose viscous drag on those created at the canopy top and prevent their further downward penetration, which results in more momentum absorption in the upper parts of the canopy. Boldes et al. (2007) suggest the formation of lower level eddies in another open forest stand, which interact with the eddies generated at canopy-top.

However the proposed mechanical explanation remains speculative, since the poor vertical resolution of the turbulence measurements does not permit a more detailed analysis of the interaction of the eddy structures.

5.4 Conclusions

This is the first time that turning moments of trees in two neighbouring stands with different canopy structures have been measured simultaneously. Specifically we investigated two larch stands, one without an understorey an one with an understorey. The three independent analysis conducted were:

- comparison of wind profiles,
- analysis of the momentum absorption as function of wind direction, and
- a direct comparison of experienced turning moments.

This analysis has been used to compare the wind and tree interaction of the neighbouring stands. The results are consistent and suggest that trees with an understorey have to withstand less severe turning moments compared to overstorey trees that lack an understorey. The results are in agreement with those from a wind tunnel study, that investigated the wind loading on trees of different stand structures (Gardiner et al., 2005). In conclusion this supports observations from continental Europe, which suggest that irregular stand structures are more stable (Dvorák et al., 2001).

At the moment we are not able to give a totally satisfactory explanation for these results, which would probably require a more sophisticated setup. The data from one field experiment are also not sufficient for a proper parametrisation so that transferring this understanding to other stand structures is not possible yet. However, with the recent progress in applying large eddy simulation for forest canopies (Yang et al., 2006; Clark and Mitchell, 2007; Dupont and Brunet, 2008a) it seems reasonable to tackle this question with the help of a modelling approach rather than field experiments.

Acknowledgement

Structured forest stands are rare as hens' teeth in Britain. All the more we have to thank Peter Hale (Hale Association) and Ian Robinson (Scottish Woodland) for letting us conducting the experiment in one of the stands in the beautiful Kyloe Wood forest. As usual the guys from the Technical Support Unit did the tough jobs for me, while I was supervising. Thanks go to Carl Foster, Brian Jones, Dai Evans, "Dickie". Sylvain Dupont, INRA (France), kindly provided the data from his LES simulations, which were used for comparison in Figure 5.9 and published in *Agricultural and Forest Meteorology.*

I also like to thank many of my colleagues at the Northern Research Station, which gave me a hand during the field season: Shaun Mochan, Bruce Nicoll, Alexis Achim, and Sophie Bertin.

References

Andersen KF, 1954: Gales and gale damage to forests, with special reference to the effects of the storm of 31st January 1953, in the northeast of Scotland. *Forestry*, 27, 97–121.

Baldocchi DD and Meyers TP, 1988: Turbulence structure in a deciduous forest. *Boundary-Layer Meteorology*, 43, 345–364.

Blackburn GRA, 1997: *The Growth and Mechanical Response of Trees to Wind Loading*. PhD, University of Manchester.

Boldes U, Scarabino A, and Colman J, 2007: About the three-dimensional behavior of the flow within a forest under unstable conditions. *Journal of Wind Engineering and Industrial Aerodynamics*, 95, 91–112.

Brunet Y and Irvine MR, 2000: The control of coherent eddies in vegetation canopies: Streamwise structure spacing, canopy shear scale and atmospheric stability. *Boundary-Layer Meteorology*, 94, 139–163.

Cheng DL and Niklas KJ, 2007: Above- and below-ground biomass relationships across 1534 forested communities. *Annals of Botany*, 99, 95–102.

Clark TL and Mitchell SJ, 2007: Three-dimensional simulations of air flow and momentum transfer in partially harvested forests. *Boundary-Layer Meteorology*, 125, 505–524.

Dupont S and Brunet Y, 2008a: Edge flow and canopy structure: A large-eddy simulation study. *Boundary-Layer Meteorology*, 126, 51–71.

Dupont S and Brunet Y, 2008b: Influence of foliar density profile on canopy flow: A large-eddy simulation study. *Agricultural and Forest Meteorology*, 148, 976–990.

Dvorák L, Bachmann P, and Mandallaz D, 2001: Sturmschäden in ungleichförmigen Beständen. *Schweizerische Zeitschrift für Forstwesen*, 152, 445–452.

Ennos AR, 1997: Wind as an ecological factor. *Trends in Ecology and Evolution*, 12, 108–111.

Finnigan J, 2000: Turbulence in plant canopies. *Annual Review of Fluid Mechanics*, 32, 519–571.

Finnigan JJ, 2004: A re-evaluation of long-term flux measurement techniques Part II: Coordinate systems. *Boundary-Layer Meteorology*, 113, 1–41.

Finnigan JJ, Clement R, Malhi Y, Leuning R, and Cleugh H, 2003: A re-evaluation of long-term flux measurement techniques Part I: Averaging and coordinate rotation. *Boundary-Layer Meteorology*, 107, 1–48.

Gao W, Shaw RH, and Paw U KT, 1989: Observation of organized structure in turbulent flow within and above a forest canopy. *Boundary-Layer Meteorology*, 47, 349–377.

Gardiner B, Marshall B, Achim A, Belcher R, and Wood C, 2005: The stability of different silvicultural systems: A wind tunnel investigation. *Forestry*, 78, 471–484.

Gardiner BA and Quine CP, 1994: Wind damage to forests. *Biomimetics*, 2, 139–147.

Ghisalberti M and Nepf H, 2006: The structure of the shear layer in flows over rigid and flexible canopies. *Environmental Fluid Mechanics*, 6, 277–301.

Hale SE, 2003: The effect of thinning intensity on the below-canopy light environment in a Sitka spruce plantation. *Forest Ecology and Management*, 179, 341–349.

Irvine MR, Gardiner BA, and Hill MK, 1997: The evolution of turbulence across a forest edge. *Boundary-Layer Meteorology*, 84, 467–496.

de Langre E, 2008: Effects of wind on plants. *Annual Review of Fluid Mechanics*, 40, 141–168.

Lu SS and Willmarth WW, 1973: Measurements of the structure of the Reynolds stress in a turbulent boundary layer. *Journal of Fluid Mechanics*, 60, 481–511.

Marshall BJ, Wood CJ, Gardiner BA, and Belcher RE, 2002: Conditional sampling of forest canopy gusts. *Boundary-Layer Meteorology*, 102, 225–251.

Mason WL, 2002: Are irregular stands more windfirm? *Forestry*, 75, 347–355.

Mason WL, Kerr G, and Simpson J, 1999: What is Continuous Cover Forestry? Information Note 29, Forestry Commission, Edinburgh.

Miller KF, 1985: Windthrow hazard classification. Leaflet 85, Forestry Commission.

Milne R, 1991: Dynamics of swaying of *Picea sitchensis*. *Tree Physiology*, 9, 383–399.

Moore JR, Gardiner BA, Blackburn GRA, Brickman A, and Maguire DA, 2005: An inexpensive instrument to measure the dynamic response of standing trees to wind loading. *Agricultural and Forest Meteorology*, 132, 78–83.

Moore JR and Maguire DA, 2004: Natural sway frequencies and damping ratios of trees: Concepts, review and synthesis of previous studies. *Trees*, 18, 195–203.

Morgan J and Cannell MGR, 1994: Shape of tree stems - a re-examination of the uniform stress hypothesis. *Tree Physiology*, 14, 49–62.

Nicoll BC, Gardiner BA, Rayner B, and Peace AJ, 2006: Anchorage of coniferous trees in relation to species, soil type, and rooting depth. *Canadian Journal of Forest Research*, 36, 1871–1883.

Pommerening A and Murphy S, 2004: A review of the history, definitions and methods of continuous cover forestry with special attention to afforestation and restocking. *Forestry*, 77, 27–44.

Py C, de Langre E, and Moulia B, 2006: A frequency lock-in mechanism in the interaction between wind and crop canopies. *Journal of Fluid Mechanics*, 568, 425–449.

Raupach MR, Finnigan JJ, and Brunet Y, 1996: Coherent eddies and turbulence in vegetation canopies: The mixing-layer analogy. *Boundary-Layer Meteorology*, 78, 351–382.

Rollinson TJD, 1987: Thinning control of conifer plantations in Great Britain. *Annals of Forest Science*, 44, 25–34.

Rudnicki M, Mitchell SJ, and Novak MD, 2004: Wind tunnel measurements of crown streamlining and drag relationships for three conifer species. *Canadian Journal of Forest Research*, 34, 666–676.

Schütz JP, Götz M, Schmid W, and Mandallez D, 2006: Vulnerability of spruce (*Picea abies*) and beech (*Fagus sylvatica*) forest stands to storms and consequences for silviculture. *European Journal of Forest Research*, 125, 291–302.

Shaw RH, 1977: Secondary wind speed maxima inside plant canopies. *Journal of Applied Meteorology*, 16, 514–521.

Shaw RH, Tavangar J, and Ward DP, 1983: Structure of the Reynolds stress in a canopy layer. *Journal of Climate and Applied Meteorology*, 22, 1922–1931.

Stacey GR, Belcher RE, Wood CJ, and Gardiner BA, 1994: Wind flows and forces in a model spruce forest. *Boundary-Layer Meteorology*, 69, 311–334.

Troen I and Petersen E, 1989: *European Wind Atlas*. Risø National Laboratory, Roskilde.

Urban ST, Lieffers VJ, and MacDonald SE, 1994: Release in radial growth in the trunk and structural roots of white spruce as measured by dendrochronology. *Canadian Journal of Forest Research*, 24, 1550–1556.

Wilczak JM, Oncley SP, and Stage SA, 2001: Sonic anemometer tilt correction algorithms. *Boundary-Layer Meteorology*, 99, 127–150.

Yang B, Morse AP, Shaw RH, and Paw U KT, 2006: Large-eddy simulation of turbulent flow across a forest edge. Part II: Momentum and turbulent kinetic energy budgets. *Boundary-Layer Meteorology*, 121, 433–457.

Chapter 6

General Discussion

6.1 Main findings from the field experiments

The data from the first field campaign in a mature Sitka spruce stand in Clocaenog Forest showed pronounced differences in the measured turning moments for the nine experimental trees. The turning moment for the tallest tree was about one order of magnitude higher than for the tree with the lowest turning moment. The vast majority of wind energy is absorbed in the upper parts of the canopy where only the crowns of the dominant trees are present. Due to the exposure of their canopy, taller trees experience higher drag and therefore higher turning moments compared to their smaller neighbours. Naturally taller trees also have higher resistance to breakage and overturning. The strongest experimental tree in Clocaenog was estimated to be more than 5 times stronger than the weakest one.

A quadratic function was fitted to the 10 min maximum turning moment and the 10 min mean wind speed data. Except for one tree R^2 values were higher or equal to 0.75. These regression models were used to predict the critical wind speeds for the experimental trees. The values obtained were similar in comparison to the measured turning moments. Predicted critical wind speeds for the nine trees covered the range 15.5-22.5 $\mathrm{m\,s^{-1}}$ (mean: 18.7 $\mathrm{m\,s^{-1}}$). The relationships between individual tree characteristics and predicted wind speeds for breakage for the nine trees were only weakly correlated. For the overturning wind speed the correlation coefficients were higher. The slope of the regression lines when either *dbh* or tree height were used as independent variable were negative, which indicates that the taller trees in the stand are at higher risk of failure.

Competition indices turned out to be a good estimator to explain the differences in wind loading among the group of experimental trees. The absolute values of the correlation coefficients for four out of six tested indices were higher than 0.89, which indicates that competition indices can explain most of the observed variance in turning moment between trees. For two of the experimental trees it was shown that wind direction also influenced the turning moment. For wind directions with lower competition, the turning moment was increased for the same wind speed compared to wind directions, with higher competition. This underlines on the one hand the suitability and sensitivity of the competition indices, but on the other hand it poses the question as to the need to include wind direction in the analysis of wind risk. In cases in which the competition is very different for different wind directions this is probably essential.

In the second field survey the wind and tree interaction in two adjacent stands was analysed. The overstorey of the two stands was made up by the same crop but only at one of the stands was a dense understorey present. The results from the experiment suggest that the presence of an understorey has an impact on the wind profile and the turbulence characteristics. In the stand without an understorey the wind profile showed a more rapid decline in the upper part of the canopy, which was related to higher momentum absorption by the canopy. These results are backed up by turbulence measurements above the canopy and at the bottom of the overstorey canopy. Normalised differences in momentum flux between the two heights were more pronounced when the wind blew from a sector without an understorey. The measured horizontal and vertical Eulerian length scales and the correlation coefficient of these two wind components were reduced compared to a sector with an understorey. This indicates that the turbulence is less organised and that the efficiency of momentum transfer is reduced at the bottom of the overstorey canopy if there is no understorey.

The differences in the wind profile and turbulence characteristics had an effect on the wind-tree interaction at the two locations. A direct comparison between a tree from the stand without an understorey with four trees from the location with an understorey suggest that the presence of an understorey reduces wind loading. Predicted critical wind speeds of breakage for the experimental trees also suggest that trees without an understorey have a higher risk of failure compared to trees with an understorey.

6.2 Relevance for wind risk modelling

The variation in wind loading between trees needs to be accounted for in any wind risk model that deals with irregular stand structures. The observed differences are too significant for only an average tree to be considered in any modelling. Such a simple approach does not represent adequately the conditions of an irregular stand.

The data analysis from the Clocaenog experiment showed that the wind energy is not distributed equally onto the individuals of the stand and that the vast amount of momentum is absorbed by the tallest members of the stand. Therefore the *average* tree is not necessarily representative of the stability of the whole stand. The prediction of the critical wind speeds for the experimental trees suggest that the taller trees are at a higher risk of failure and hence determine the overall stability of the stand.

Accounting for the differences in wind loading requires that the wind risk models perform their calculations at the individual tree level rather than at the stand level. Individual tree resolution is also required to estimate the impact of any thinning on the stability of the stand.

The wind and turning moment relationships for the trees in Clocaenog Forest were influenced by wind direction. For a wind sector with a gap, the turning moment was increased compared to a wind direction without gap for the same wind speed. Due to the low tree density in the Clocaenog stand and the advanced maturity of the trees, the removal of any tree would inevitable create a considerable gap and hence would increase the wind loading and risk for the remaining trees in a downwind direction. This adds another component to the analysis of the wind and tree interaction. Unfortunately the data from only nine trees was not sufficient for a parametrisation of the impact that gaps have on the wind and tree relationship.

6.3 Application for forest management

The stability of the experimental stand in Clocaenog Forest shows that the transformation of even-aged stands towards an irregular structure is possible. From the field survey in Kyloe Wood we found that it is likely that an irregular stand is beneficial in terms of wind risk. The results should encourage British foresters to promote the transformation of regular into irregular stands. However,

forest stands will always be vulnerable to wind damage particularly following any stand manipulation and any thinning will inevitable lower the stability of any stand at least in the short term.

Due to the pronounced differences in momentum absorption and turning moments, that were measured in the Clocaenog experiment, it is hard to imagine that trees, which are not dominant, would bear up to the wind loading of a taller and more exposed member of the stand. Non-dominant trees are reliant on a sheltered wind environment, that is created for them by their taller neighbours. In comparison, the removal of smaller trees will have less impact on the bigger trees, since the smaller trees do not contribute much shelter to the bigger ones. Therefore the removal of smaller trees during stand intervention is generally preferable from a stability point of view.

However, the comparison of the wind and tree interaction of individual trees in adjacent stands in Kyloe Wood, suggests that the overstorey trees benefit in part from an understorey in terms of wind loading and risk. Turbulence characteristics and comparison of the wind profiles in the two stands support this observation with increased momentum absorption in the overstorey in the absence of an understorey. The results from the field experiment are in agreement with those from Gardiner et al. (2005) derived from wind tunnel studies. Early and less intense thinning is still the preferred way to establish an irregular stand structure. For mature forest stands in exposed areas any thinning might result in an unacceptable high risk of wind damage. However, the Kyloe Wood and Clocaenog stands are two examples of a successful implementation of continuous cover forestry in Britain and proof that it is possible to introduce irregular stand structures if done carefully.

Stability of forests is dependant on a multitude of factors. Since the time scale of the rotation period of forests is in line with those that are discussed in the global change debate, forestry will be very much affected. Changes in air temperature, precipitation, and CO_2 concentrations are only some of many parameters, that need to be considered as factors affecting tree growth. Today's silviculture defines the forest structure for the forthcoming decades. Therefore, a clear understanding of the trees response to any environmental change is a necessary precondition for sensible decision making processes.

6.4 Recommendations for further work

The field data from the two field surveys give valuable information of the wind and tree interaction in irregular structured forest stands and will help to improve wind risk models. However, the data from the two field experiments only represent a snapshot in the life time of a stand.

The performance of competition indices as independent variables for explaining differences in wind loading is encouraging and worth further investigation. However, at the moment the available data are not sufficient for an exhaustive parametrisation. In particular the impact of gaps on the wind loading, that was shown for two experimental trees in Clocaenog Forest, seems to be a major aspect and needs to be considered in the modelling of wind risk. Long-term measurements, or repeated measurements in a stand before and after a thinning intervention, are necessary to achieve a more general parametrisation of this approach. At the moment the estimated relationships are only applicable to the experimental stand, since it can not be assured that they are independent from general stand characteristics. Measurements in different stand types are therefore required.

The establishment of natural regeneration below the canopy is a precondition for a successful transformation of regular forest stands towards CCF. Therefore any approach which neglects the light regime is of limited practicability. A linkage of growth, light, and wind risk models is essential to estimate the success of the transformation process. Results from the experiment in Kyloe Wood are in agreement with those from Gardiner et al. (2005) obtained in the wind tunnel. The differences that were worked out are based on the separation of the data pools regarding the wind direction to distinguish a stand structure with and without an understorey. Due to the heterogeneity of any forest it can not be assumed that the observed differences are caused by the presence of an understorey, although there is strong evidence. A controlled experiment in which the understorey is removed and measurements are taken before and after the removal are desirable and would increase the reliability of the results.

So far only coniferous species are incorporated in the ForestGALES model. Besides the encouragement to transform regular structured stands into irregular ones, British foresters are also encouraged to increase the proportion of broadleaved species. At the moment a parametrisation of deciduous species is not possible due to a lack of data. Adding broadleaved species to the model is

another desirable step to increase the applicability for stands under continuous cover management.

References

Gardiner B, Marshall B, Achim A, Belcher R, and Wood C, 2005: The stability of different silvicultural systems: A wind tunnel investigation. *Forestry*, 78, 471–484.

Appendix A

Strain transducers

A.1 Design

The aluminium strain transducers used in the field studies were designed by Blackburn (1997) and the Forest Research workshop at the Northern Research Station (NRS) (see Fig. A.1). Blackburn required long term measurements of growth and wind loading in living Sitka spruce (*Picea sitchensis* (Bong.) Carr.) trees.

Several examples can be found in the literature where strain gauges were used to measure the strain of living plants (e.g. Ennos, 1995) and where the strain gauges were glued directly onto the prepared bark of a tree. However, this setup is not feasible for long term experiments, since the installation does not generally last long. In particular Sitka spruce produces significant amounts of resin as a defence reaction if it gets wounded, which is unavoidable when the bark is prepared for the mounting of the strain gauge.

The main requirements the strain transducer design has to fullfill for long term measurements are:

1. the possibility of sealing the strain gauges to protect them from weather,
2. a high signal to strain ratio,
3. and linearity between signal to strain.

The linear response of the strain transducers was tested on a precision millimetre machine. For the calibration the strain transducer was fixed with a bole in one screwhole while the other end of the strain transducer was moved

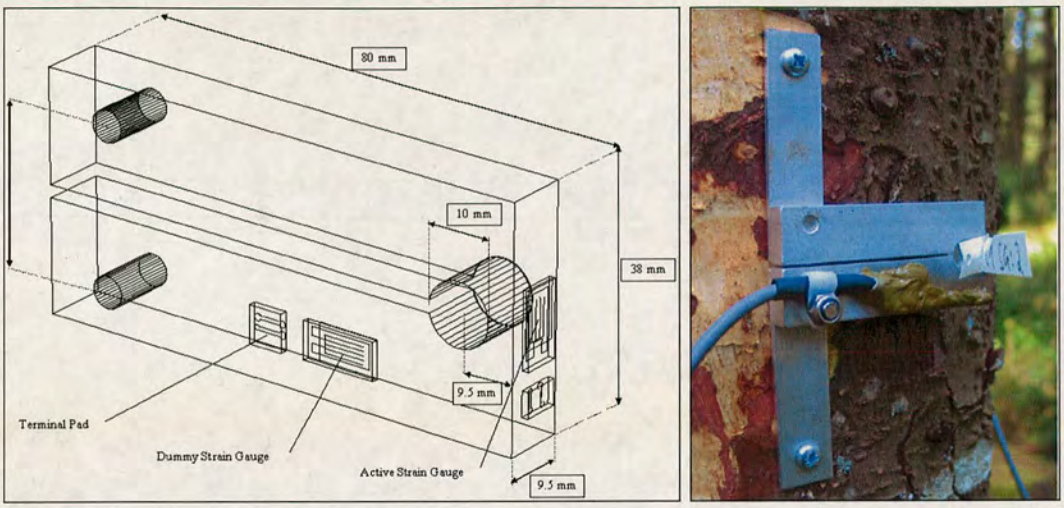

Figure A.1: Schematic illustration of the strain transducer design (left hand side; figure taken from Blackburn (1997)) and strain transducer attached to a Sitka spruce tree in Clocaenog Forest (right hand side).

in steps of 0.01 or 0.02 mm. The displacement was measured with a dial gauge. In Figure A.2 the signal output of the bridge is plotted versus the displacement. For the chosen example the correlation coefficient is -1 and the mean square error is 0.00033. These numbers prove the high linearity of the strain transducers. The scatter around the regression line near zero displacement is due to some slack, because the holding pivot did not exactly fit the screwholds of the strain transducers. This is not a problem in the field, since the transducers are screwed into the trees (see Fig. A.1).

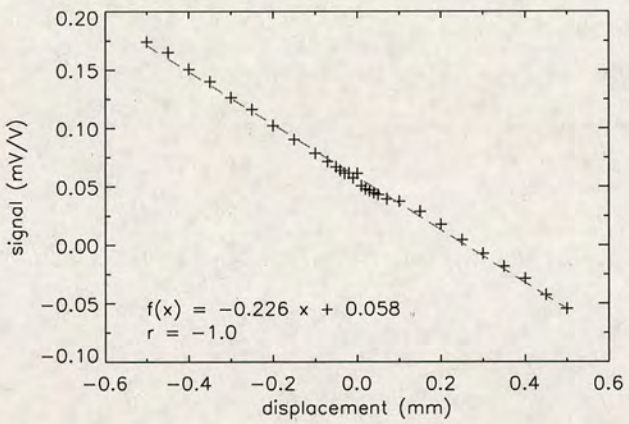

Figure A.2: Example of a strain transducer calibration on the precision millimetre machine in the workshop at the Northern Research Station. The strain transducer signal is plotted versus the displacement.

A more extensive description and background information about the strain transducers can be found in Blackburn (1997) and Moore et al. (2005).

A.2 Measurement

The most common strain gauge type is the foil strain gauge. A metallic foil pattern is combined with an insulating flexible backing. Any kind of deformation causes a *small* change in electrical resistance. To achieve a sufficient accurate measurement of such changes the strain gauges are incorporated into a Wheatstone bridge as it is shown in Figure A.3. The four resistors of the bridge can all be strain gauges or any number can be supplemented by a high precision constant resistor. When the bridge is balanced the voltage across the two legs is zero. Strain gauges are relatively power demanding. This can cause problems if batteries are relied on to supply power. The signal output of the bridge is related linearly with the applied voltage (see Eq. A.3). Higher excitation voltage gives a higher signal output.

$$V = \left(\frac{R_x}{R_3 + R_x} - \frac{R_2}{R_1 + R_2} \right) \cdot V_{Ex} \qquad \text{(A.1)}$$

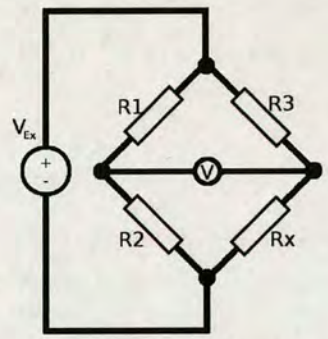

Figure A.3: Circuit diagram of a Wheatstone bridge and the formula to calculate the output of the bridge as function of the four resistances (R_x, R_1, R_2, R_3) and the excitation voltage (V_{Ex}).

For many data loggers the resolution of the differential voltage measurement is linked to the measurement range. High resolution means a narrow signal range and vice versa. This can cause problems when the strain gauge is not close to balance in the resting position of the tree. Small changes can than cause the signal output to exceed the data loggers measurable range. Care should therefore be taken that the bridge is balanced in the trees resting position. A work-around for this problem is the implementation of a potentiometer into the bridge, which can be used to balance the bridge. The downside of this method is, that the potentiometer might be too responsive to temperature changes which have to

then be accounted for.

A.3 Calibration

General

Every strain transducer has individual characteristics and every tree has its specific rigidity. Therefore an individual calibration is required for each strain transducer to calculate the turning moment on the tree from the strain transducer signal.

For the calibration of the strain transducer an artificial known turning moment is applied to the tree while the output of the strain transducer (Wheatstone bridge) is measured. Since the process is supposed to copy the wind loading under natural conditions the calibration procedure should mimic this process as closely as possible.

Theory

The strain transducers respond to changes in distance between its two anchor points. Strain (ε) is defined as the relative change in distance:

$$\varepsilon = \frac{\Delta L}{L} \tag{A.2}$$

where L (m) is the total distance, which is in our case the distance between the two attachment points of the strain transducer (see Fig. A.1). The strain a tree experiences is a function of its stiffness and the applied load, and the strain and turning moment are linearly related:[1]

$$\varepsilon = \frac{32 \cdot M}{\pi \cdot E \cdot d^3} \tag{A.3}$$

where M (N m) is the applied turning moment, E (Pa) is Young's modulus, and d (m) is the diameter of the tree at the height, where the strain transducer is mounted.

When the tree bends to one side the outer fibres on the opposite side get stretched. Since the strain transducer is screwed into the outer part of the tree, it follows this stretching. The opposite happens when the tree bends in the

[1]Blackburn (1997) carried out tree pulling tests to estimate the Young's modulus of several Sitka spruce trees and got unreasonable high values in freezing conditions. Hence the rigidity of a stem is also a function of the weather condition.

other direction. Than the fibres in the tree get squeezed and so does the strain transducer.

Since a strain transducer works in one direction of the xy-plane, two strain transducers are needed per tree to reproduce the sway pattern and applied moment in the xy-plane.

Setup

In terms of wind loading the tree crown can be regarded as the sail of a boot, where wind acts on an area (Mattheck, 1991). This is impossible to completely mimic in a tree pulling test. Thom (1971) showed that the zero plane displacement of the wind profile can be considered as the acting height of the wind force. Therefore, this height would be the optimal attachment height for the pulling rope (Wood, 1995). In practise this height is often not accessable, since it is located within the crown, but the rope should be placed as close to the zero plane displacement height as possible. For most plant canopies 0.66–0.80 times canopy height is a good estimate of the zero plane displacement (Oke, 1987).

The anchor point for the pulling rope should be aligned with the strain transducer and as far away from the subject tree as feasible to achieve a low angle for the pulling rope (see Fig. A.6). In a forest other tree trunks can provide suitable anchor points. The applied load is measured with a load cell, which is located in between the anchor point and the pulling rope.

If possible the strain transducer and the load cell should be attached to the same data logger and logged automatically. For calibration the following measurements are necessary:

- attachment height on the tree of the pulling rope,
- angle of the pulling rope at the beginning of the procedure,
- angle deviation (*Azimuth*) of alignment of strain transducer and rope,
- strain transducer signal, and
- load measurements.

Calibration procedure

Tree pulling tests should be carried out on calm days to reduce any signal noise caused by wind loading. The tree pulling should be carried out with increasing

and decreasing loads. First of all the turning moment is increased to the maximum load. Then the load is decreased stepwise, until the tree is in its rest position again.

Operating the winch will cause unwanted tree movement, since its design makes a steady increase/decrease of loading impossible (see Fig. A.4). Therefore, the tree should be left for 20 to 30 seconds after every step to damp on any tree swaying. Figure A.4 shows the time series of a single calibration procedure. Before each plateau in the time series there is a short overshooting of the signal, while the winch is in operation.

To avoid any kind of structural damage to the tree the maximum applied turning moment should be well below the trees critical moment. As a rule of thumb the maximal applied force should not exceed 30 % of the critical moment and the rotation angle at the base of the tree should not exceed 5 ° from the trees rest position.

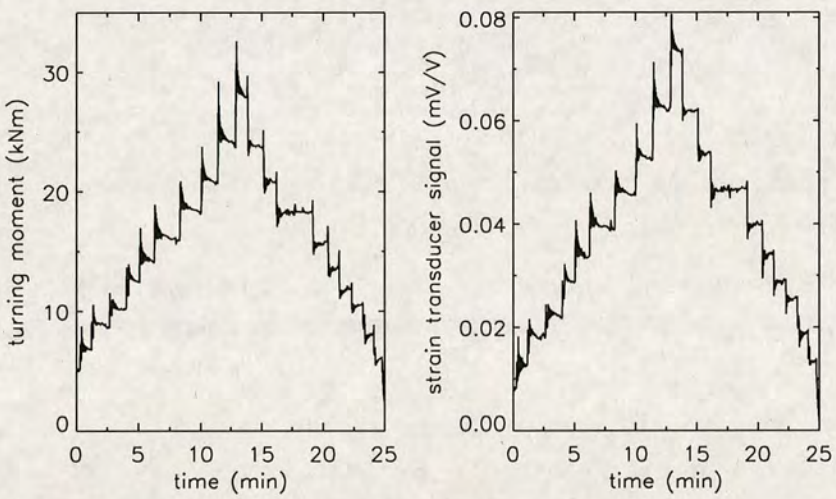

Figure A.4: Time series of applied turning moment and strain transducer signal from the calibration procedure for the NS strain transducer of tree 38 in Clocaenog Forest (date: 09.Nov.2005).

Data analysis

The turning moment is calculated from the height (h in m) of attachment point on the subject tree, the measured load (F in N), the angle (α in deg) of the rope, and the deviation of the pulling direction from a straight line between the strain transducer and the anchor tree (see Fig. A.6):

$$M = F \cdot h \cdot cos(\alpha) \cdot cos(\beta) \tag{A.4}$$

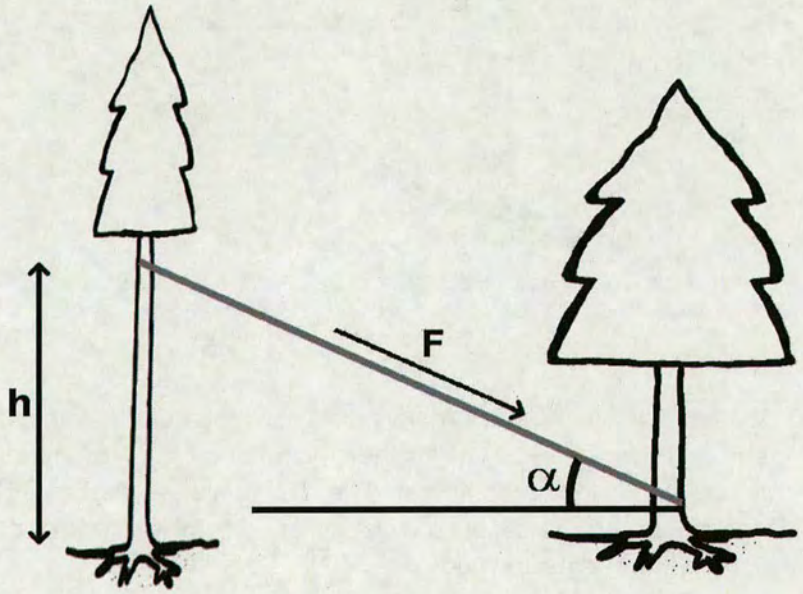

Figure A.5: Illustration of the tree pulling procedure for calibrating the strain transducers in the field.

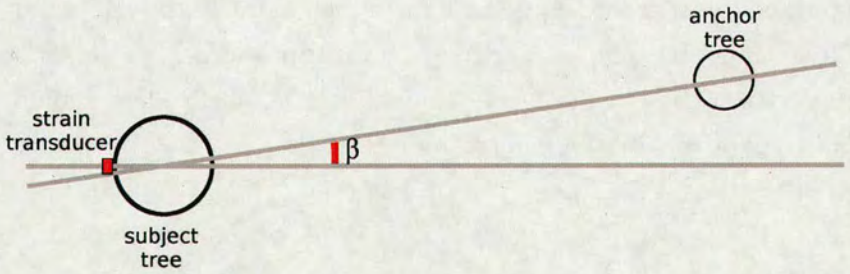

Figure A.6: Accounting for the angle deviation between the anchor tree and the strain transducer.

The calibration coefficient for the strain transducer is determined by performing a linear regression analysis of the strain transducer signal (STS) and the applied turning moment (M):

$$M(STS) = a \cdot STS + b \tag{A.5}$$

The calibration coefficient is the slope (a) of the regression line. In Figure A.7

the turning moment is plotted versus the strain transducer signal for one calibration procedure in Clocaenog Forest. The dashed line represents the calibration function.

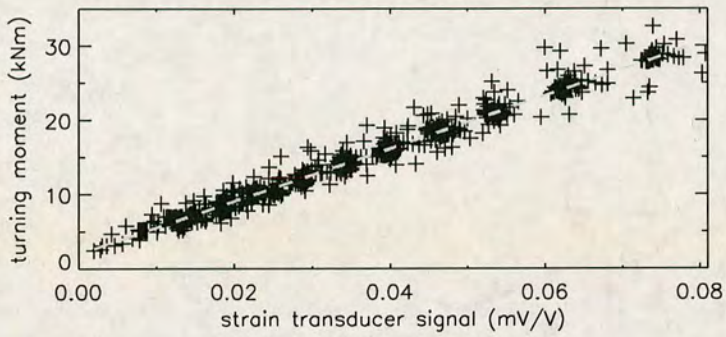

Figure A.7: Scatter plot of applied turning moment versus strain transducer signal (same data as in Fig. A.4) for the calibration of the NS strain transducer of tree 38 in Clocaenog Forest. The dashed line is the best fit of a linear regression and the calibration coefficient for the strain transducer is the slope of the regression line ($R^2 = 0.98, SE = 0.62$).

Blackburn (1997) observed in some of his calibrations a hysteresis in the data of his tree pulling experiments, which he accounts to the complex structural properties of wood (Morgan and Cannell, 1994). In such cases the time series of the tree pulling experiment should be split at the point of the maximum load, so that the two time series represent the part with increasing load and the one for decreasing force. The calculation of the calibration coefficients should than be carried out separately for the two sets of data.

References

Blackburn GRA, 1997: *The Growth and Mechanical Response of Trees to Wind Loading*. PhD, University of Manchester.

Ennos AR, 1995: Development of buttresses in rainforest trees: The influence of mechanical stress. In Coutts MP and Grace J, eds., *Wind and Trees*, chap. 17, pp. 293–304. Cambridge Univ. Press.

Mattheck C, 1991: *Trees: The mechanical design*. Springer-Verlag, Berlin, Germany.

Moore JR, Gardiner BA, Blackburn GRA, Brickman A, and Maguire DA, 2005: An inexpensive instrument to measure the dynamic response of standing trees to wind loading. *Agricultural and Forest Meteorology*, 132, 78–83.

Morgan J and Cannell MGR, 1994: Shape of tree stems - a re-examination of the uniform stress hypothesis. *Tree Physiology*, 14, 49–62.

Oke T, 1987: *Boundary layer climates*. Routledge, London, 2nd edn.

Thom AS, 1971: Momentum absorption by vegetation. *Quarterly Journal of the Royal Meteorological Society*, 97, 414–428.

Wood CJ, 1995: Understanding wind forces on trees. In Coutts MP and Grace J, eds., *Wind and Trees*, chap. 7, pp. 133–164. Cambridge Univ. Press.

Appendix B

Clocaenog Forest

B.1 Logging system

The logging system for the field campaign in Clocaenog Forest consisted of several data loggers, communication devices, and one industrial PC (see Fig. B.1). All strain transducer were measured by CR10 data loggers (Campbell Scientific, Logan, US). Each data logger measured 6 strain transducers (3 experimental trees). The CR10s were equipped with 32 kB memory, which was sufficient to store about 12 minutes of strain transducer data. Therefore it was not possible to just use the data loggers without any additional data storage facility. For the purpose of data storage all data loggers were implemented into a RS485-network using communication modules (MD-485, Campbell Scientific). The RS485 protocol allows addressing of a number of devices such as data loggers. For the final data storage an industrial PC (PIP6, MPL, Switzerland [1]) was added to the network, which ran permanently using LOGGERNET software (Campbell Scientific). The data from the CR10s were sent on request every 3 minutes to the industrial PC for final data storage. No processing of the data took place in the field. All raw data were stored as plain text files on the hard disk of the industrial PC.

The cup anemometers were logged with two different data logger types. One was a 21X (Campbell Scientific) which logged the two wind vanes and the four upper cup anemometers and was also part of the RS485-network. Final data storage of the 21X data was also done by the industrial PC. The four lower cup anemometers were logged by a Holtech data logger (Durham, UK), with a time

[1] For the 2nd half of the experiment the PIP was replaced by a PC4 (OR-Industrial Computers, Germany)

resolution of one minute. The Holtech logger wrote all data to a PCMCIA Flash Card, which was taken to the office for downloading at the end of every run.

For the second half of the experiment a sonic anemometer was available (USA-1, METEK GmbH, Germany). The sonic was equipped with an internal A/D converter. The sonic anemometer permanently streamed the 10 Hz raw data as a RS422 signal. The RS422 signal was converted to an RS232 signal and connected to the second serial port of the industrial PC. All raw data were stored in hourly files using the manufacturer's software (tcopy.exe).

The whole logging system was relatively power demanding. In particular the industrial PC, which required 12 W, made it impossible to run the logging system permanently, since no mains power was available on site. Because the focus of the experiment was to investigate the interaction of wind and tree in high winds, the decision was made to switch the system on manually, whenever a low pressure system was approaching. Therefore, no continuous time series are available.

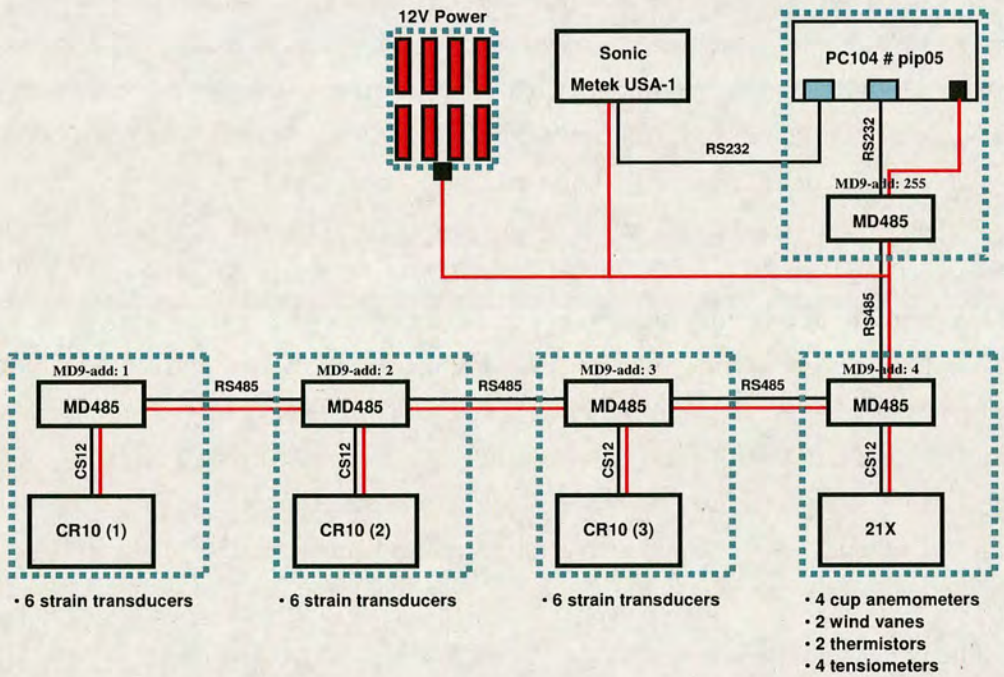

Figure B.1: Schematic illustration of the measuring system as it was used during the field survey in Clocaenog Forest.

Table B.1: List of sensors and data logging equipment used during the field experiment in Clocaenog Forest.

Sensor	Location	logging	time res.
ST#001[2]	Tree 80.E	CR10#3.DIFF1[3]	4 Hz
ST#002	Tree 80.N	CR10#3.DIFF2	4 Hz
ST#003	Tree 39.E	CR10#3.DIFF3	4 Hz
ST#004	Tree 39.N	CR10#3.DIFF4	4 Hz
ST#005	Tree 37.E	CR10#3.DIFF6	4 Hz
ST#006	Tree 37.N	CR10#3.DIFF5	4 Hz
ST#007	Tree 40.E	CR10#2.DIFF1	4 Hz
ST#008	Tree 40.N	CR10#2.DIFF2	4 Hz
ST#009	Tree 41.E	CR10#2.DIFF3	4 Hz
ST#010	Tree 41.N	CR10#2.DIFF4	4 Hz
ST#011	Tree 43.E	CR10#2.DIFF5	4 Hz
ST#012	Tree 43.N	CR10#2.DIFF6	4 Hz
ST#013	Tree 38.E	CR10#1.DIFF1	4 Hz
ST#014	Tree 38.N	CR10#1.DIFF2	4 Hz
ST#015	Tree 42.E	CR10#1.DIFF3	4 Hz
ST#016	Tree 42.N	CR10#1.DIFF4	4 Hz
ST#017	Tree 4.E	CR10#1.DIFF5	4 Hz
ST#018	Tree 4.N	CR10#1.DIFF6	4 Hz
NRG#40[4]	30.8 m	21X.P1	1 s
NRG#40	27.0 m	21X.P2	1 s
NRG#40	24.0 m	21X.P3	1 s
NRG#40	21.0 m	21X.P4	1 s
NRG#40	18.0 m	Holtech	1 min
NRG#40	15.0 m	Holtech	1 min
NRG#40	10.0 m	Holtech	1 min
NRG#40	5.0 m	Holtech	1 min
NRG#200P[5]	27.0 m	21X.SE1	1 s
NRG#200P	15.0 m	21X.SE2	1 s
USA-1[6]	29.8 m	PC (serial port)	10 Hz
SKT600#1[7]		21X.DIFF4	15 min
SKT600#2		21X.DIFF5	15 min
SKT600#3		21X.DIFF6	15 min

— continued on next page —

[2]ST: strain transducer

[3]reading from left to right: DATALOGGER#ID.CHANNEL (e.g. CR10#3.DIFF1 is the 1st differential channel on the 3rd CR10.

[4]NRG#40: cup anemometer (NRG Systems, US)

[5]NRG#200P: wind vane (NRG Systems, US)

[6]USA-1: sonic anemometer (METEK GmbH, Germany)

[7]SKT600: Skye tensiometer (Skye Instruments, Powys, UK)

— continued from previous page —

Sensor	Location	logging	time res.
Thermistor#1	27.0 m	21X.SE5	15 min
Thermistor#2	5.0 m	21X.SE6	15 min

B.2 Photographs - Clocaenog Forest

Figure B.2: Photographs taken in the experimental plot in Clocaenog Forest. First row shows representative fish-eye photographs taken within the experimental stand. The other pictures show the amount of natural regeneration on the forest floor and the general stand structure.

Appendix C

Kyloe Wood

C.1 Logging system

The field campaign in Kyloe Wood was the second part of my PhD project. In comparison to the first campaign in Clocaenog Forest the logging system underwent considerable improvements. The use of simple Gigalog8 (Audon Electronics, Nottingham, UK) data loggers allowed us to dispense with the industrial PC, which was needed in the Clocaenog experiment for final data storage and which was the main consumer of power.

The heart of the system was a CR23X data logger (Campbell Scientific, Logan, US) which on its own measured all 18 strain transducers, two wind vanes, and eight cup anemometers. Since the amount of differential channels on the wiring panel of the data loggers is not sufficient for the 18 strain transducers a relay multiplexer (AM416, Campbell Scientific) was used to increase the number of differential channels.

Table C.1: List of sensors and data logging equipment used during the field experiment in Kyloe Wood.

Sensor	Location	logging	time res.
ST#001[1]	Tree 103.E	CR23X.DIFF2.AM416.DIFF8[2]	4 Hz
ST#002	Tree 103.N	CR23X.DIFF2.AM416.DIFF7	4 Hz
ST#003	Tree 104.E	CR23X.DIFF2.AM416.DIFF6	4 Hz
ST#004	Tree 104.N	CR23X.DIFF2.AM416.DIFF5	4 Hz

— continued on next page —

[1]ST: strain transducer

[2]reading from left to right: DATALOGGER#ID.CHANNEL.DEVICE.CHANNEL (e.g. CR23X.DIFF2.AM416.DIFF8: measured the 8th differential channel on the AM416 multiplexer, which is connected to the 2nd differential channel of the data logger (CR23X).

— continued from previous page —

Sensor	Location	logging	time res.
ST#005	Tree 105.E	CR23X.DIFF2.AM416.DIFF4	4 Hz
ST#006	Tree 105.N	CR23X.DIFF2.AM416.DIFF3	4 Hz
ST#007	Tree 106.E	CR23X.DIFF2.AM416.DIFF2	4 Hz
ST#008	Tree 106.N	CR23X.DIFF2.AM416.DIFF1	4 Hz
ST#013	Tree 107.E	CR23X.DIFF12	4 Hz
ST#014	Tree 107.N	CR23X.DIFF11	4 Hz
ST#015	Tree 108.E	CR23X.DIFF10	4 Hz
ST#016	Tree 108.N	CR23X.DIFF9	4 Hz
ST#017	Tree 109.N	CR23X.DIFF8	4 Hz
ST#018	Tree 109.N	CR23X.DIFF7	4 Hz
ST#019	Tree 102.E	CR23X.DIFF6	4 Hz
ST#020	Tree 102.N	CR23X.DIFF5	4 Hz
ST#021	Tree 101.E	CR23X.DIFF4	4 Hz
ST#022	Tree 101.N	CR23X.DIFF3	4 Hz
NRG#40[3]	Mast-II@30.8 m	CR23X.P1	1 s
NRG#40	Mast-II@27.0 m	CR23X.P2	1 s
NRG#40	Mast-II@24.0 m	CR23X.P3	1 s
NRG#40	Mast-II@21.0 m	CR23X.P4	1 s
NRG#40	Mast-II@18.0 m	CR23X.C5.LLAC4.P1	1 s
NRG#40	Mast-II@15.0 m	CR23X.C6.LLAC4.P2	1 s
NRG#40	Mast-II@10.0 m	CR23X.C7.LLAC4.P3	1 s
NRG#40	Mast-II@5.0 m	CR23X.C8.LLAC4.P4	1 s
NRG#40	Mast-I@30.8 m	Gigalog8#1	1 s
NRG#40	Mast-I@27.0 m	Gigalog8#1	1 s
NRG#40	Mast-I@24.0 m	Gigalog8#1	1 s
NRG#40	Mast-I@21.0 m	Gigalog8#1	1 s
NRG#40	Mast-I@18.0 m	Gigalog8#1	1 s
NRG#40	Mast-I@15.0 m	Gigalog8#1	1 s
NRG#40	Mast-I@10.0 m	Gigalog8#1	1 s
NRG#40	Mast-I@5.0 m	Gigalog8#1	1 s
NRG#200P[4]	Mast-II@27.0 m	CR23X.SE1	1 s
NRG#200P	Mast-II@15.0 m	CR23X.SE2	1 s
USA-1[5]	Mast-II@29.8 m	Gigalog8#2	10 Hz
USA-1	Mast-II@16.0 m	Gigalog8#3	10 Hz
SKT600#1[6]		CR10X.DIFF4	15 min
SKT600#2		CR10X.DIFF5	15 min
SKT600#3		CR10X.DIFF6	15 min

— continued on next page —

[3]NRG#40: cup anemometer (NRG Systems, US)
[4]NRG#200P: wind vane (NRG Systems, US)
[5]USA-1: sonic anemometer (METEK GmbH, Germany)
[6]SKT600: tensiometer (Skye Instruments, Powys, UK)

— continued from previous page —

Sensor	Location	logging	time res.
SKT600#3		CR10X.DIFF7	15 min
Thermistor#1	27.0 m	CR10X.SE5	15 min
Thermistor#2	5.0 m	CR10X.SE6	15 min

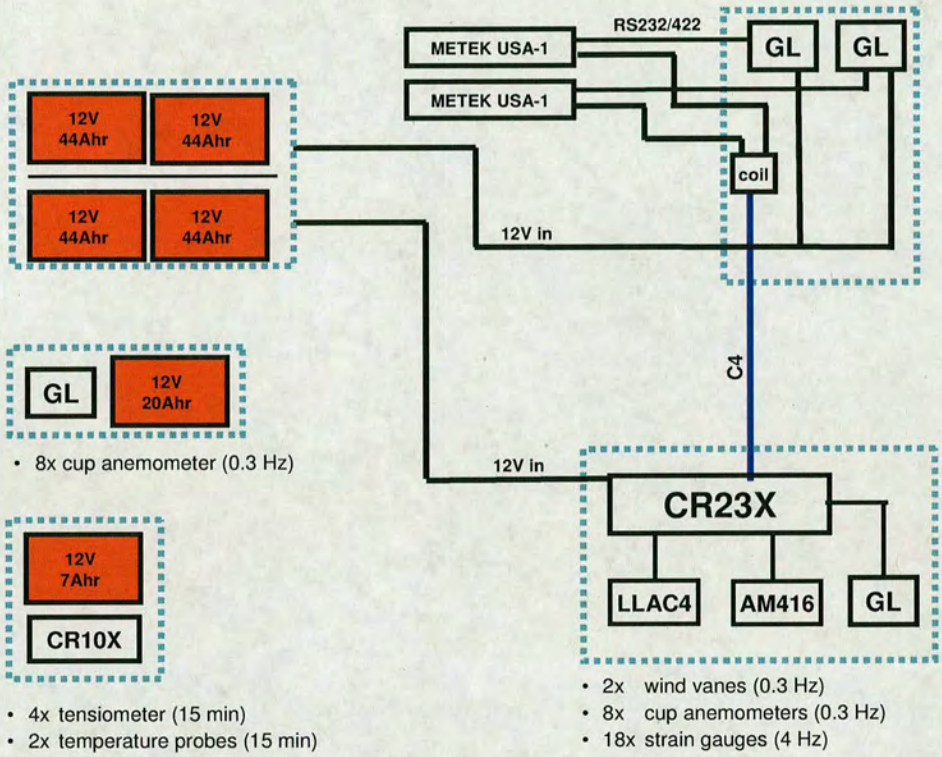

Figure C.1: Schematic illustration of the measuring system as it was used during the field survey in Kyloe Wood.

C.2 Photographs - Kyloe Wood

Figure C.2: Photographs from the experimental plot in Kyloe Wood. The first row shows the two experimental plots. Left hand side is the location *without* an understorey and on the right hand side is the stand *with* an understorey. The two pictures in the middle row are taken from within the understorey. The pictures in the bottom row show identical scenery before (left hand side, date: 22.Mar.2006) and after bud burst (right hand side, date: 31.May.2006).